

UNCLASSIFIED

AD NUMBER
AD820118
NEW LIMITATION CHANGE
TO Approved for public release, distribution unlimited
FROM Distribution authorized to U.S. Gov't. agencies and their contractors; Critical Technology; AUG 1967. Other requests shall be referred to Army Electronics Command, Attn: AMSEL-VL/C, Fort Monmouth, NJ.
AUTHORITY
USAEC ltr, 27 Jul 1971

THIS PAGE IS UNCLASSIFIED

AD820118

AD

TECHNICAL REPORT ECOM-00477-4

COMPACT H-F AIRCRAFT ANTENNAS (2-30 MHz)

FINAL REPORT

BY

J. H. HENDERSHOT

AUGUST 1967

.....
ECOM

UNITED STATES ARMY ELECTRONICS COMMAND - FORT MONMOUTH, N.J.

CONTRACT DA 28-043-AMC-00477(E)

MARTIN MARIETTA CORPORATION

Baltimore Division

Baltimore, Maryland 21203

DISTRIBUTION STATEMENT

This document is subject to special export controls and each transmittal to foreign governments or foreign nationals may be made only with prior approval of CG, U.S. Army Electronics Command, Attn: AMSEL-VLC

NOTICES

Disclaimers

The findings in this report are not to be construed as an official Department of the Army position, unless so designated by other authorized documents.

The citation of trade names and names of manufacturers in this report is not to be construed as official Government indorsement or approval of commercial products or services referenced herein.

Disposition

Destroy this report when it is no longer needed. Do not return it to the originator.

TECHNICAL REPORT ECOM-00477-4

AUGUST 1967

COMPACT H-F AIRCRAFT ANTENNAS (2-30 MHz)

FINAL REPORT

21 JANUARY 1965 TO 1 AUGUST 1967

Report No. 4

CONTRACT NO. DA 28-043-AMC-00477(E)

DA Project No. 1J6-41203-D-528-04

Prepared by

J. H. HENDERSHOT

MARTIN MARIETTA CORPORATION

BALTIMORE DIVISION

BALTIMORE, MARYLAND 21203

For

U. S. ARMY ELECTRONICS COMMAND, FORT MONMOUTH, N. J.

ABSTRACT

The program effort reported here is primarily concerned with the design and development of a broadband, compact, omnidirectional airborne antenna in the H-F communications range (2 to 30 MHz) to be used on several U. S. Army aircraft, both fixed and rotary wing.

Additional investigations are presented on a low profile wire antenna located on the aircraft tail at close proximity to the aircraft skin.

The various exploratory element configurations reported here are loop-type structures intended to induce currents on the airframe for a predominantly vertical polarized system. The final model H-F antenna delivered as the result of this program is a two-turn grounded loop.

Scaled models of two aircraft, one rotary and one fixed wing, were built for pattern, impedance, and gain measurements. Data are presented illustrating the effect of the antenna configuration, orientation, and location on the particular scale model aircraft. Pattern measurements were performed on a 1/50-scale Caribou aircraft and a 1/25-scale Iroquois helicopter. Impedance and gain measurements were made on 1/5-scale models of the same two aircraft.

Manual L-C tuners were built for the 1/5-scale antennas to facilitate impedance matching for the relative gain comparison measurements.

The application of ferrite to the H-F antenna has been considered. Measured field strength of a matched transmitting coil, with and without ferrite material, is presented.

A full-scale breadboard model of the two-turn loop was successfully tested with a Univac automatic tuner for high power and impedance tuning.

Environmental tests were performed on the full-scale final model antenna. The antenna was subjected to various vibration levels which resulted in structural modifications to the delivered model antennas.

Two full-scale final model antennas, a Univac automatic tuner and a Collins tunable filter were delivered during this program.

The Design Plan, Test Plan, and Environmental Test Results are included in the appendix.

CONTENTS

	Page
Abstract	iii
List of Illustrations	vii
List of Tables	xiii
Introduction	1
Concept	2
Element Configuration Investigated	3
Impedance	3
Radiance Coverage	7
Gain Measurement	8
Automatic Tuner	10
Ferrite Investigation	10
Structural Considerations	12
Environmental Tests	13
Final Model Full-Scale Antenna	15
Low Profile Antenna	15
Conclusion	17
References/Reports	59
Appendix A--Design Plan for Compact H-F Aircraft Antennas	A-1
Appendix B--Test Plan for Compact H-F Aircraft Antennas	B-1
Appendix C--Environmental Test Results	C-1

ILLUSTRATIONS

Fig.	Title	Page
1	Outboard Grounded Loop Feed Element on Vertical Stabilizer	18
2	1/5-Scale 4-Turn Loop	19
3	1/5-Scale Cap-Coil	19
4	1/5-Scale Submerged Coil	19
5	Full-Scale Outboard Patch	19
6	1/5-Scale 2-Turn Loop	20
7	1/5-Scale Multiturn Coil Loop Antenna	21
8	1/5-Scale Caribou Impedance Model	22
9	1/5-Scale Iroquois Impedance Model	22
10	Preliminary Element Configurations and Reactance Parameter Tuning Requirement	23
11	H-F Antenna Element Impedance Characteristics, 1/5-Scale Caribou	24
12	R and X Components, 4-Turn Loop at Location No. 1 on 1/5-Scale Caribou	25
13	Typical Full-Scale 2-Turn Loop Reactance Characteristics with Antenna Mounted on a Metal Building	26
14	1/50-Scale Caribou Pattern Model	27
15	1/25-Scale Iroquois Pattern Model	27
16	H-F Antenna Element Patterns, 1/50-Scale Caribou, Location No. 3	28
17	H-F Antenna Element Patterns, 1/25-Scale Iroquois, Location No. 2	29
18	3-ft Monopole and 12-ft x 12-ft Ground Plane	30

ILLUSTRATIONS (continued)

Fig.	Title	Page
19	1/5-Scale Caribou on Turntable Support	30
20	Manual Tuner for 1/5-Scale HF Antenna and 3-ft Monopole	31
21	Relative Gain (4-turn loop/3-ft whip) Versus Frequency	32
22	Relative Gain (4-turn loop/3-ft whip) Versus Frequency for Two Orientations on Tail of 1/5-Scale Caribou	33
23	Drag Versus Antenna Configuration	34
24	Relative Gain (2- and 4-turn loop/2-ft whip) Versus Frequency as a Function of Size	35
25	Full-Scale H-F Compact Antenna	36
26	Test Unit Antenna (lateral plane)	37
27	Test Unit Antenna (modified)	38
28	H-F Antenna (final model)	39
29	Low Profile H-F Antenna	40
30	Low Profile Antenna Impedance	41
31	Low Profile Gain	42
32	Low Profile Gain Continued	43
33	Patterns of Low Profile Wire Antenna, 1/50 Caribou	44
34	Patterns of Low Profile Wire Antenna, 1/50 Caribou	45
35	Patterns of Low Profile Wire Antenna, 1/50 Caribou	46
36	Patterns of Low Profile Wire Antenna, 1/50 Caribou	47

ILLUSTRATIONS (continued)

Fig.	Title	Page
37	Patterns of Low Profile Wire Antenna, 1/50 Caribou	48
38	Patterns of Low Profile Wire Antenna, 1/50 Caribou	49
39	Patterns of Low Profile Wire Antenna, 1/50 Caribou	50
40	Patterns of Low Profile Wire Antenna, 1/50 Caribou	51
41	Patterns of Low Profile Wire Antenna, 1/50 Caribou	52
42	Patterns of Low Profile Wire Antenna, 1/50 Caribou	53
43	Patterns of Low Profile Wire Antenna, 1/50 Caribou	54
44	Patterns of Low Profile Wire Antenna, 1/50 Caribou	55
45	Patterns of Low Profile Wire Antenna, 1/50 Caribou	56
46	Patterns of Low Profile Wire Antenna, 1/50 Caribou	57
47	Patterns of Low Profile Wire Antenna, 1/50 Caribou	58
A-1	1/50-Scale Model of Caribou	A-7
A-2	Pattern Model--1/5 Scale	A-7
A-3	Aircraft Model Coordinate System (right-hand spherical coordinates)	A-8
A-4	Azimuth Patterns--Location 1, 100 MHz, E	A-9
A-5	Azimuth Patterns--Location 1, 100 MHz, E	A-10

ILLUSTRATIONS (continued)

Fig.	Title	Page
A-6	Azimuth Patterns--Location 1, 750 MHz, E	A-11
A-7	Azimuth Patterns--Location 1, 750 MHz, E	A-12
A-8	Azimuth Patterns--Location 1, 1500 MHz, E	A-13
A-9	Azimuth Patterns--Location 1, 1500 MHz, E	A-14
A-10	Azimuth Patterns--Location 2, 100 MHz, E	A-15
A-11	Azimuth Patterns--Location 2, 100 MHz, E	A-16
A-12	Azimuth Patterns--Location 2, 750 MHz, E	A-17
A-13	Azimuth Patterns--Location 2, 750 MHz, E	A-18
A-14	Azimuth Patterns--Location 2, 1500 MHz, E	A-19
A-15	Azimuth Patterns--Location 2, 1500 MHz, E	A-20
A-16	Azimuth Patterns--Location 3, 100 MHz, E	A-21
A-17	Azimuth Patterns--Location 3, 100 MHz, E	A-22
A-18	Azimuth Patterns--Location 3, 750 MHz, E	A-23
A-19	Azimuth Patterns--Location 3, 750 MHz, E	A-24
A-20	Azimuth Patterns--Location 3, 1500 MHz, E	A-25
A-21	Azimuth Patterns--Location 3, 1500 MHz, E	A-26
A-22	Typical Construction of Impedance Mockup (Sikorsky CH-3C shown)	A-27
A-23	Test Setup for Determining Tuner Losses	A-28
B-1	Impedance Test Setup	B-5
B-2	Test Setup to Verify VSWR $\leq 2:1$	B-5
B-3	HF and Monopole Manual Tuner	B-6

ILLUSTRATIONS (continued)

Fig.	Title	Page
B-4	Gain Measurement Test Setup	B-7
B-5	3-ft Monopole with Ground Plane and 1/5-Scale Caribou on Rotary Platform	B-8
B-6a	Reference Level Setup for Manual Tuner Calibration	B-9
B-6b	Manual Tuner Insertion Loss Test Setup	B-9
B-7	Decoupling Test Setup	B-9
C-1	Compact H-F Aircraft Antenna	C-2
C-2	Vibration Requirements Qualification Level	C-3

INTRODUCTION

The investigation and development reported here were concentrated on new approaches to an H-F antenna design with the goal of fabricating a compact and efficient antenna operating over the frequency range of 2 to 30 MHz. It is desired that the antenna, when mounted on a fixed-wing or rotary-wing aircraft, shall demonstrate a significant improvement over performance achieved by existing wire, whip, and other antennas currently used in this frequency range.

The design objectives for this antenna are listed as follows:

- (1) Tuning range--2 to 30 MHz with one or more controls.
- (2) Efficiency and gain--better than a 15-ft monopole over a good ground plane.
- (3) Polarization--vertical.
- (4) Azimuth coverage--omnidirectional.
- (5) Power input--400 watts average.
- (6) VSWR--2:1 maximum (with tuner).
- (7) Impedance--50 ohms unbalanced.
- (8) Bandwidth--at least 6 KHz at 1/2 power points.
- (9) Isolation (retransmission mode)--60 db between 2 antennas spaced 5 ft apart.
- (10) Size--24 in. in the maximum dimension.
- (11) Weight--10 lb.

The specific aircraft with which this antenna will be used are as follows:

<u>Fixed Wing</u>	<u>Rotary Wing</u>
CV-2 Caribou	UH-1 Iroquois
OV-1 Mohawk	CH-47 Chinook
U-8 Seminole	OH-13 Sioux
	OH-23 Raven

The two aircraft selected here for the impedance, pattern, and gain investigations were the fixed-wing Caribou and the rotary-wing Iroquois. The Caribou and Iroquois impedance models were built at 1/5 scale while the pattern models were made of a 1/50-scale Caribou and 1/25-scale Iroquois for this program.

The basic Martin Marietta grounded two-loop antenna design described here is an equivalent outboard notch type coupling element that will ef-

ficiently couple R-F currents on the aircraft structure. The complete antenna system consists of the antenna and an automatic tuner.

Subsequent to the design and delivery of the final model full-scale Martin Marietta loop antenna, a low profile wire antenna was investigated. The intent here was to arrive at an extremely low-silhouette H-F wire antenna that would exhibit a substantial reduction in aerodynamic drag with no degradation in the electrical performance such as gain and pattern coverage.

Final evaluation of the full-scale antenna system through a flight test program has not been performed at the time of this reporting. Thus, measured results obtained from future flight tests will provide a basis of comparison of the H-F antennas presently used.

Concept

The object of the investigations to be described is to arrive at the design of a coupling element which may be externally mounted on an aircraft in such a fashion that substantial H-F current flow will be induced on the structure. Thus, the aircraft serves as the antenna; the coupling element itself is much too small to possess good radiation characteristics in the frequency range under consideration.

The advantages to be derived from this approach, as compared to existing H-F aircraft antennas, are the following:

- (1) Small size. The major constraint specified for this "antenna" is that the maximum dimension must not exceed 2 ft.
- (2) Minor structural modification. Excluding the trailing wire antenna, the other types in use are:
 - (a) Electrical (probe, tail cap and wing cap)
 - (b) Magnetic (notch).

Both of these involve substantial structural modification, and the antenna cannot be separated from the particular aircraft for which it was designed.

- (3) General applicability. This antenna is to be externally mounted, in contrast to the types mentioned above, and, therefore, may be used on a variety of aircraft.

These advantages are not to be realized without some sacrifice in electrical properties. The coupling to the aircraft will not be as good, in general, as that realized by a larger probe or notch, for example, specifically designed for a given aircraft. For best coupling, the electric

type must be located in the region of a voltage maximum, corresponding to the airframe extremities. Conversely, the magnetic type was chosen since it afforded more flexibility in location, according to the above remarks, and also since voltage breakdown problems are reduced by its use. High current problems are involved, instead, which must be accommodated in the ultimate design.

The basic design configuration is shown at a possible location on the vertical stabilizer in Fig. 1. R-F current flowing in the loop conductor creates a changing magnetic field, which induces currents on the aircraft skin 90 deg out of phase with the magnetic field. The magnetic lines which encircle the stabilizer are the ones which produce coupling.

Element Configurations Investigated

Several antenna element configurations investigated in this program are discussed in the sections on impedance, pattern, and gain. These configurations shown in Figs. 2 through 7 are the Four-Turn Loop, Cap-Coil, Submerged Coil, Outboard Notch, Two-Turn Loop and a 21-Turn Coil shaped into a half loop. Another configuration of a low-profile wire antenna is discussed in a later section. The four-turn loop and cap-coil are considered equivalent one-turn loops with series inductance. In addition, the cap-coil is top loaded with a capacitive hat. The submerged coil consists of a series grounded coil enclosed within a slit cylinder. The scheme here is to induce currents on the inner wall of the cylinder which continue on around to the exterior walls and then couple to the airframe. Insofar as reactance is concerned, the outboard notch may be considered analogous to a length of two-wire transmission line shorted at one end.

The 1/5-scale antennas were fabricated to a maximum dimension of 4.8 in. which corresponds to a maximum allowable full-scale dimension of 2 ft.

The various configurations were investigated primarily through impedance and pattern studies. Another factor was the aerodynamic drag that resulted from the different shapes studied. The final configuration selected was a two-turn loop and was principally dictated by reduced drag and justified by the measured results of relative gain presented in the section on gain.

Impedance

Caribou and Iroquois 1/5-scale impedance mockups are shown in Figs. 8 and 9. The models were built to the same 1/5 scale to facilitate measurement of the 1/5-scale antennas on each. The models are made of wood covered with hardware wire mesh. The antenna locations are numbered 1, 2 and 3 as shown for the Caribou, while two locations, also

numbered, are shown on the Iroquois. Also shown is a movable wood tower support that is interchangeable with each aircraft. The test equipment was mounted inside the aircraft for the actual impedance measurement. An access door is provided for installing the equipment.

Preliminary impedance investigations were performed on a full-scale outboard notch-fed element. A 1/5-scale outboard notch and various 1/5-scale grounded loops were also evaluated for their impedance characteristics. The initial concern here was to determine the magnitude of the reactance parameter that would require tuning out eventually by an automatic tuner.

Discussions on automatic tuner capabilities with the Univac Division of Sperry Rand indicated it was feasible to tune out values of $+j20$ ohms reactance at 2 MHz. The maximum tuning capacity required is 4000 pf.

The full-scale outboard notch was measured to only 4 MHz. Excessive cable lengths were required to transform the impedance through a transmission line. Below 4 MHz, the cable losses masked out the sensitivity of the measurement apparatus, and the full-scale model was abandoned in favor of the 1/5-scale configurations. A 1/5-scale outboard notch and loop elements were then tested at 10 MHz. Each element was mounted on an existing 1/3-scale model aircraft which provided a suitable simulated ground plane. A Q-meter technique was then employed for the measurement of the reactance parameter. The results of these preliminary measurements are shown in Fig. 10. The resultant capacity required for tuning each element is noted for the scale frequency and the full-scale equivalence. The measured results indicated the notch-fed element was undesirable due to the required high capacity values of 7,000 to 12,000 pf. This effort was then concentrated upon the multiturn grounded loops that included some additional series inductance. The grounded element was chosen to reduce high voltage breakdown problems; otherwise, a breakdown arrester would be required. Preliminary adjustments were made from the roof of the laboratory building with the mockup adjacent to the building. The support tower with a 1/5-scale model was then moved away from the building and the test instrument remotely tuned by a 16-ft wooden pole. An umbilical connection for the a-c line is provided on a small chassis box beneath the fuselage of each model. Three R-F filter chokes in series with the two-wire line with ground are housed within this box to isolate the R-F current from the input a-c line.

The Q-meter required a minimum number of controls during the remote tuning adjustment. Values of Q_1 and capacitance C_1 were recorded for no antenna connection, and then Q_2 and C_2 were taken by remote measurement with the instrument connected to the antenna terminals through a length of transmission line. Various lengths of transmission

The other antenna locations on the aircraft required interconnection of various lengths of RG-8A/U coaxial cable. The adjusted impedance transformed through the length of line and measured at the R-X meter terminals is accounted for in Eq (1). Values of parallel capacity and parallel resistance were recorded for each antenna over a frequency range of 10 through 150 MHz. The same computer program was used for the data reduction to the series equivalent components.

The measured results of impedance tests performed on the 1/5-scale Caribou are plotted on simplified Smith Charts in Fig. 11. The three 1/5-scale antenna elements consisting of the cap-coil, four-turn loop and the submerged coil were measured for the three locations illustrated. At Location No. 1, both inductive and capacitive components are noted from 10 through 150 MHz. At Location No. 2, the cap-coil reactance component is entirely inductive. This is due to the altered configuration when mounting the element at the tail base position. At Location No. 3, the measured results indicate that the reactive component is entirely inductive. Plotted results of reactance and resistance versus frequency for the four-turn loop at Location No. 1 are shown in Fig. 12. Very low resistance values of approximately 100 milliohms are noted at the low frequencies. The measured results of the cap-coil element showed slightly higher values of resistance at the higher frequencies while the submerged coil element showed a maximum value of 3 to 6 ohms. This compares to 61 and 14 ohms for the four-turn loop and cap-coil elements, respectively.

The measured results obtained from the 1/5-scale Iroquois impedance model indicated essentially the same results as measured at Location No. 1 of the Caribou. Rotor blade position effect was noted for the top location while little effect was noted for the bottom location. This effect was noted by a change in the reactance parameter.

Impedance measurements were made relative to antenna orientation at all locations on both aircraft models. No change in the impedance characteristics was noted when the element ground point connection was rotated 90 deg about the feed point.

A Smith Chart plot of the impedance characteristics of the two-turn loop full-scale breadboard model antenna is shown in Fig. 13. The antenna was mounted on the exterior of a small metal building for the measurements. The main parameter desired from these measurements was the reactance at 2 MHz. The shunt capacity required for tuning is approximately 3500 pf which is well within the automatic tuner capability of 4200 pf. The plot is representative of the reactance parameter only, since the antenna relies on the aircraft itself for radiation resistance, especially at the lower frequencies.

The other antenna locations on the aircraft required interconnection of various lengths of RG-8A/U coaxial cable. The adjusted impedance transformed through the length of line and measured at the R-X meter terminals is accounted for in Eq (1). Values of parallel capacity and parallel resistance were recorded for each antenna over a frequency range of 10 through 150 MHz. The same computer program was used for the data reduction to the series equivalent components.

The measured results of impedance tests performed on the 1/5-scale Caribou are plotted on simplified Smith Charts in Fig. 11. The three 1/5-scale antenna elements consisting of the cap-coil, four-turn loop and the submerged coil were measured for the three locations illustrated. At Location No. 1, both inductive and capacitive components are noted from 10 through 150 MHz. At Location No. 2, the cap-coil reactance component is entirely inductive. This is due to the altered configuration when mounting the element at the tail base position. At Location No. 3, the measured results indicate that the reactive component is entirely inductive. Plotted results of reactance and resistance versus frequency for the four-turn loop at Location No. 1 are shown in Fig. 12. Very low resistance values of approximately 100 milliohms are noted at the low frequencies. The measured results of the cap-coil element showed slightly higher values of resistance at the higher frequencies while the submerged coil element showed a maximum value of 3 to 6 ohms. This compares to 61 and 14 ohms for the four-turn loop and cap-coil elements, respectively.

The measured results obtained from the 1/5-scale Iroquois impedance model indicated essentially the same results as measured at Location No. 1 of the Caribou. Rotor blade position effect was noted for the top location while little effect was noted for the bottom location. This effect was noted by a change in the reactance parameter.

Impedance measurements were made relative to antenna orientation at all locations on both aircraft models. No change in the impedance characteristics was noted when the element ground point connection was rotated 90 deg about the feed point.

A Smith Chart plot of the impedance characteristics of the two-turn loop full-scale breadboard model antenna is shown in Fig. 13. The antenna was mounted on the exterior of a small metal building for the measurements. The main parameter desired from these measurements was the reactance at 2 MHz. The shunt capacity required for tuning is approximately 3500 pf which is well within the automatic tuner capability of 4200 pf. The plot is representative of the reactance parameter only, since the antenna relies on the aircraft itself for radiation resistance, especially at the lower frequencies.

Radiation Coverage

Solid copper skin models of the 1/50-scale Caribou and 1/25-scale Iroquois shown in Figs. 1 and 15 were built for the radiation pattern measurement tests. Element locations for each aircraft are numbered as shown. Three locations were chosen for Caribou while two were chosen for the Iroquois. The coordinate system employed for the pattern measurements is illustrated in Fig. A-3 of the Design Plan.

It was desirable to keep the frequency range as high as possible in order to minimize ground reflections on the test range. Thus for the Caribou, the lowest frequency required is 100 MHz. The 1/50-scale factor was impractical for the Iroquois model since the model size becomes too small to accommodate detector mounting within the model. The lowest scale frequency for the 1/25-scale Iroquois is therefore 50 MHz at some sacrifice in range performance with regard to reflections. Due to the small physical size of the models, complete tuning compensation is not practical. This further compounds the measurement problems for adequate signal strength. A compromise in the line lengths, at each location, between the element and the internally mounted detector was made to get the best overall signal levels at all frequencies.

Four element configurations were evaluated on the Caribou. They were the four-turn loop, cap-coil, submerged coil and outboard notch. At Locations Nos. 1 and 3 each element was evaluated for two orientations. The orientations at each location consisted of rotating the element ground point by 90 deg. At Location No. 2 only one orientation was tested. This location would result in an antenna differing from those suitable for the other locations and is considered undesirable due to the consequent loss of universality.

The measurements consisted of taking radiation patterns of the azimuth, longitudinal and transverse planes with horizontal and vertical polarization for each antenna location. Since the principal emphasis here is on omnidirectional coverage in the azimuth plane with vertical polarization, only those results are presented. The measured pattern coverage of the 1/50-scale Caribou, azimuth plane, with vertical polarization is shown in Fig. 16. The results indicate best omnidirectional coverage at Location No. 3 on the tail for the four-turn loop and the cap-coil. The order of preference for the element location is Nos. 3, 2 and 1. The predominance of a vertical polarized system was also confirmed when compared to the measured results with horizontal polarization. The 1/50-element size was held to a full scale equivalent, 2- x 2-ft dimensions.

Pattern measurements on the 1/25-scale Iroquois aircraft were taken with a four-turn loop and the cap-coil. Azimuth plane, vertical polarization patterns are shown in Fig. 17. The effect of rotor blade position

is also evident here. The measured results showed that both antennas are nearly the same in coverage at either location.

Patterns were also taken on the 21-turn half loop and the two-turn loop. The 21-turn half loop showed good azimuth plane coverage but still not as optimum as the four-turn loop. This 21-turn configuration was tried late in the program in an effort to reduce aerodynamic drag. The 21-turn element was arrived at by simulating the impedance characteristics of the four-turn loop and, thus, not imposing any additional requirements on the automatic tuner. The two-turn loop patterns were essentially the same as for the four-turn loop.

The pattern studies indicate good omnidirectional vertical polarization in the azimuth plane on the 1/50-scale Caribou with fair coverage for the 1/25-scale Iroquois. Full size patterns of the outboard notch on the 1/50 Caribou (Figs. A-4 through A-21) are shown in the Design Plan in the appendix.

Gain Measurements

Gain measurements required comparison of the H-F antenna relative to a full-scale, 15-ft monopole. The measurements were performed on 1/5-scale models. A 3-ft vertical monopole mounted on a 12 x 12-ft wire mesh ground screen, shown in Fig. 18, was fabricated for these tests. In addition, a support stand with a turntable support for the model aircraft is shown in Fig. 19. Gain measurements were performed on each antenna (H-F antenna and whip) located equidistant from a vertically polarized source antenna, 70 ft away (see Fig. B-4 of the Test Plan). Mockup proximity effects were reduced by providing an adequate distance between the two mockups. This safe distance was verified by rotating the 1/5-scale aircraft about its support while noting no perceptible change on the whip monitor.

Each antenna was matched out with a manual tuner for each frequency of measurement. The manual tuner is comprised of lumped L-C networks as shown in Fig. 20. Series inductive, shunt or series capacitive tuning of the reactance parameter is utilized, dependent on the frequency to be matched out. Each antenna is both inductive or capacitive over the 1/5-scale frequency range of 10 to 150 MHz. The 3-ft whip is capacitive to approximately 80 MHz and then inductive through 150 MHz. The scaled four-turn loop H-F antenna is inductive to about 85 MHz and then becomes capacitive through 150 MHz. A variable inductor enables the transformation of the resistance component to the characteristic impedance of the input transmission line. Clip lead connections facilitate the appropriate connection as required for the L-C combination or L and C separately. Calibration of the tuners for insertion loss was accomplished by utilizing a conjugate impedance tuner to simulate the antenna impedance of the scale H-F or whip antenna. The model H-F

and whip manual tuner controls remain fixed for the matched-out condition of each antenna, while the conjugate tuner is connected back-to-back and manipulated for a matched condition of maximum output power and minimum VSWR as monitored by an impedance bridge and receiver. Once this is accomplished an insertion loss measurement is made, and the total loss is divided by two since only one tuner is involved in the gain measurements. After calibration, true relative gain comparisons accounting for the tuner losses can be made. A similar test setup (Fig. 23) is discussed in the appendix on the Design Plan.

A vertically polarized source antenna located equidistant from each test antenna was used to transmit to power monitoring equipment housed within each receiving antenna mockup. Gain measurements were then taken independently for each test antenna. The tuner losses were accounted for at each test frequency from previous calibration.

Relative gain measurements were performed at two locations of the 1/5-scale Caribou aircraft. The 1/5-scale multiturn loop antenna gain was compared to that of a 3-ft whip from 10 through 150 MHz. The measured gains reported here are for the best aircraft orientation at the particular frequency of interest. This corresponds to the direction of maximum gain of the radiation pattern.

The measured results with the four-turn grounded loop located atop the fuselage and two orientations are shown in Fig. 21. Peaks in the data occur at 30 and 100 MHz which may be attributed to the physical dimensions of the aircraft model. Gain variations of +2 to -14 dB were measured from 10 through 150 MHz. The measured results for two orientations of the four-turn loop at the midtail location of the Caribou are shown in Fig. 22. Gain variations are similar to those for the fuselage location. A more definite orientation preference is noted here for the loop element oriented parallel to the tail. This corresponds to the loop-axis parallel to the tail.

Computations of drag on the four-turn loop indicated loads of 133 lb for speeds of 225 kn. The four-turn loop provided the lowest drag of the three configurations illustrated in Fig. 23. These loads are almost prohibitive for the preferred tail installation. Additional effort was made to reduce the antenna size and drag while not altering the electrical performance. Gain measurements were performed for a reduced height, width and number of turns. The measured results shown in Fig. 24 indicate little degradation for a two-turn loop of reduced height. These results and a drag of 40 lb at 225 kn merited the element size reduction. The full-scale equivalent dimensions for the final smaller element are shown in Fig. 25.

Automatic Tuner

An automatic tuner, Model 3260A-1, was supplied by Univac, and acceptance tests were performed at their facility in St. Paul, Minnesota. The Martin Marietta two-turn loop breadboard model and a simulated H-F antenna load by Univac were used for these tests. The tuner performed exceptionally well at all frequencies from 2 to 30 MHz. A matched condition (VSWR 1.6:1) was verified throughout this frequency range. Most of the measurements were performed at 100 watts CW input power. At 2 and 30 MHz, the automatic tuner and breadboard antenna were subjected to 400 watts CW with no apparent degradation in performance. Some slight heating of 20° to 40° C above ambient temperature was noted at 30 MHz for a continuous power application of about 1-min duration. One significant point in these tests is that the breadboard antenna was tuned out while attached only to a metal bench which provided a poor mockup for a simulated aircraft. Measured output current of 33 amp was noted at 5 MHz, while a gradual decrease to 1 amp at 30 MHz was noted for 100 watts input power. At frequencies from 2 to 4 MHz, the current was not measured due to the monitor ammeter limitation of 33 amp. Tuner efficiencies of 80 to 90% were measured from 2 to 9 MHz, while 50% or greater efficiencies were measured from 10 to 30 MHz. The efficiencies were measured on a Univac load that simulated the H-F compact antenna impedance from 2 to 30 MHz.

The efficiency as defined here is the ratio of the measured output average power to the measured input average power $\frac{P_{out\ avg}}{P_{in\ avg}}$. The input power was measured on a M. C. Jones micromatch Model MM-252 coupler indicator unit. For the output power measurement, a simulated H-F antenna load consisting of a 5-in. diameter coil with 13 turns was employed. The final six turns were shorted with an ammeter and 50 ohm resistor in series to ground. Hence, the measured I^2R values provided an approximate value of the average output power.

Additional equipment delivered during this program was a Collins 635V-1 tunable filter to be utilized for a retransmission mode requirement.

Ferrite Investigation

It has been shown by Wheeler* that the radiation power factor of an inductor operating as a small antenna is increased by increasing the relative permeability of its core. Thus, it is of interest to consider this technique for the present application.

* Wheeler, H. A., "Fundamental Limitations of Small Antennas," Proc., IRE, December 1947, pp 1479 to 1484.

It should first be noted that the type of antenna under development involves the radiating properties of the aircraft structure. The extent to which the airframe may be coupled to the feedpoint determines the radiation resistance and, consequently, the radiation power factor. For an antenna with a maximum dimension of 2 ft, the radiation resistance will be extremely low at a wavelength of 500 ft such that even if the core permeability were increased several times, the result would still be small in comparison to ohmic losses in the antenna-tuner system. If currents are excited to any degree on a large extent of airframe, however, the effective antenna size is thereby made substantially larger than 2 ft with a consequent increase in effective radiation resistance. Therefore, any means of increasing coupling to the airframe is a step in the right direction.

Currents are induced on the airframe by the changing magnetic field of the inductor antenna. The magnetic field strength will be increased for the same current input by using a high permeability core in the antenna, thus, intensifying the current flow on the airframe. Thus, in concept, this approach appears attractive.

The drawbacks to such a scheme are due to the weight and electrical losses of the magnetic material. In the frequency range under consideration, ferrites are the only materials which do not have prohibitive losses. A sample rod was obtained for investigation from Trans-Tech, Inc., one of the leaders in this field. The material recommended by them as best suited to our requirement from the loss standpoint was a nickel-cobalt ferrite designated TT 2-101, which has a curie temperature of 585° C. With this material, there would obviously be no loss of effectiveness due to heating. Ferrites are, however, temperature sensitive and heating changes would cause detuning which would have to be corrected by the automatic tuning system.

A coil was wrapped around the sample, and relative field strengths were measured in the near field with and without the core sample. The power input was held constant by matching the signal generator output to the two different loads with the manual tuner designed for the exploratory development model antenna. The results are shown in the following table.

<u>Relative Field Strength</u>	
<u>Frequency (MHz)</u>	<u>(with core/without core) ± dB</u>
15	+4.5
16	+3.0
17	+4.8
18	+5.0
19	+4.0
20	+3.0

<u>Frequency (MHz)</u>	<u>(with core/without core) \pm dB</u>
21	+3.6
22	+2.5
23	+3.0
24	+3.0
25	+3.1
26	+3.0
27	+2.8
28	+2.8
29	+3.0
30	+3.0

Insofar as weight is concerned, the specific density of TT-201 is 5.44 gm/cm³. In order to stay within the 10-lb antenna weight limitation, let us assume that half of the weight could be assigned to ferrite. Five pounds of this material occupies a volume of 25.4 cu in. This is very small compared to the amount required for a 2-ft diameter inductor, so that the effect would be negligible even if there were no losses.

On the basis of the above observations, it is concluded that ferrites have no useful application in this particular antenna development, since the weight required for electrical improvement is prohibitive.

Structural Considerations

A test-unit antenna was designed and fabricated to withstand the qualification test program. Primary emphasis was placed on the vibration tests. These tests are essential to ensure the antenna will withstand the aircraft environments without deteriorating the aerodynamic and electrical characteristics of the antenna. The necessary structural modifications would be made as required to ensure the best mechanical configuration.

The first full dynamic spectrum sweep resulted in a failure of the bond of the fairing to the fairing block. Data obtained from this run revealed a dynamic magnification of 30 at the antenna tip, resulting in the equivalent of 260 g. The design was reviewed, and the following revisions were made.

- (1) The fiberglass fairings were increased to 0.180 in. thick at the base, with a tapered thickness to 0.060 in. at the tip.
- (2) The fairing block was extended to increase the bond area to the fairing.
- (3) The fairing was terminated at the base with a flanged condition, permitting the direct connection of the baseplate and fairing, through the fairing block.

The above revisions were considered the most practical solution in light of the total weight, aerodynamic drag, and electrical requirements.

The dynamic test results are given in the appendix. About 90% of the total dynamic test program was completed when cracks were noted in the baseplate, primarily in the vicinity of the plate-to-tube weld. Test was suspended, and the following revisions were made.

- (1) Attachment bolt pattern of the baseplate to fixture (or aircraft) was modified to provide better bending moment distribution in the plate at the fairing block.
- (2) Welding sequence at the tube to baseplate weld was revised to include heat control to reduce the heat affected zone, thus increasing strength in the areas of baseplate bolts.

Environmental Tests

The environmental tests consisted of shock and vibration only. The test antenna mounted on the shock test apparatus is shown in Fig. 26. These tests constituted a small portion of the overall tests and were performed with no difficulty.

The principal effort on the environmental test was expended on the vibration tests. In these tests, the antenna was vibrated at rated levels in the three principal planes as illustrated in Fig. C-1 of the appendix. The vibration requirements, shown in Fig. C-2 of the appendix, were run in accordance with the MIL-E-500H specification. For the initial test with the antenna mounted as shown in Fig. 26, the frequency range is swept from 5 to 500 cps and then from 500 to 5 cps at the g levels indicated on the vibration requirements curve. During these sweeps, the resonant frequencies are noted. The sweeps are run for 1-hr minimum lapse time. A maximum of four resonant frequencies are then dwelled for intervals of 1/2 hr each at rated levels. Thus, the dwell time is a 2-hr maximum in one plane. The total time required for each principal plane is 3 hr. In some cases, the sweep time was 2 hr plus 2 dwells of 1/2 hr each. Since three planes are tested, a total of 9 hr testing is required. The 1/2 hr dwells at the resonant frequencies are the severest part of the tests. Extremely high g levels as well as fatigue are experienced at the dwell frequencies.

Initially, the test antenna was tested in the lateral plane which was anticipated to be the severest of the three to be tested. The unit failed early while performing the sweep portion of the tests. One of the fiberglass fairing supports broke away from the metal baseplate and sheared the dielectric screws holding the fairing at the baseplate. The fairing was rebonded, and all dielectric screws were replaced by metal screws. Again the same test was run, and the epon adhesive bond at the fiber-

glass fairing attaching to the solid fiberglass foot-base broke. The epon bond-metal screw combination, where the first failure occurred, did not fail during this second test. Tests were then run with two fairings floating, and the loads experienced were even more severe.

Remedial action was then taken by increasing the fiberglass fairing thickness by a factor of two. In addition, the fiberglass base supports interconnecting the fairing and the metal baseplate were enlarged. After this modification, low level tests were run to determine if the test unit would withstand the rated levels. The modified unit is shown in Fig. 27.

The low level tests indicated loads in excess of 400 g would be experienced at full vibration levels. Mechanical and stress engineering analysis indicated the modified structure would be capable of withstanding loads near 600 to 700 g. The effects of sustained vibration and the resulting fatigue could not be calculated. A crossbar was tried at low levels to determine if bracing would be desirable but was not needed at the rated levels.

Full rated levels were then run again with about 90% completion of all tests. All tests were completed with the antenna mounted in the vertical plane. In the lateral axis, all but two 1/2-hr dwells were completed. In the longitudinal axis, all testing except 8 min of the final dwell was completed. During tests with the antenna mounted in the longitudinal plane, the metal baseplate cracked in the vicinity of the baseplate corners. The two factors contributing to this failure were lack of screws to hold the metal baseplate at the corners and additional holes in the plate for metal screws added adjacent to the dielectric screws.

The following revisions resulted in the configuration shown in Fig. 28.

- (1) Increased baseplate area at corners with screw holes for securing the corners.
- (2) Metal screws replaced dielectric screws for securing the fiberglass base supports.
- (3) New holes through the baseplate around the periphery of each fiberglass fairing were added to provide additional tie points in these areas.
- (4) Increased fiberglass thickness of fairings.
- (5) Increased overall size of fiberglass base supports.

These changes were incorporated into the first two delivered models.

A tabulation of the environmental test results is shown in Table 1.

TABLE 1

Environmental Test Results

<u>Axis</u>	<u>Number of Frequency Sweeps (15 min/sweep)</u>	<u>Number of Resonant Dwells (30 min/dwell)</u>	<u>Lapsed Time (hr)</u>
Vertical	4	4	3
Lateral	6	1	2
Longitudinal	8	2	<u>2.87</u>
		Total	7.87 hr

Results: % compliance $\frac{7.87}{9.00} \times 100 = 87.5\%$

Final Model Full-Scale Antenna

The final model of the H-F compact antenna shown in Fig. 28 is a two-turn grounded loop supported by four foam-filled fiberglass fairings attached to a metal baseplate. One end of the loop is grounded to the metal baseplate by a weld connection while the feed point end protrudes through a fiberglass insulator and baseplate. A flexible connector is filled with plastic internally to maintain concentricity and prevent collapsing. An antistatic black paint covers the externally exposed portion of the antenna. The overall dimensions are 18 x 24 x 12 in. The total weight is 13-3/4 lb. Two of these final model antennas were delivered during this program. An adapter plate is required between aircraft skin and antenna baseplate. The aircraft and aircraft location will determine the adapter configuration.

Low Profile Antenna

The original program called for the delivery of eight antennas. The last six were to be production models. Each would require its own automatic tuner involving additional cost. Since this antenna has to be evaluated in future flight tests, it was determined that the two delivered antennas and the one automatic tuner would be adequate for an evaluation test program. Thus, a redefinition effort study phase on a low profile wire antenna was established, and the delivery of six additional antennas was deleted.

The basic idea of the low profile wire antenna was to arrive at a "paste-on" configuration for the H-F frequency range that would have essentially zero drag.

This study involved measurement of impedance, gain, and patterns of the configuration shown in Fig. 29. A 1/4-in. diameter wire runs up the leading edge of the tail to the top and then abruptly extends down on each side where it is grounded. These tests were made for four different spacings above the aircraft skin. The spacings for the 1/5-scale tests were 1/4, 1/2, 3/4 and 1 in. The 1/5-scale length dimensions are 4 ft 3 in. for the length going up to the leading edge of the tail and 11-1/2 in. for the length on each side of the tail. The full scale length is approximately 26 ft.

The results reported here were obtained for only the Caribou models. Previous gain data were taken only on this model, and thus a basis of comparison could be made, mainly on the gain characteristics.

A plot of the measured results of the low profile impedance for a 1 in. spacing is shown in Fig. 30. The other three spacings of 1/4, 1/2 and 3/4 in. showed little change in the reactance parameter, while an increase was noted in resistance with the increased spacing. Multiple resonance and antiresonance are noted which is typical of a wire antenna with appreciable length.

The results of the relative gain measurements are plotted in Fig. 31 for each of the four spacings. These results indicate a degradation in gain with the smaller spacing. A comparison of these data with Fig. 22 indicates improved gain values for the low profile wire. Additional gain data are shown in Fig. 32 for slight variations in the configuration. For one case shown, the side elements on this tail were removed; while, for the other, wire mesh of 1 ft width at the top was tapered to a point at the external feed connection. Removal of the side elements shows a degradation at this low frequency end; while, for the second case with larger cross-section, there is improved gain at the high frequencies.

Patterns were measured on the 1/50-scale Caribou for each of the four spacings of the configuration shown in Fig. 29. The measured azimuth plane patterns with vertical polarization for a 0.050-in. spacing (1/2 in. at 1/5 scale) are shown in Figs. 33 through 47. The measured results of the other three spacings indicated very little change in radiation coverage. The results presented here indicate fair coverage throughout the whole frequency band with no deep nulls.

The results of this investigation indicate a minimum spacing for the wire element should be at least 2-1/2 in. for the full-scale configuration. Multiple resonance and antiresonance as indicated in the impedance data impose additional requirements on an automatic tuner, particularly in the regions of low resistance and low reactance, commonly referred as the "no tune area." These impedances can be tuned by adding a fixed capacitor in series with the antenna to transform the effective impedance out of the no match area.

Conclusion

This program has been concerned with the design and development of an H-F compact antenna operating over the frequency range of 2 to 30 MHz. Investigations have been concentrated on impedance, pattern, and gain characteristics of various element considerations. The necessary mockups and scaled model aircraft were built to implement the measurement tests. As a result of the investigations, the final selected configuration is a two-turn grounded loop with a maximum external dimension of 2 ft and a weight of 13-3/4 lb.

The basic antenna system is comprised of the antenna and its automatic tuner. The tuner is compatible for interconnection with the 618T H-F transceiver communications equipment. A retransmission mode involves the use of two antennas--an automatic tuner and a tunable filter. This mode will allow simultaneous transmission and reception at a slight separation of frequencies. Two antennas, one Univac automatic tuner and a Collins tunable filter were delivered during this program.

This antenna system is scheduled for a flight test evaluation program at Ft. Monmouth. These tests will entail measurement of in-flight radiation patterns and signal level versus distance throughout the 2 to 30 MHz frequency range. This system is to be tested on both fixed- and rotary-wing aircraft. The choice of aircraft for these tests will depend on their availability.

The preferred location of the antenna is the midtail location for the fixed-wing and the bottom fuselage for the rotary-wing aircraft. An adapter plate may be required between the aircraft skin and antenna baseplate. The aircraft and its antenna location will determine the adapter configuration.

Additional investigations on a low profile 1/5-scale wire antenna have been presented here. It is apparent from the measured results that poor coupling results from close spacing of the wire element of the aircraft skin. The gain results of this configuration are comparable to the two-turn loop. Slight variations of the configuration have shown improvement over portions of the frequency band. The simplicity of this antenna configuration merits further investigation at full-scale frequencies.

It is apparent from the measured results of relative gain versus frequency that there is relation to the aircraft physical dimension with the maximum gain indications. Thus it would be expected that the gain maxima will be influenced by the particular aircraft on which it is installed.

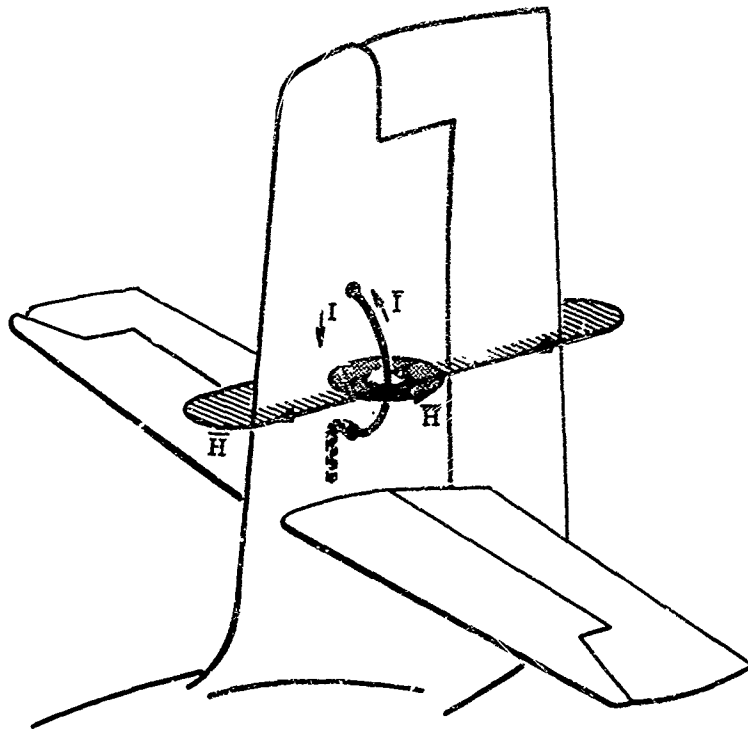


Fig. 1. Outboard Grounded Loop Feed Element on Vertical Stabilizer



Fig. 2. 1/5-Scale 4-Turn Loop

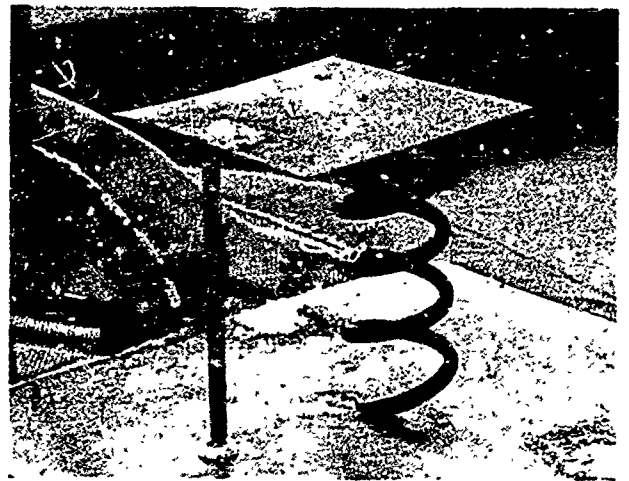


Fig. 3. 1/5-Scale Cap-Coil



Fig. 4. 1/5-Scale Submerged Coil

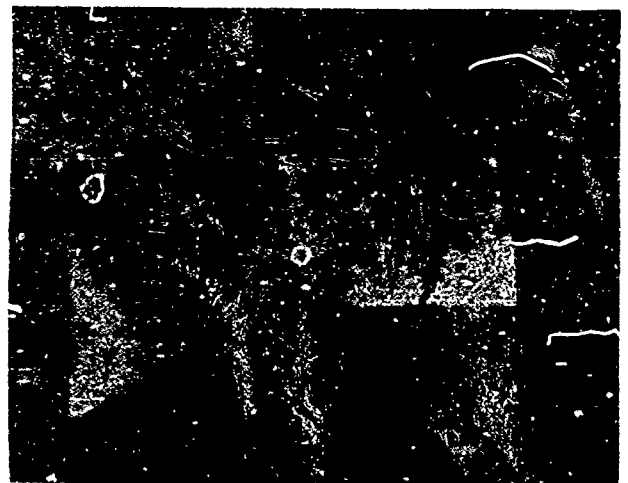


Fig. 5. Full-Scale Outboard Patch



Fig. 6. 1/5-Scale 2-Turn Loop

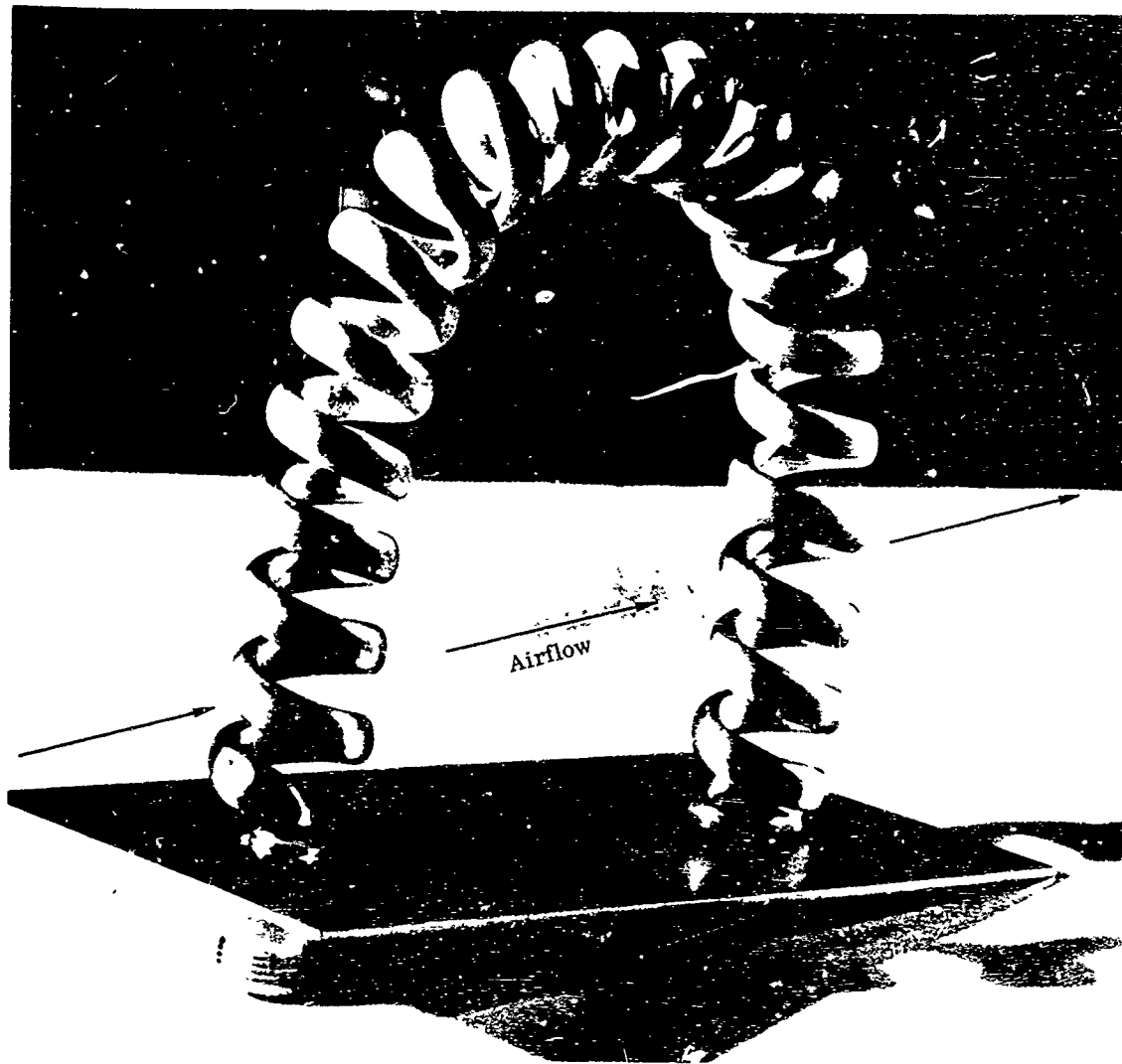


Fig. 7. 1/5-Scale Multitrans Coil Loop Antenna

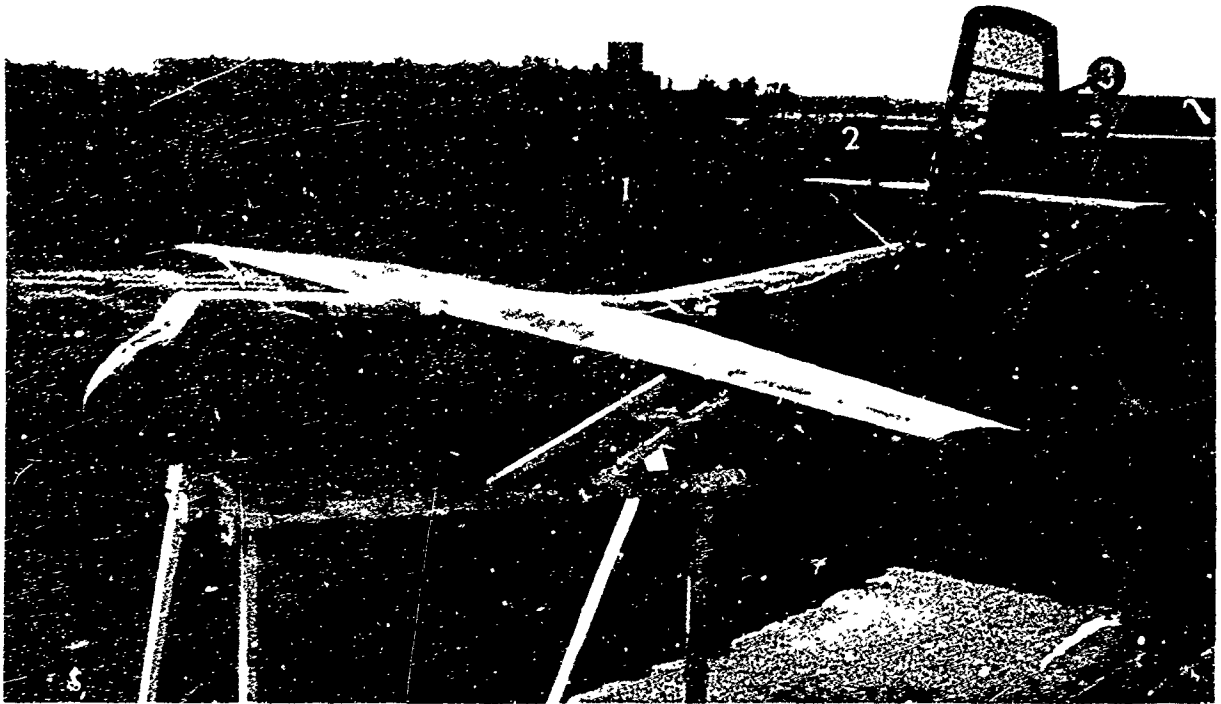


Fig. 8. 1/5-Scale Caribou Impedance Model

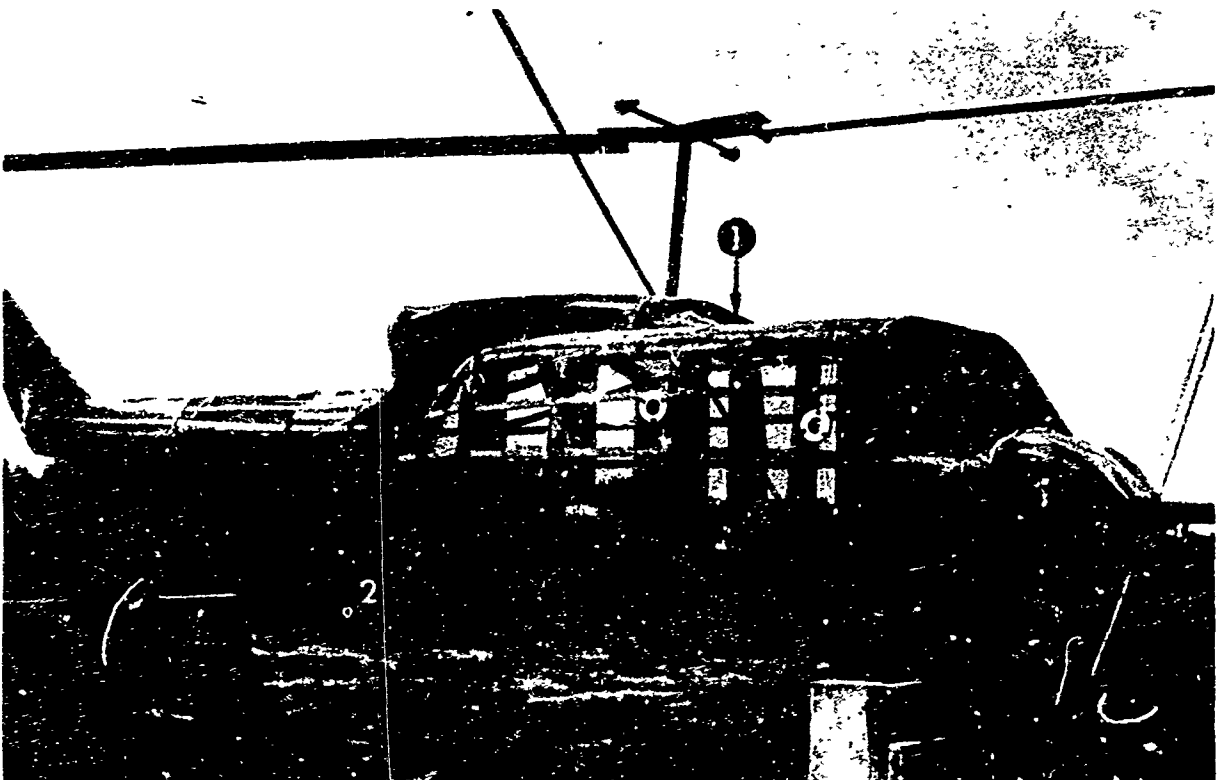
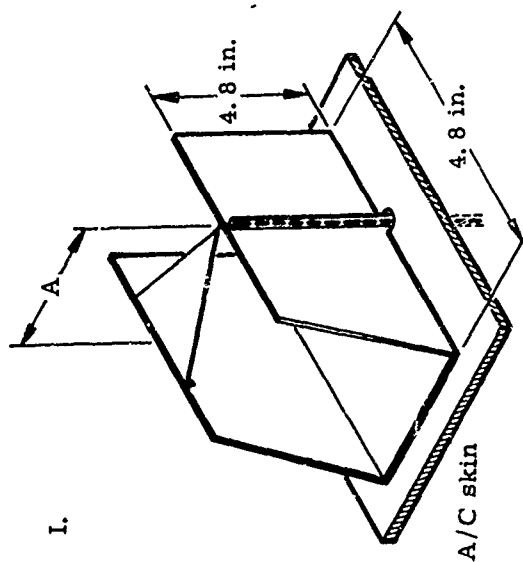
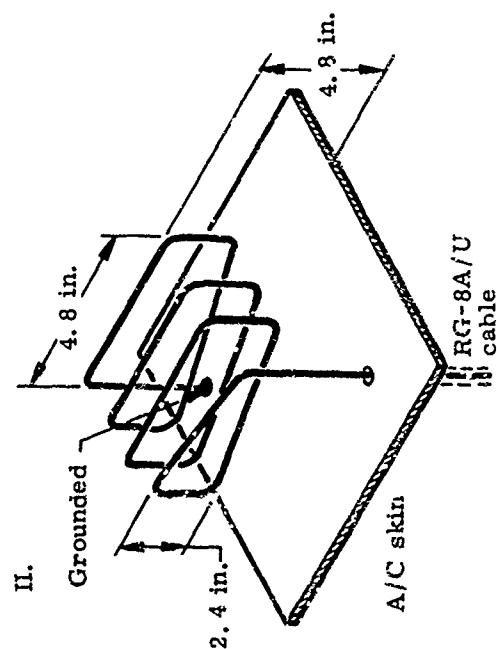


Fig. 9. 1/5-Scale Iroquois Impedance Model



Capacity Required for Tuning

1/5 Scale		
Frequency (MHz)	Dimension A (in.)	Tuning Capacity Required (pf)
(a) 10	4.8	1,410
(b) 10	2.4	2,360
Full-Scale Equivalent		
2	24	7,050
2	12	11,800



1/5 Scale			Full-Scale Equivalent	
Frequency (MHz)	Tuning Capacity Required (pf)	Frequency (MHz)	Tuning Capacity Required (pf)	
(c) 1-Turn Loop				
10	760	2	3800	
(d) 2-Turn Loop				
10	374	2	1870	
(e) 3-Turn Loop				
10	219	2	1095	

Fig. 10. Preliminary Element Configurations and Reactance Parameter Tuning Requirement

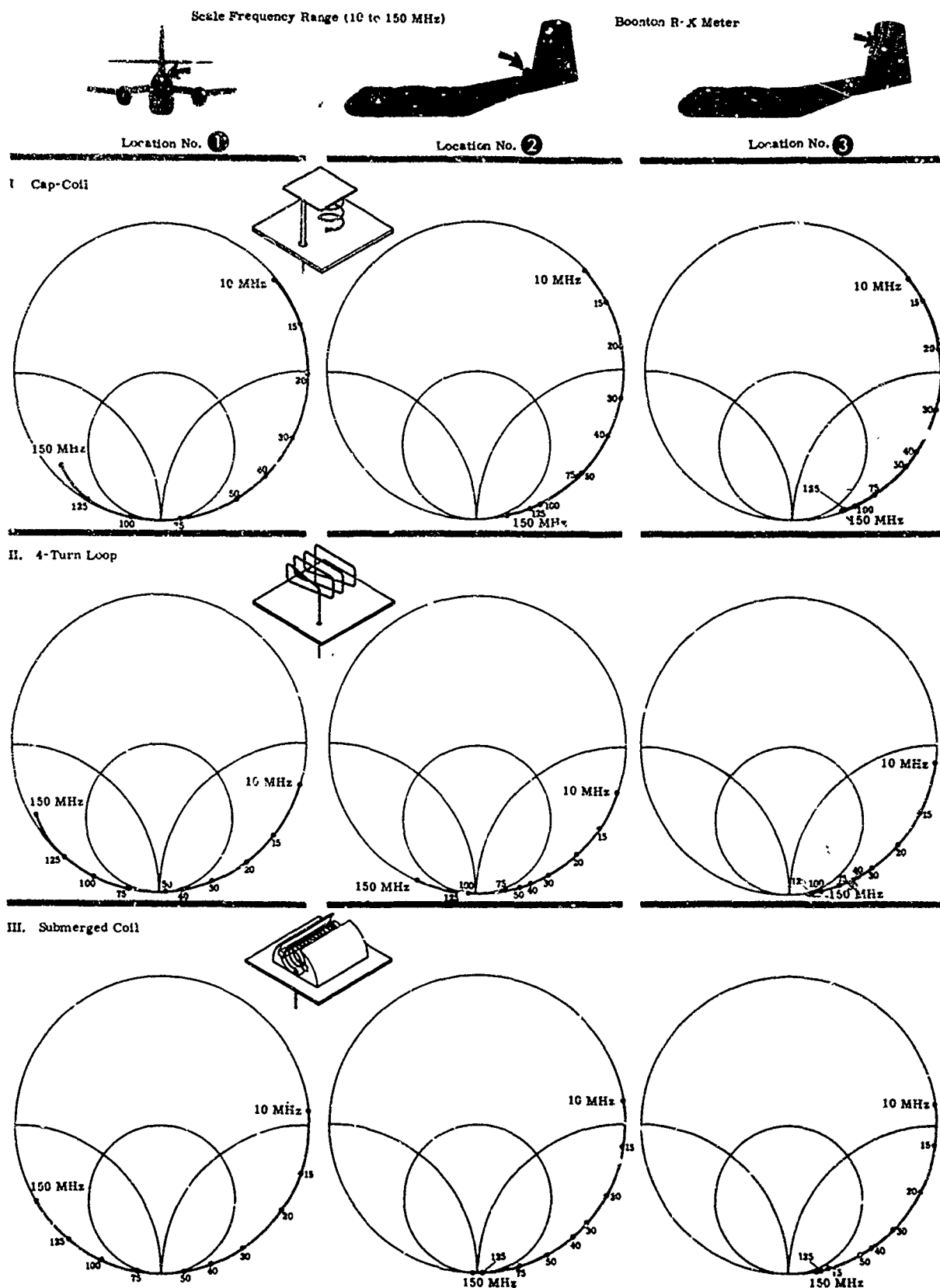


Fig. 11. H-F Antenna Element Impedance Characteristics, 1/5-Scale Caribou

Frequency (MHz)	R (Ω)	X (Ω)
10	0.146	+71
15	0.156	+108
20	0.303	+158
30	0.778	+292
40	2.93	+593
50	1.1	+2650
75	2.39	-489
100	1.82	-235
125	2.20	-149
150	6.98	-93

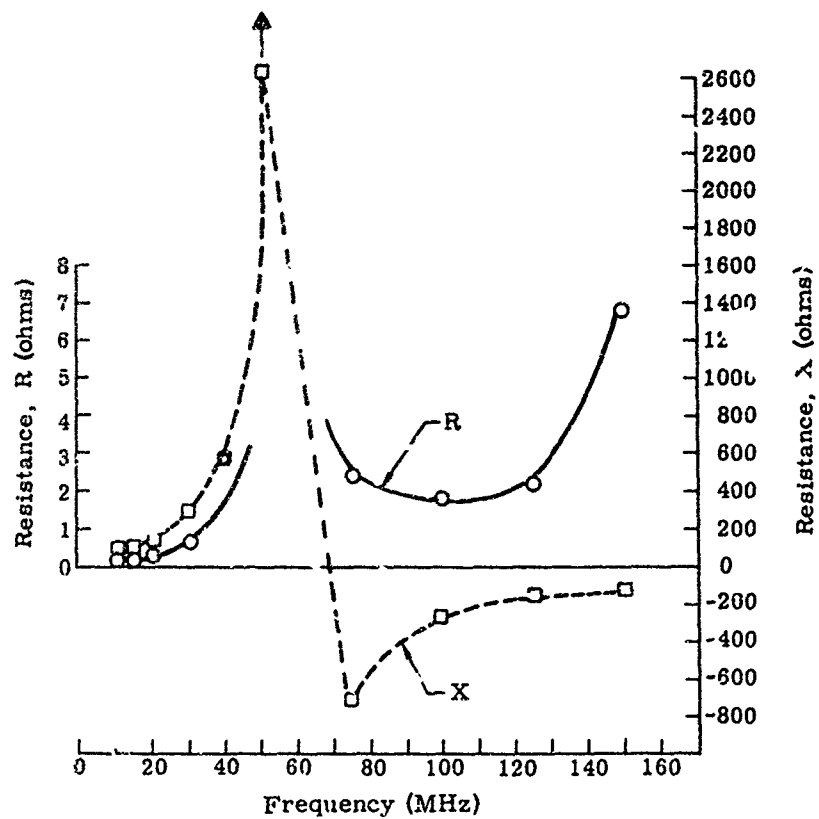


Fig. 12. R and X Components, 4-Turn Loop at Locator 1 on 1/5-Scale Caribou

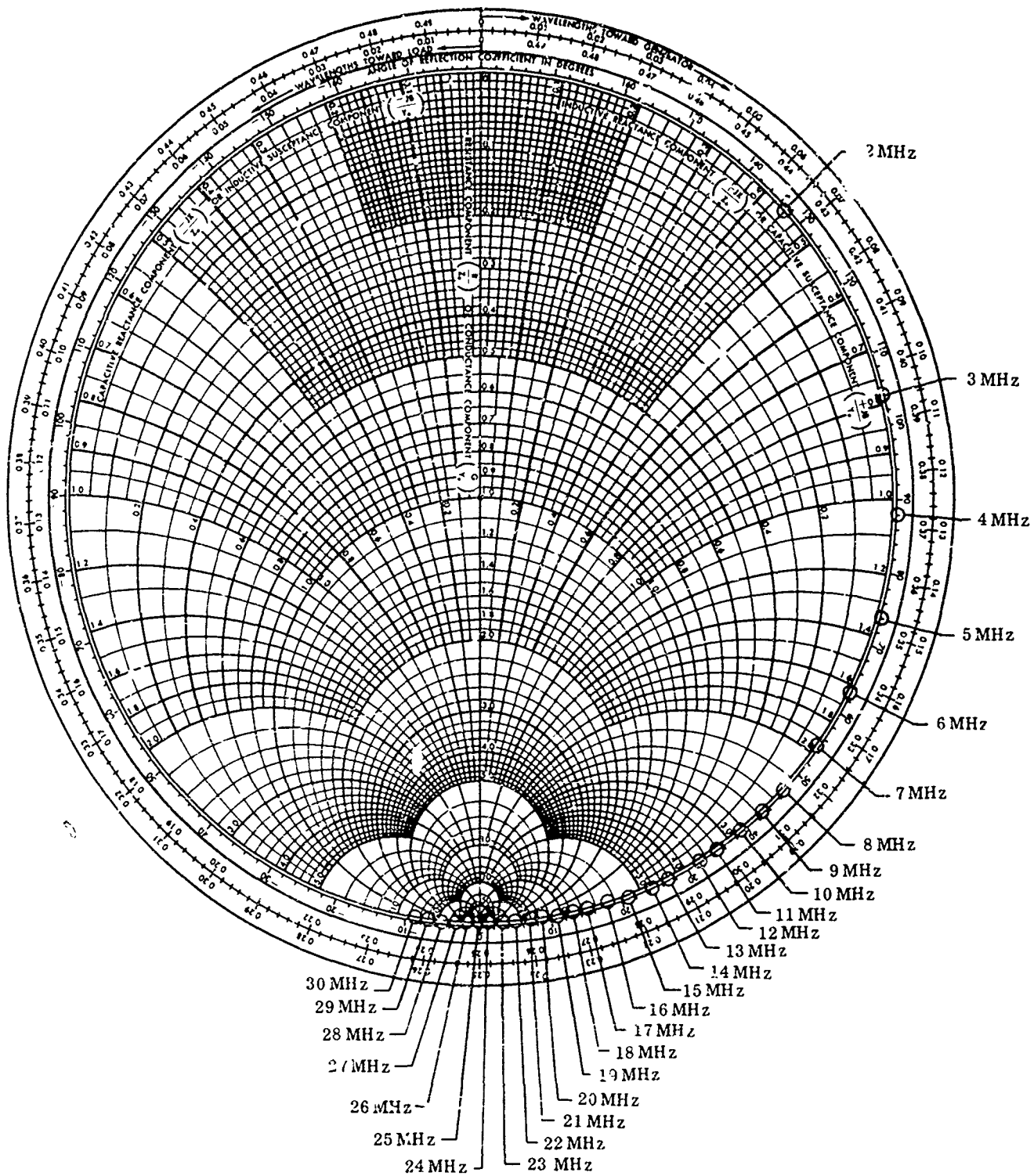


Fig. 13. Typical Full-Scale 2-Turn Loop Reactance Characteristics with Antennae Mounted on a Metal Building

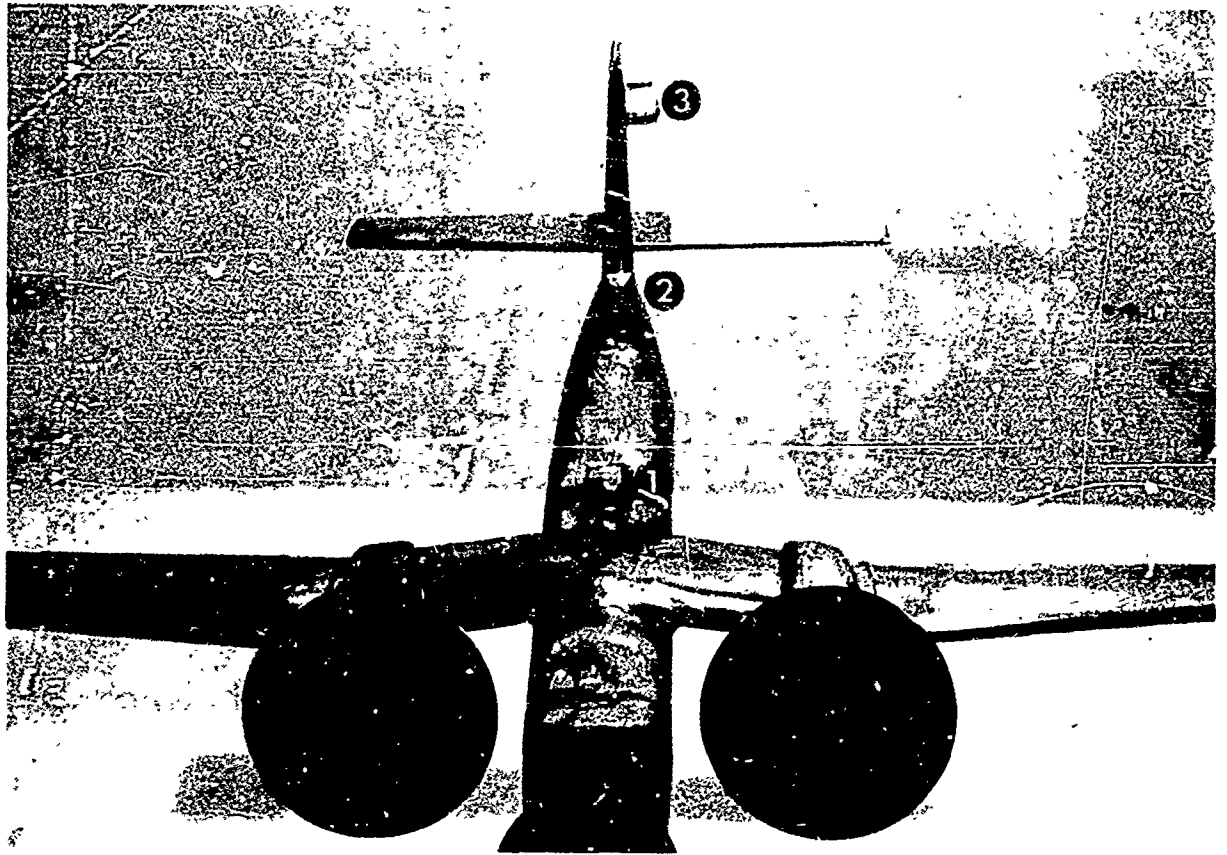


Fig. 14. 1/50-Scale Caribou Pattern Model

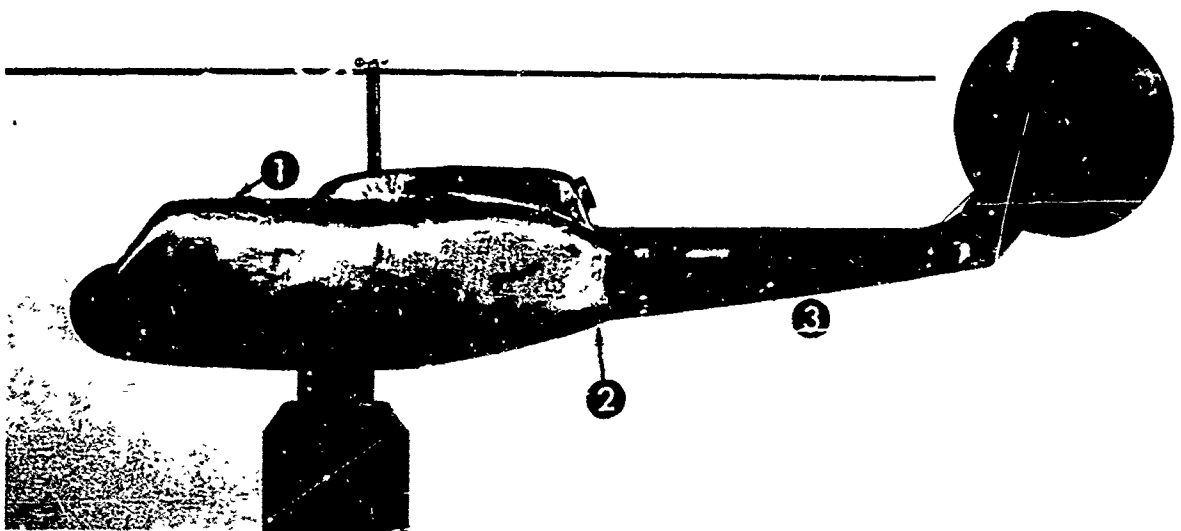


Fig. 15. 1/25-Scale Iroquois Pattern Model

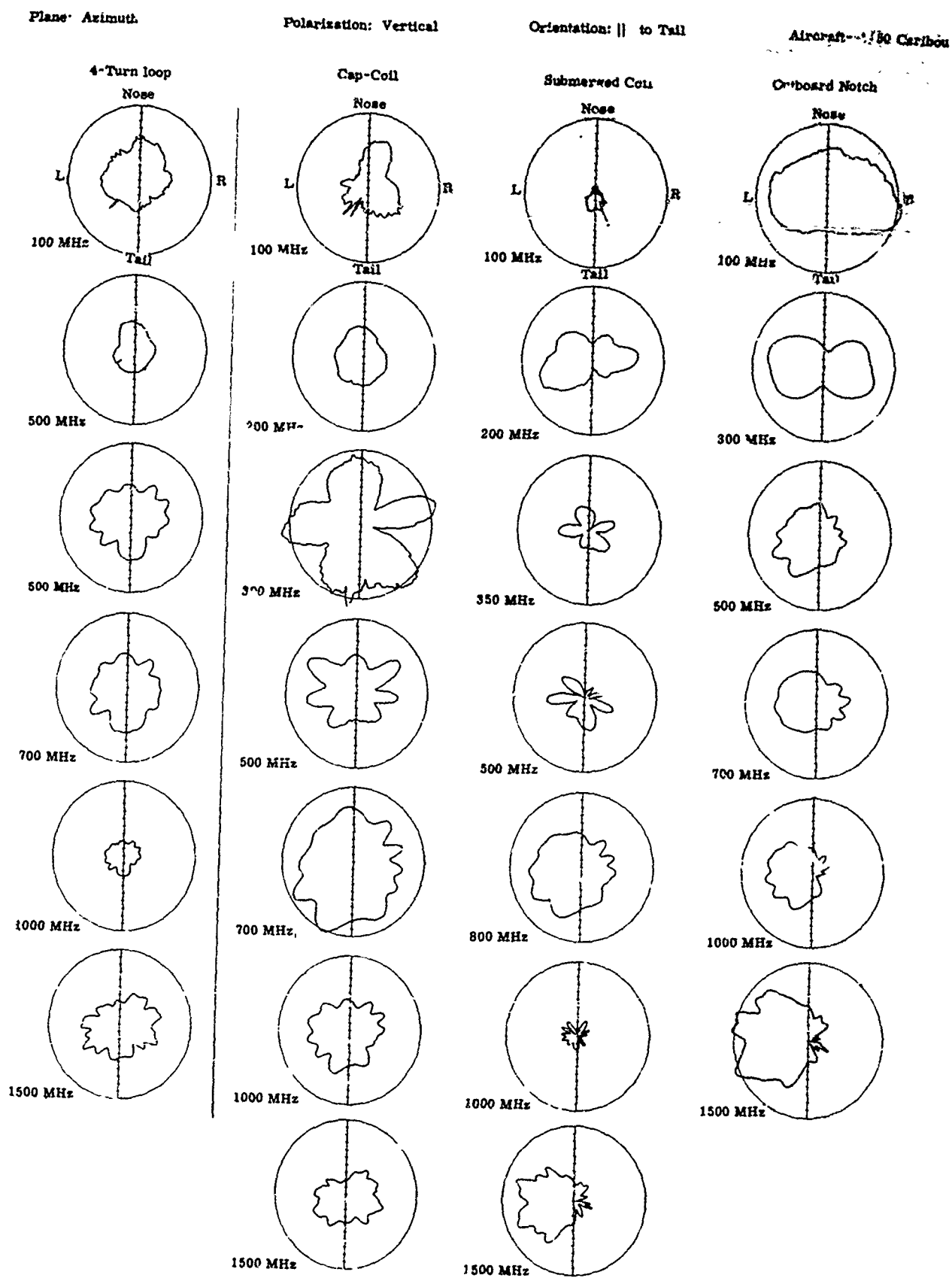


Fig. 16. H-F Antenna Element Patterns, 1/50-Scale Caribou, Location No. 3

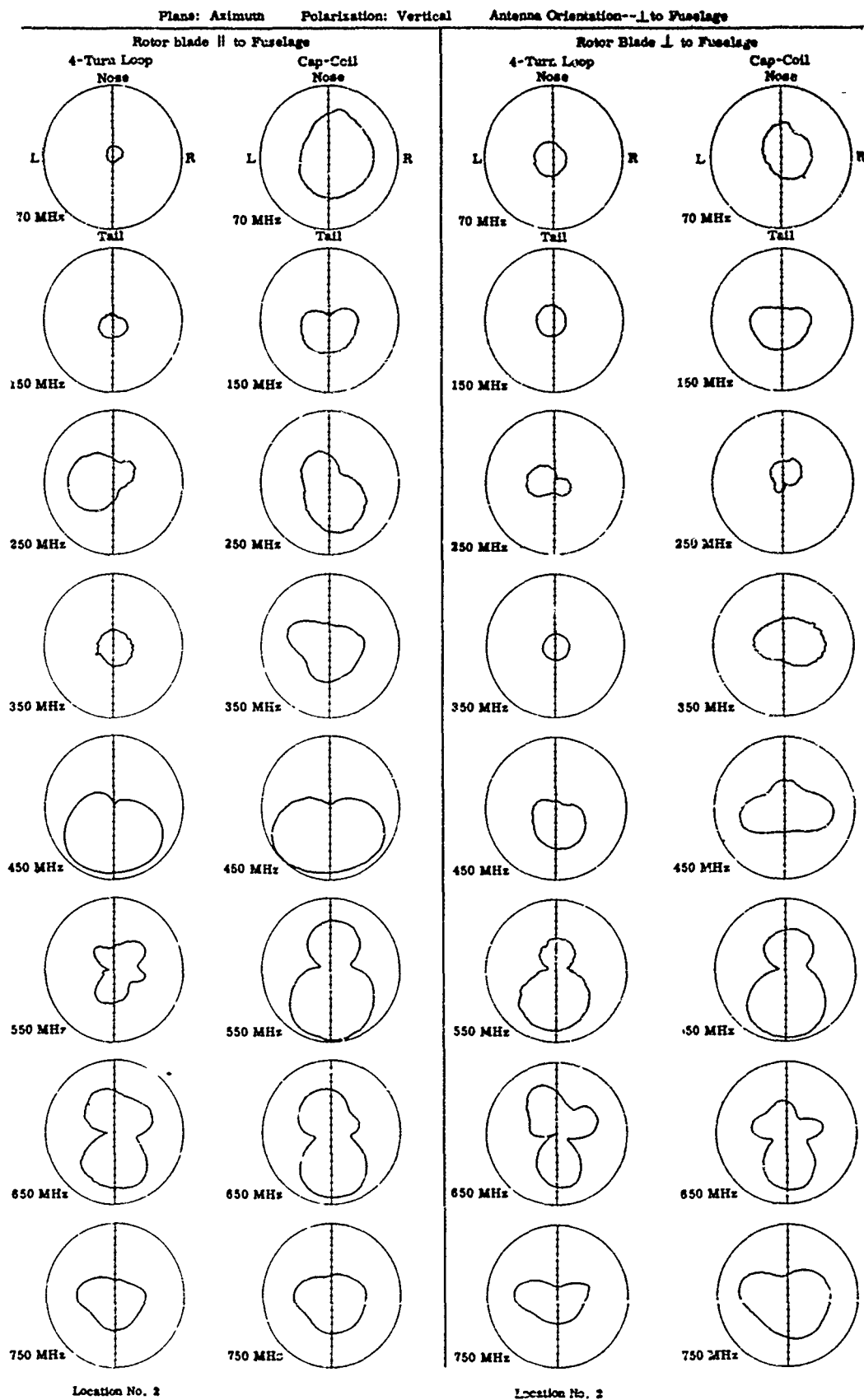


Fig. 17. H-F Antenna Element Patterns, 1/25-Scale Iroquois, Location No. 2

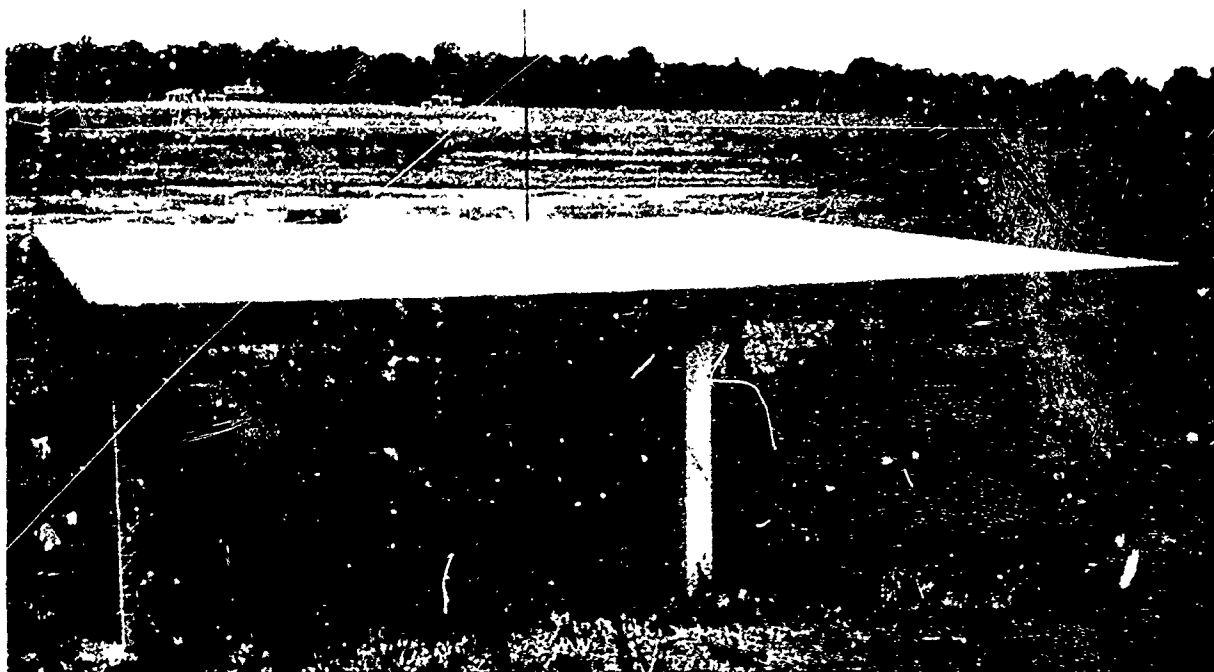


Fig. 18. 3-ft Monopole and 12- x 12-ft Ground Plane

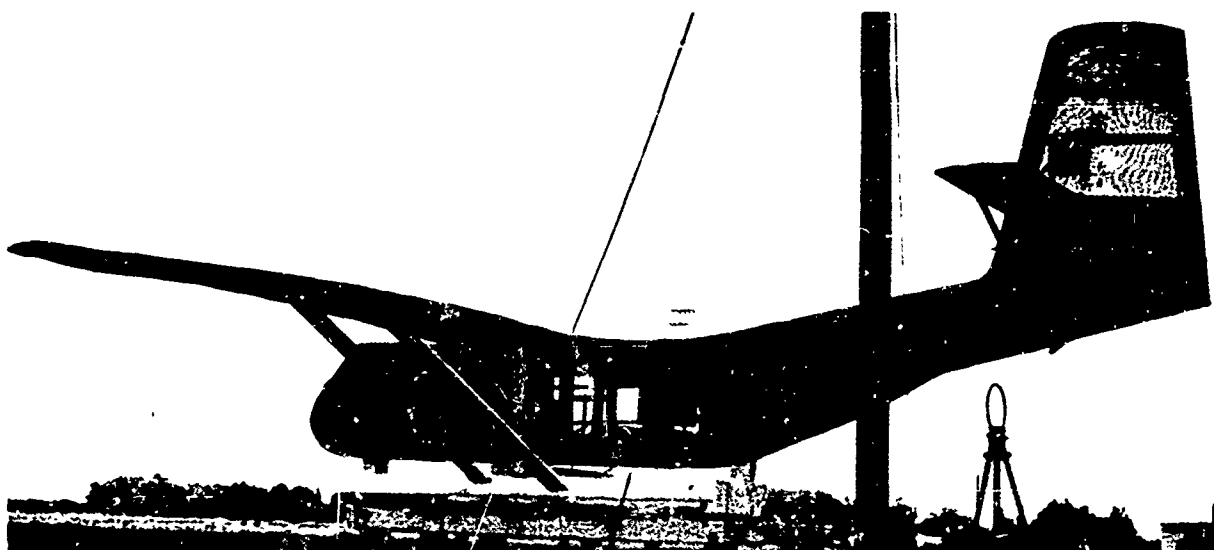


Fig. 19. 1/5-Scale Caribou on Turntable Support

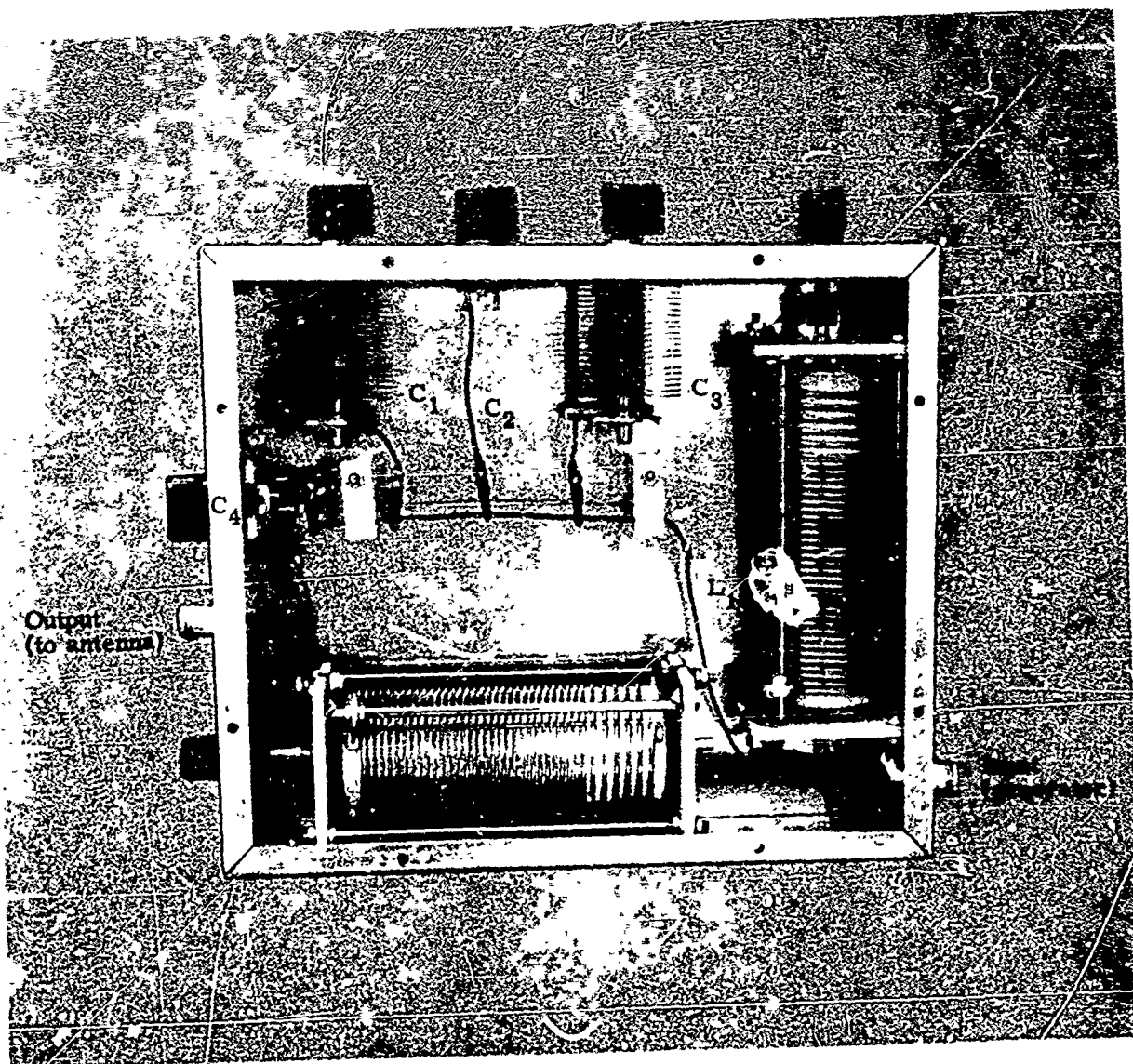
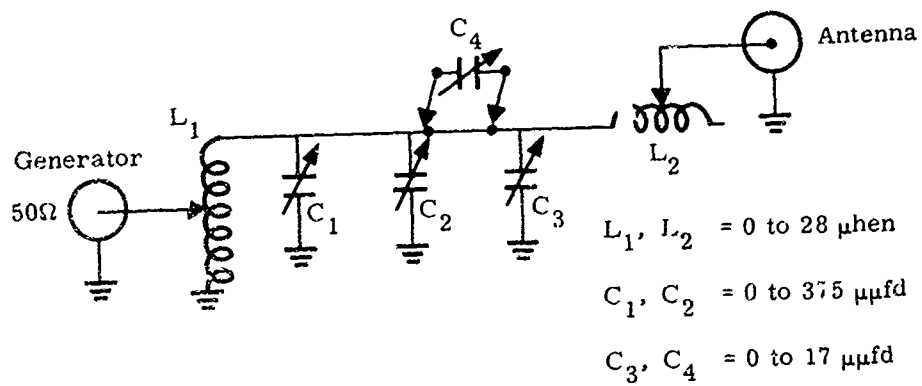


Fig. 20. Manual Tuner for 1/5-Scale HF Antenna and 3-ft Monopole

1/5-scale 4-turn loop
2 orientations, location No. 1
1/5 Caribæu

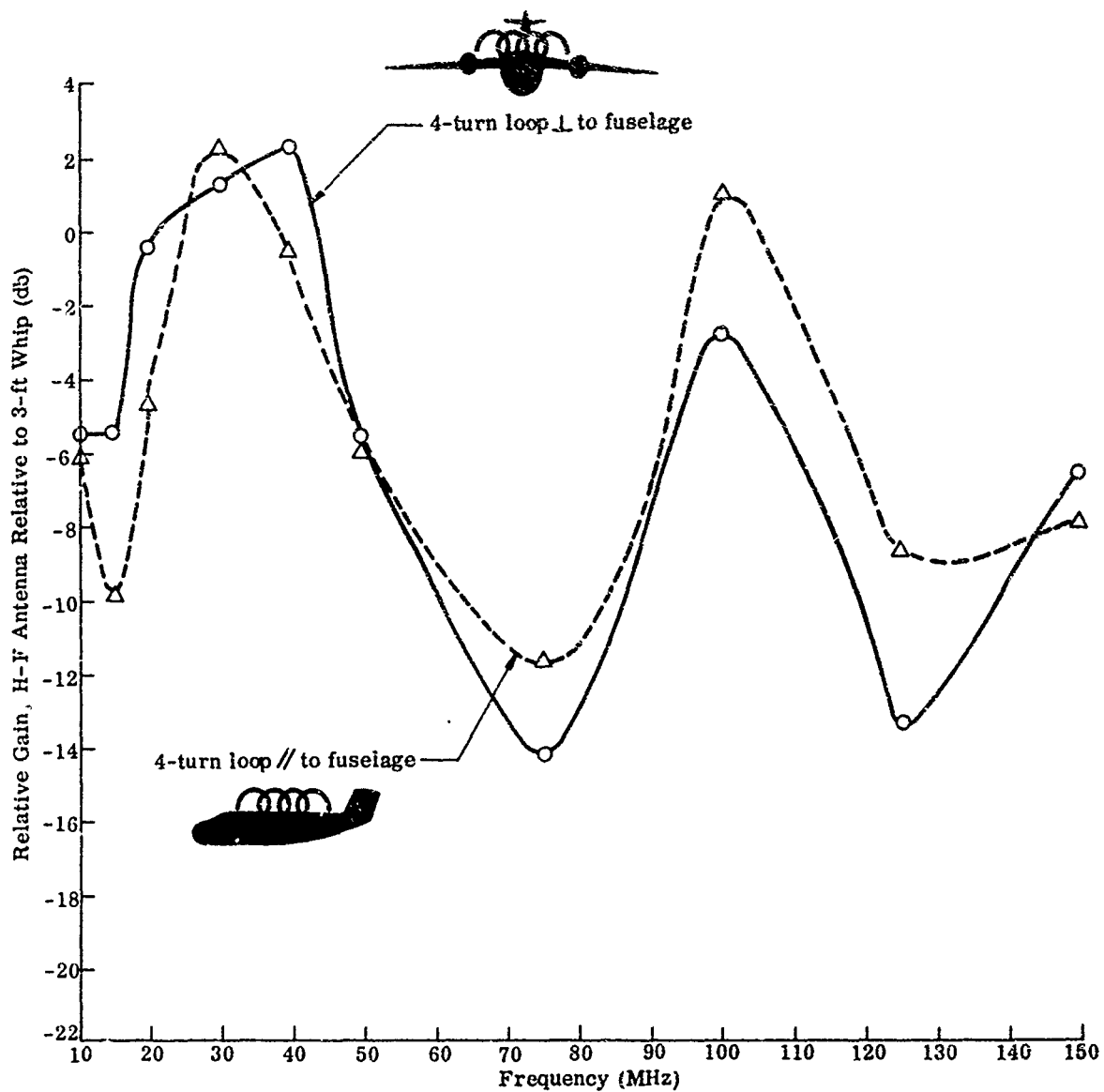


Fig. 21. Relative Gain (4-turn loop/3-ft whip) Versus Torquing

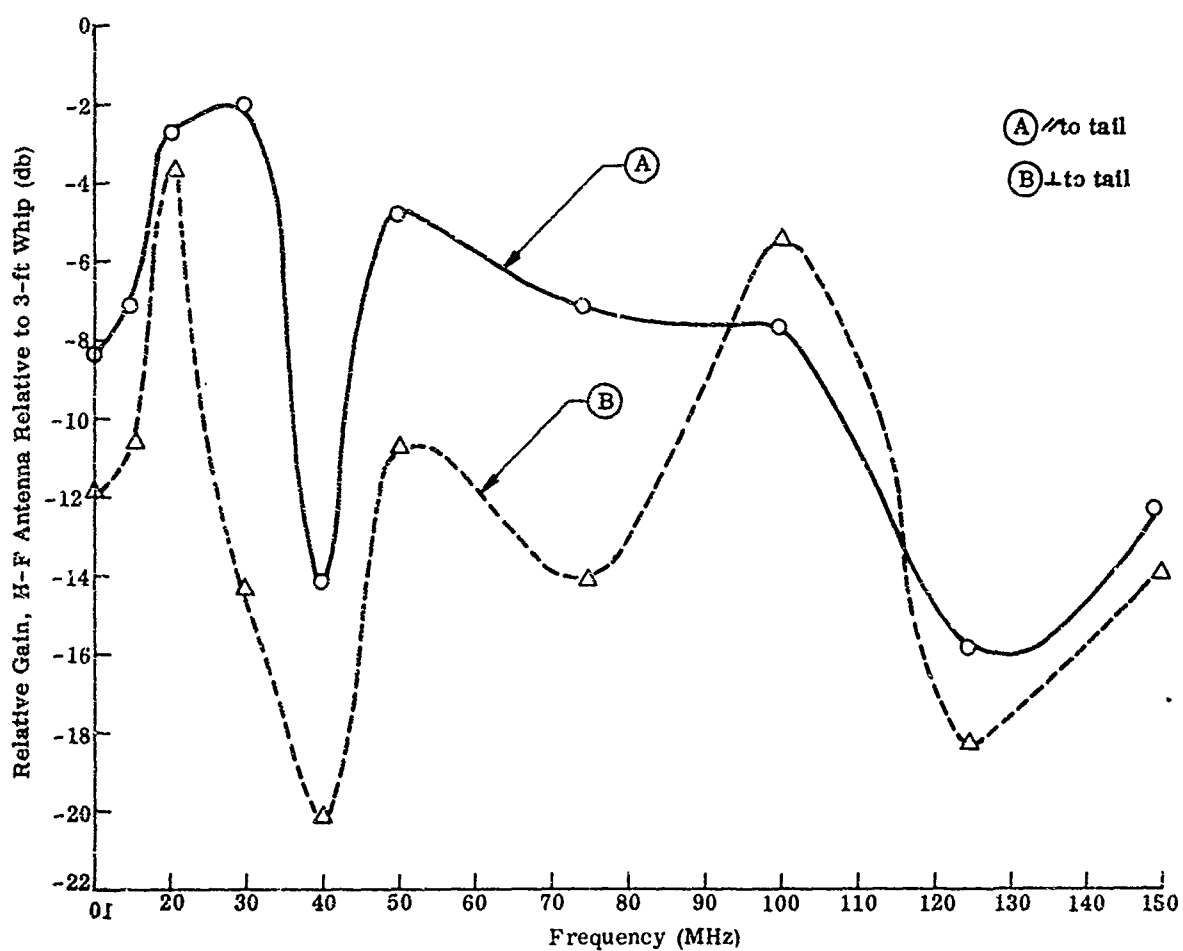
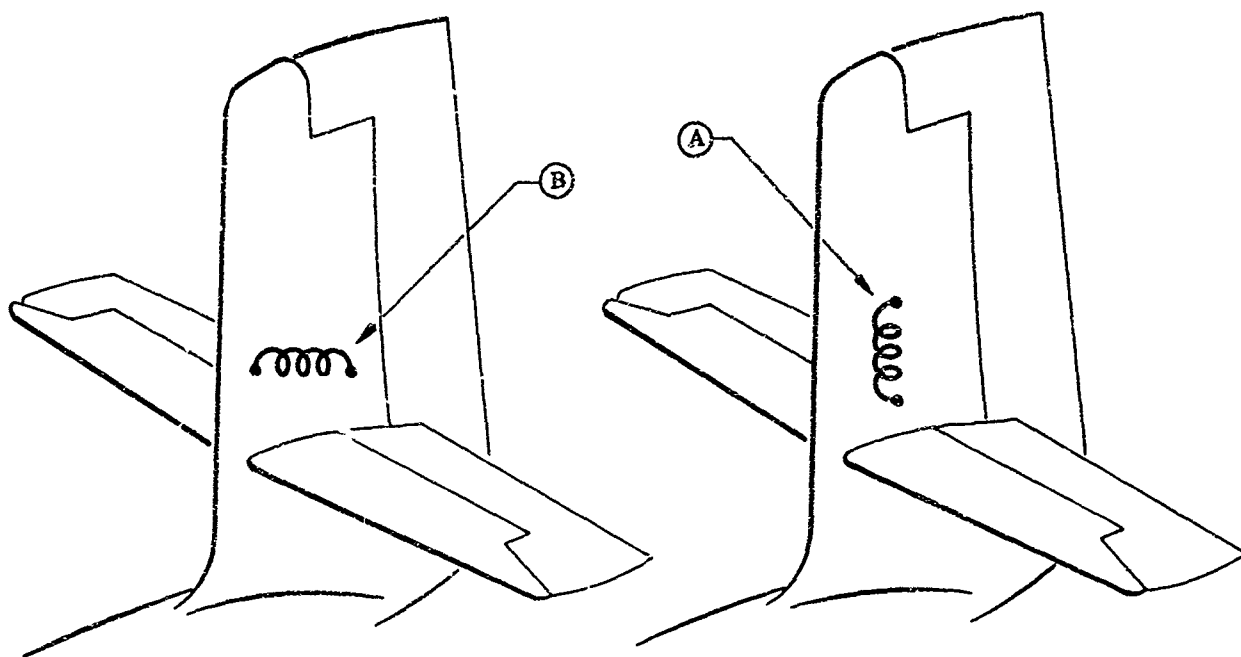
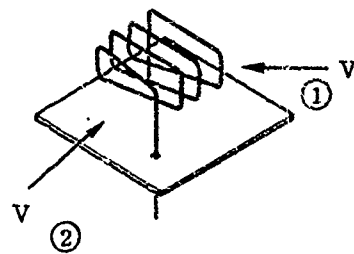


Fig. 22. Relative Gain (4-turn loop/3-ft whip) Versus Frequency for Two Orientations on Tail of 1/5-Scale Caribou

I. 4-Turn Loop

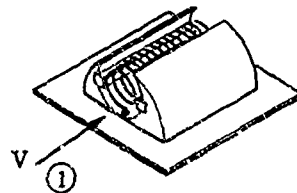


Case

$$\textcircled{1} \quad D = 0.837 \frac{V^2}{295} \text{ lb}$$

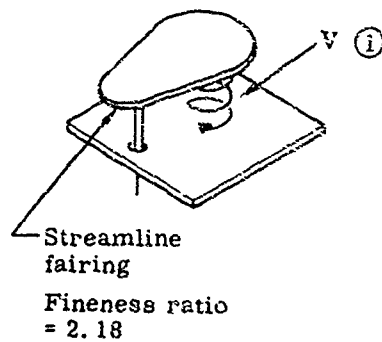
$$\textcircled{2} \quad D = 0.562 \frac{V^2}{295} \text{ lb}$$

II. Submerged Coil



$$\textcircled{1} \quad D = 2.13 \frac{V^2}{295} \text{ lb}$$

III. Cap-Coil



$$\textcircled{1} \quad D = 1.045 \frac{V^2}{295} \text{ lb}$$

where V is in knots

Fig. 23. Drag Versus Antenna Configuration

1/5-scale 4-turn loop mounted across fuselage, location No. 1
on 1/5-scale Caribou

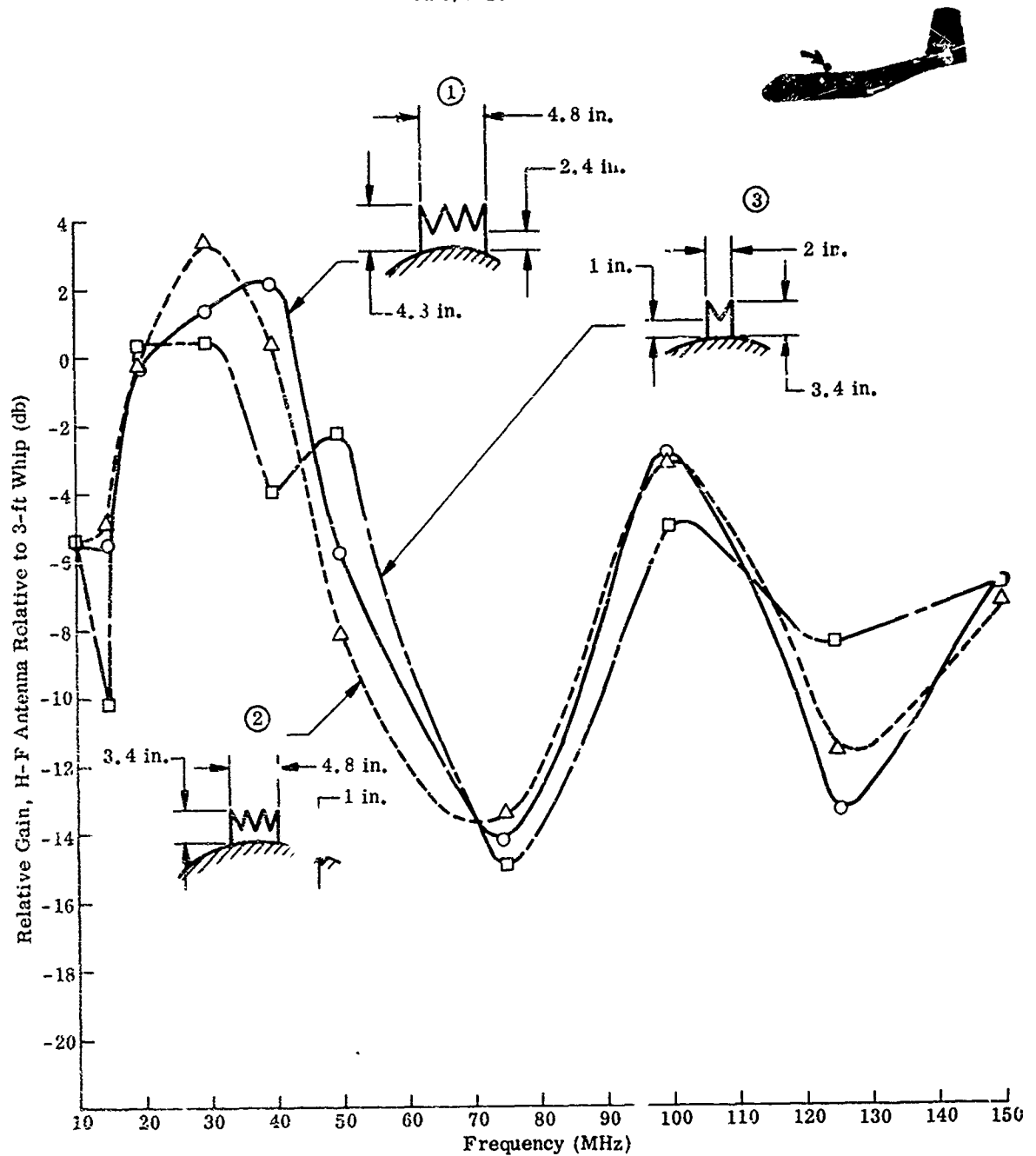


Fig. 24. Relative Gain (2- and 4-turn loop/2-ft whip) Versus Frequency as a Function of Size

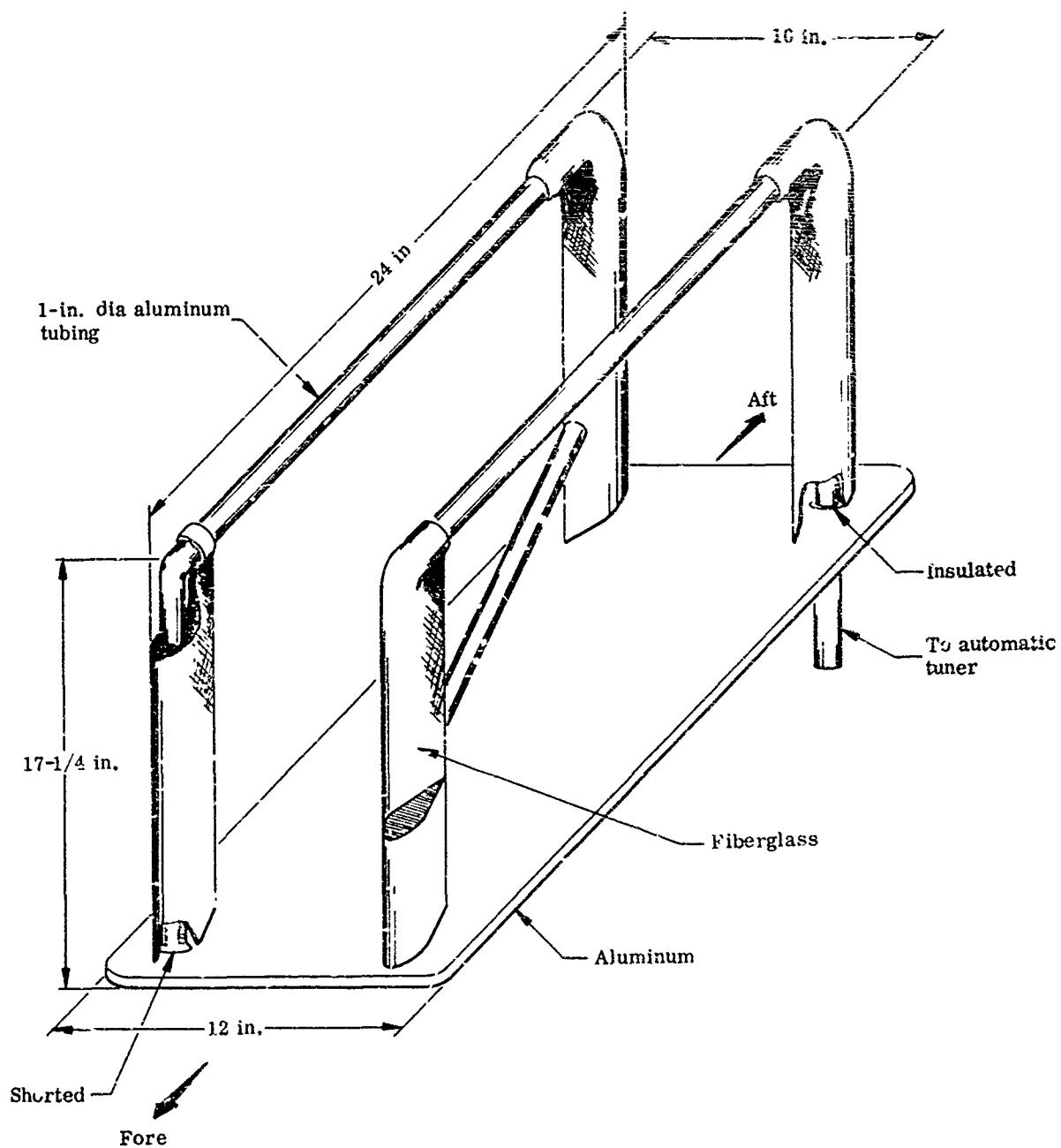


Fig. 25. Full-Scale H-F Compact Antenna

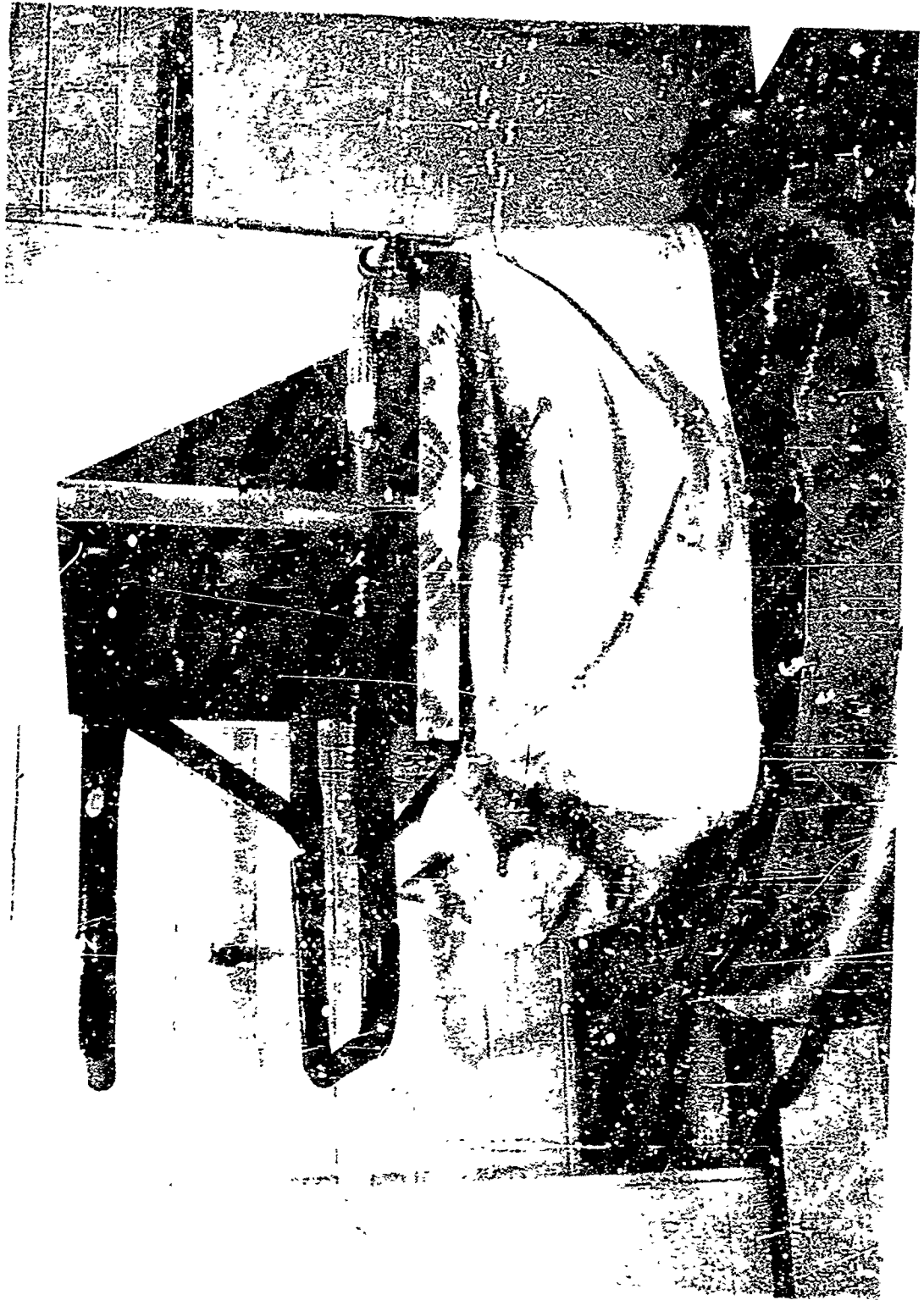


Fig. 26. Tes Unit Antenna (lateral plane)

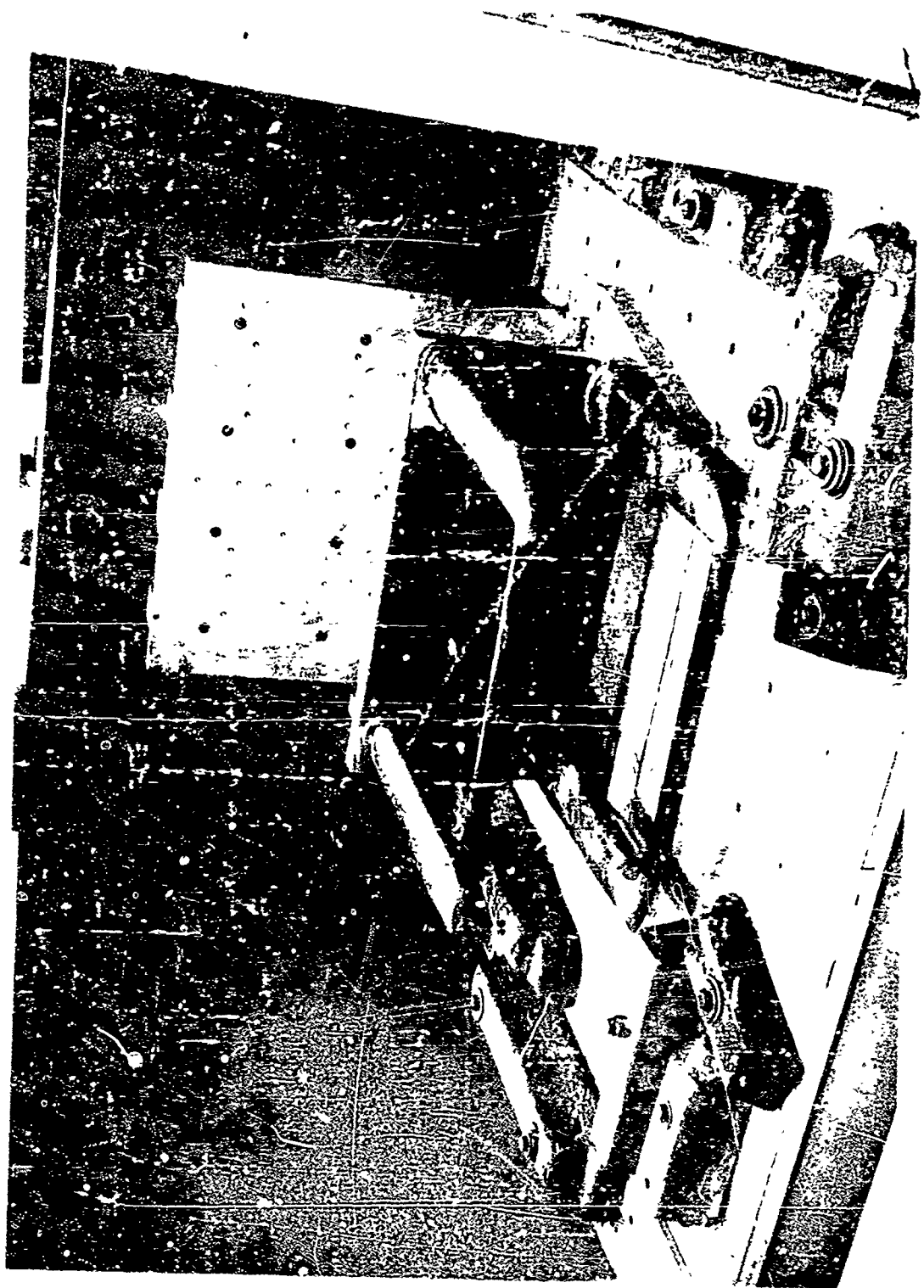


Fig. 27. Test Unit Antenna (modified)

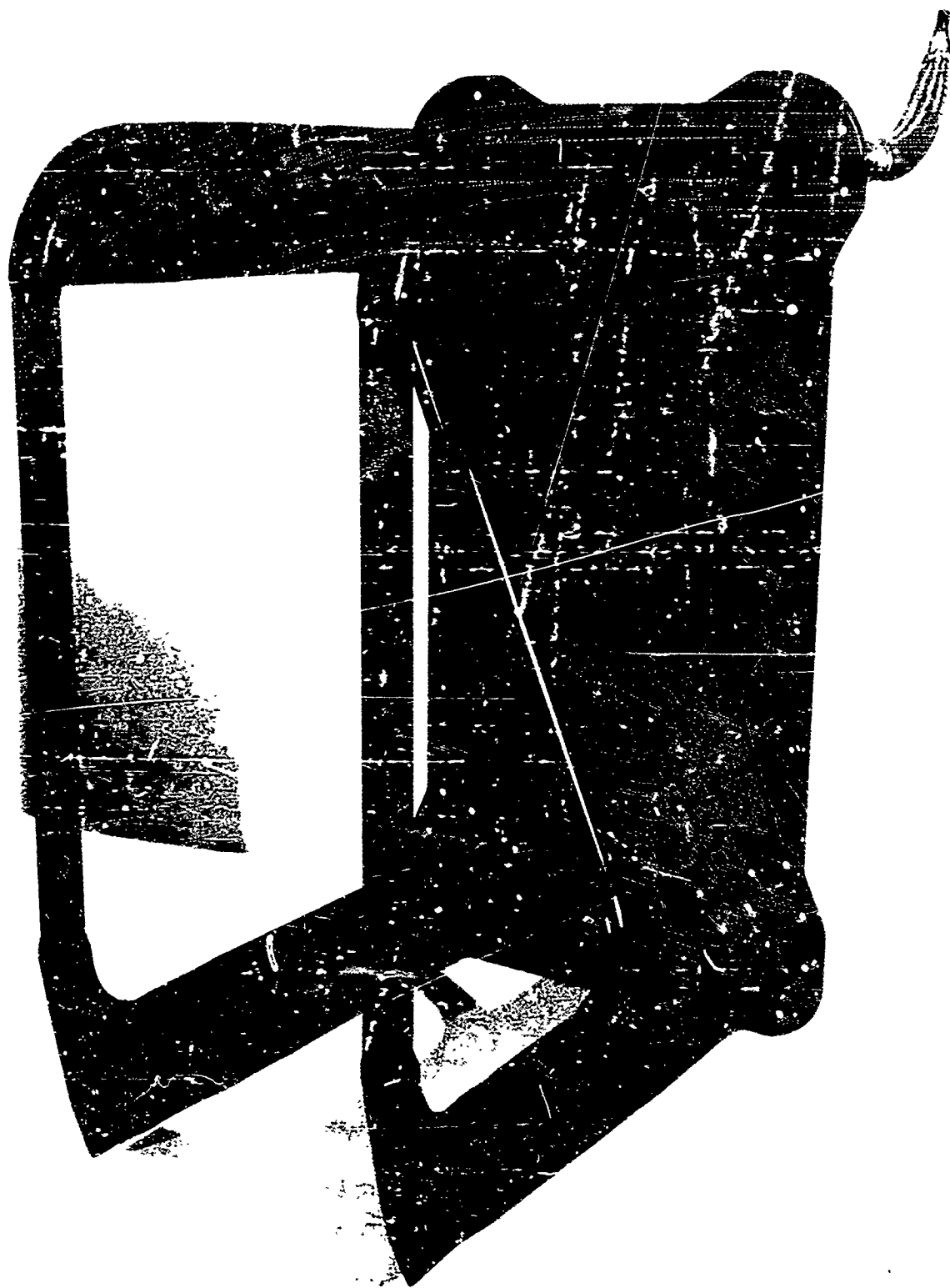


Fig. 28. H-F Antenna (Final Model)

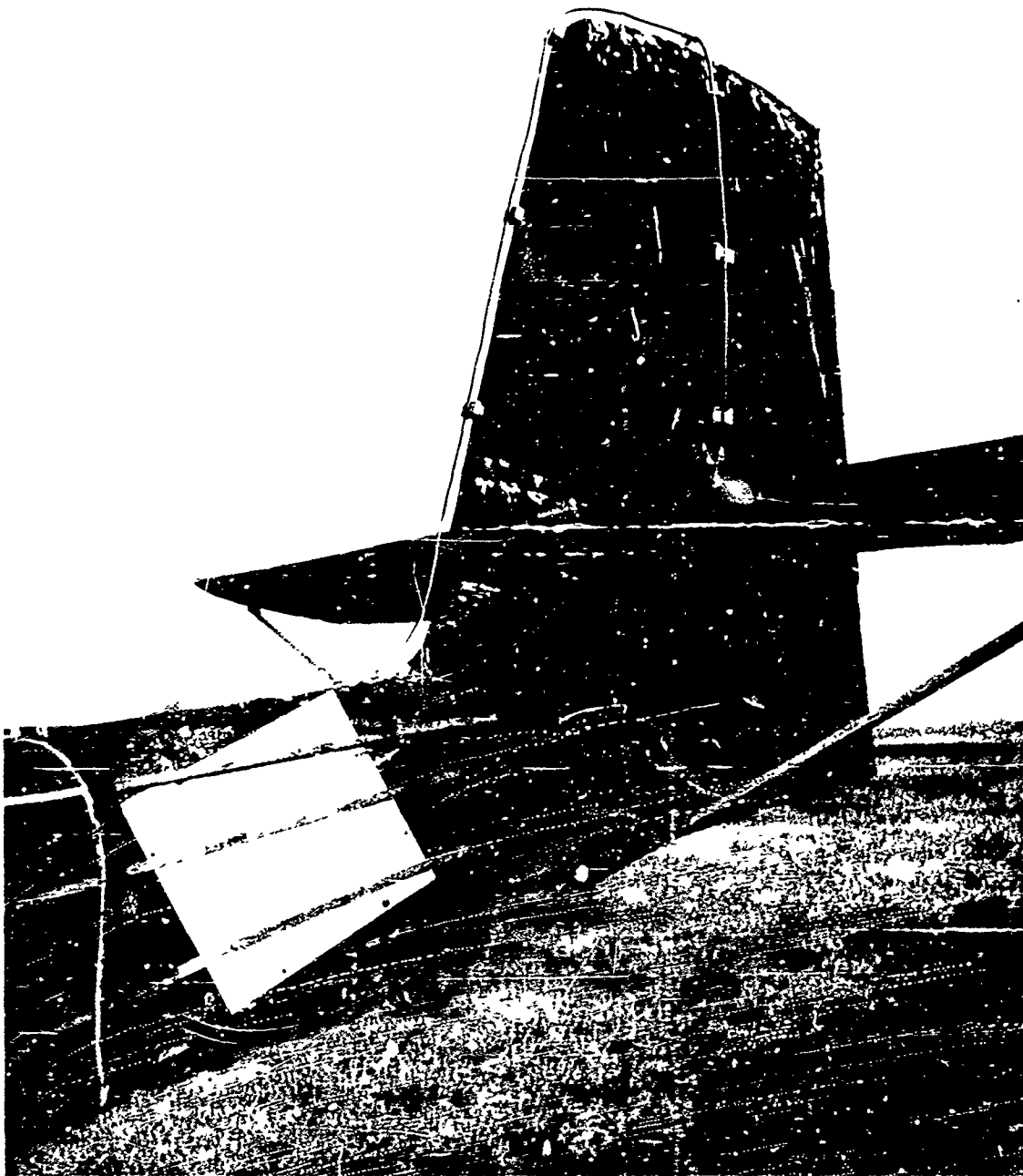


Fig. 29. Low Profile H-F Antenna

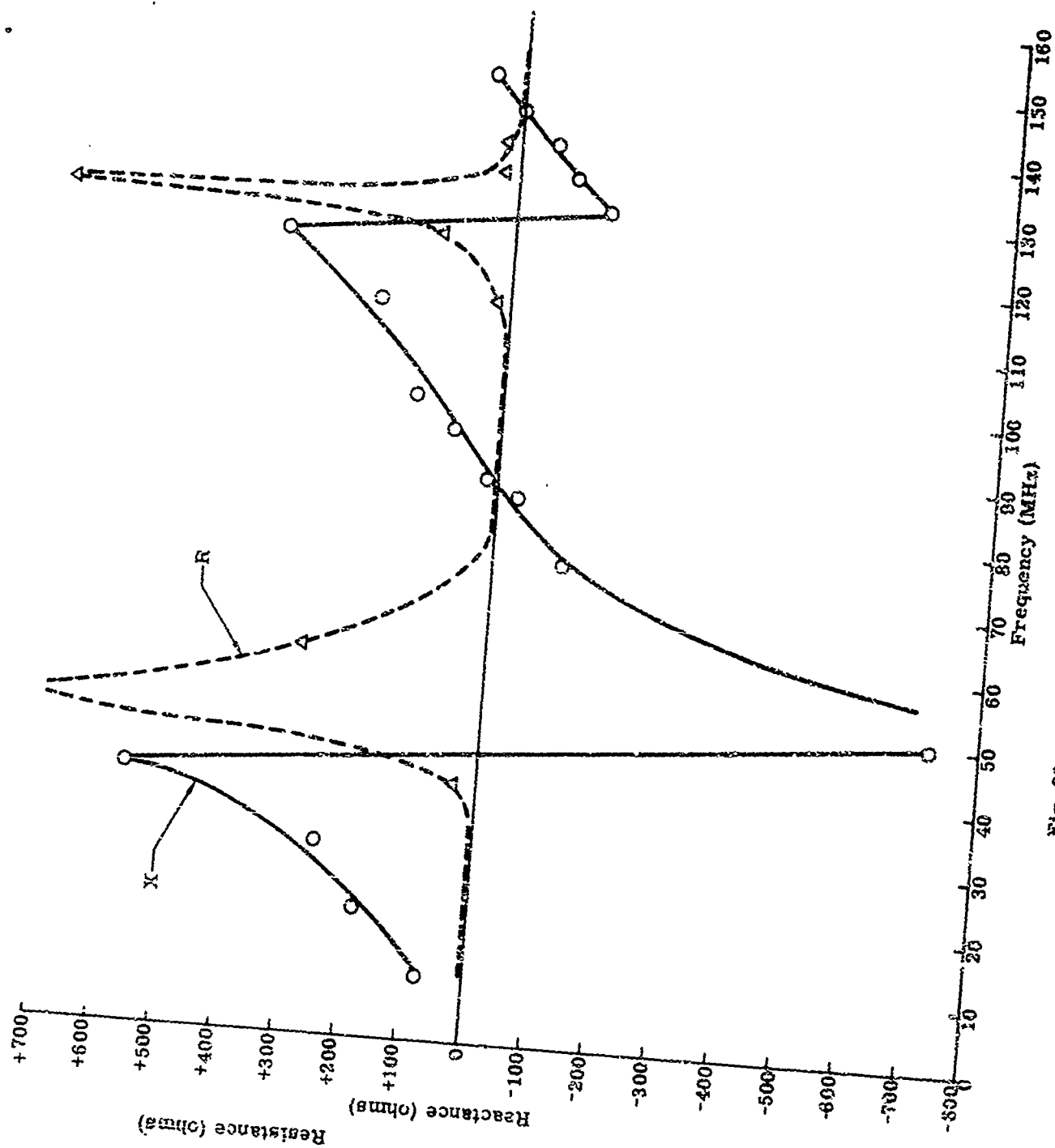


Fig. 30. Low Profile Antenna Impedances

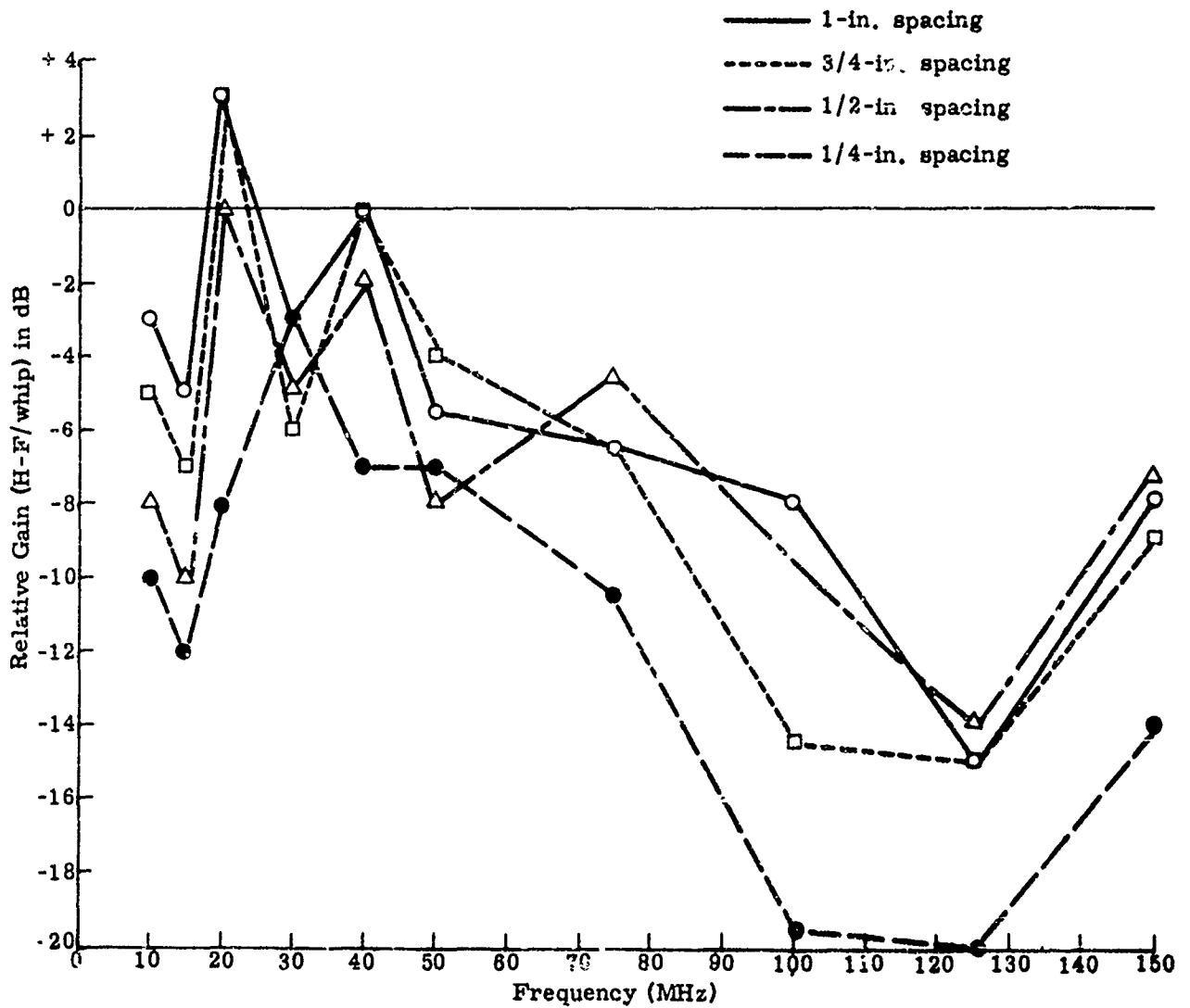
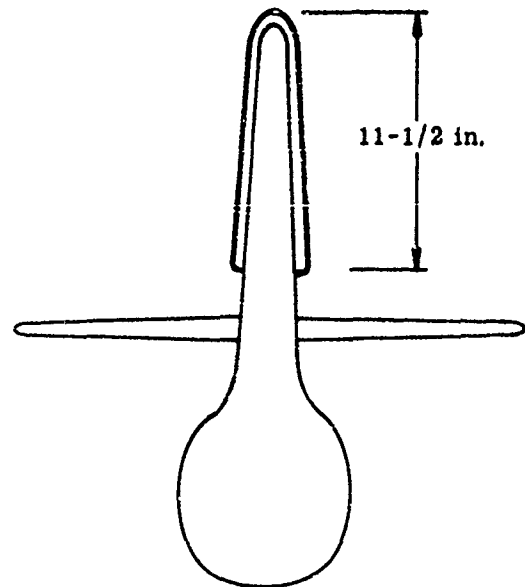
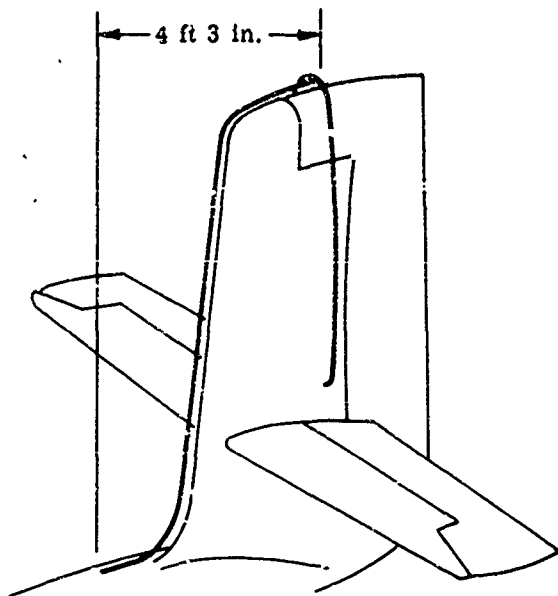


Fig. 31. Low Profile Gain

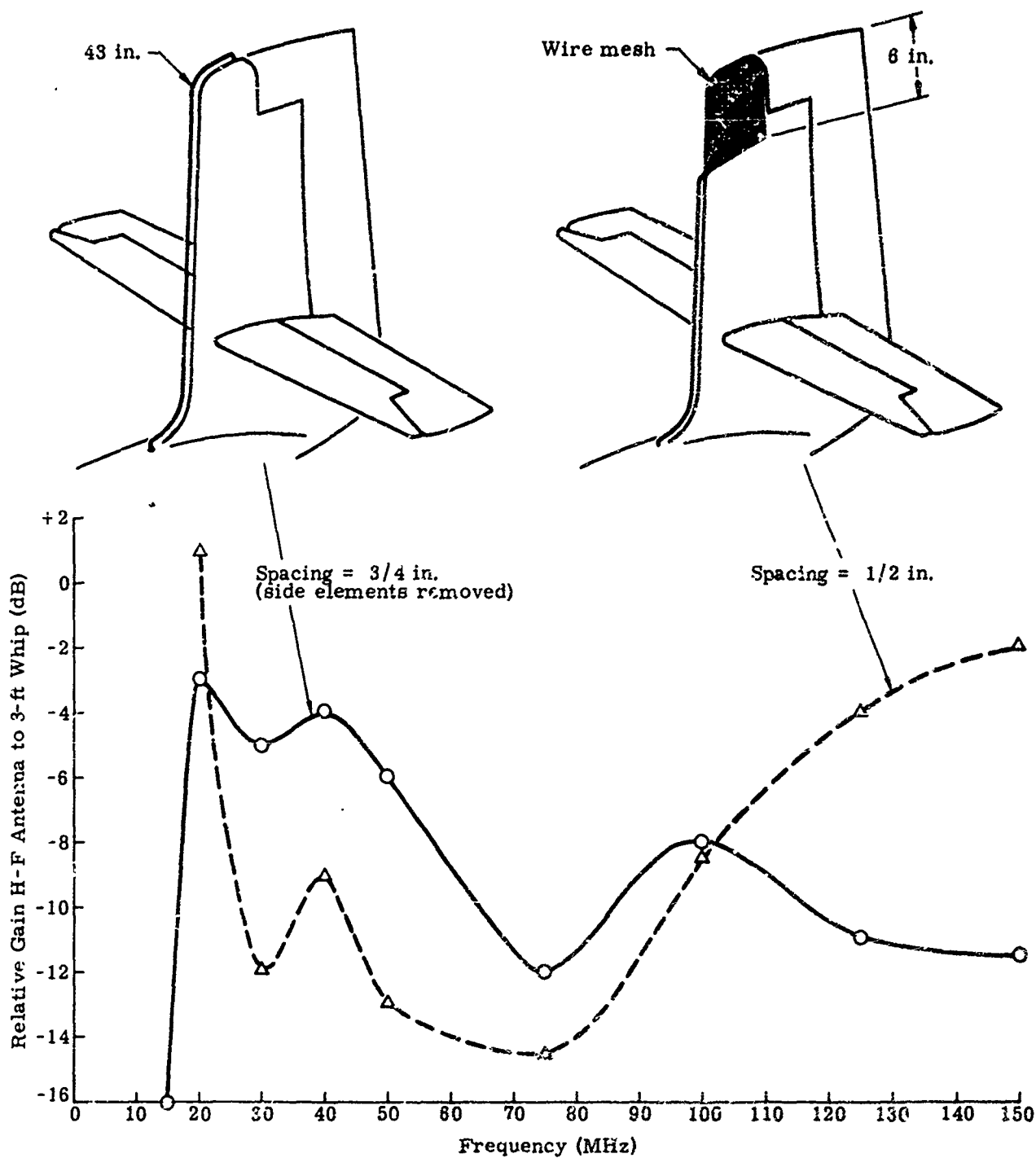


Fig. 32. Low Profile Gain Continued

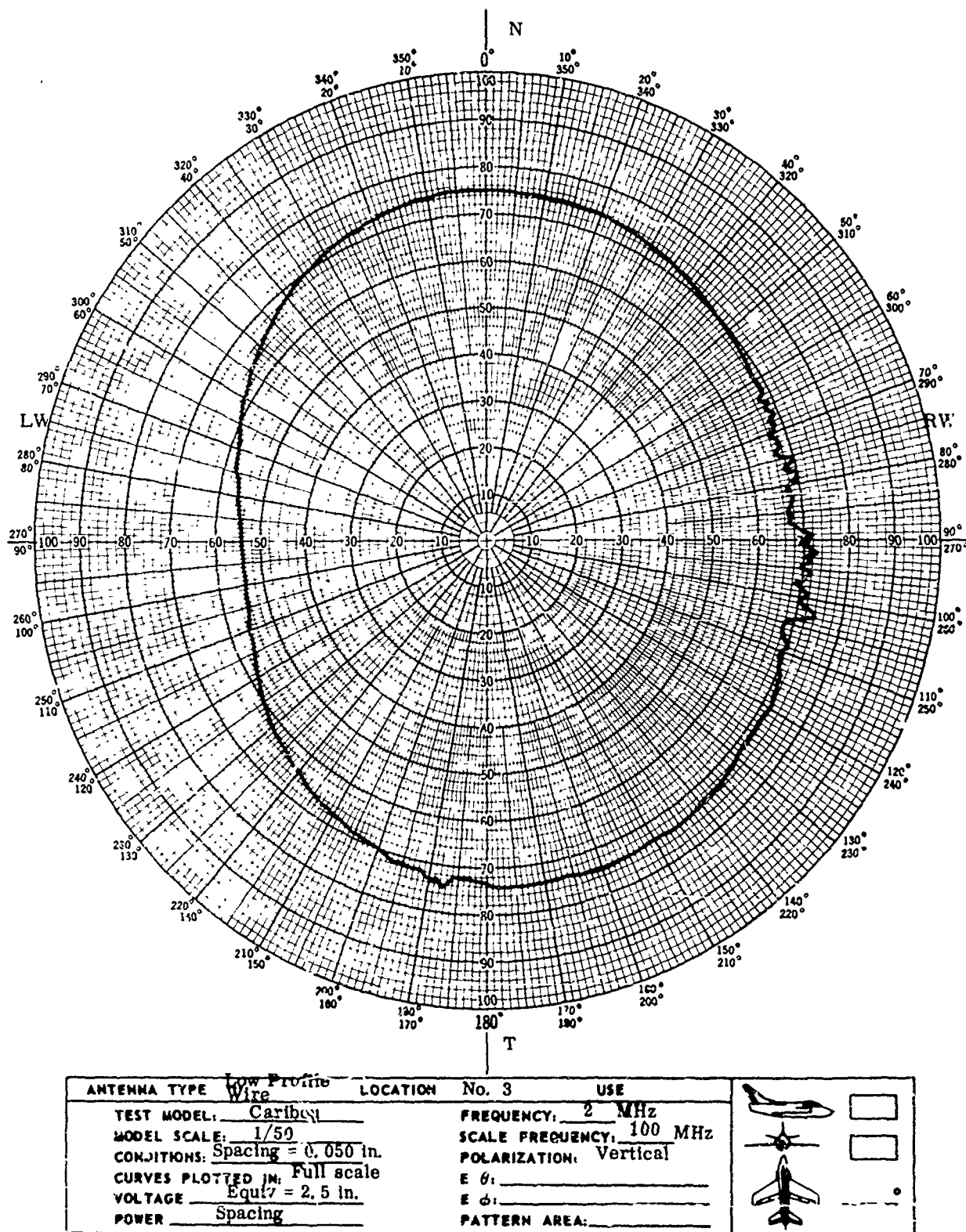
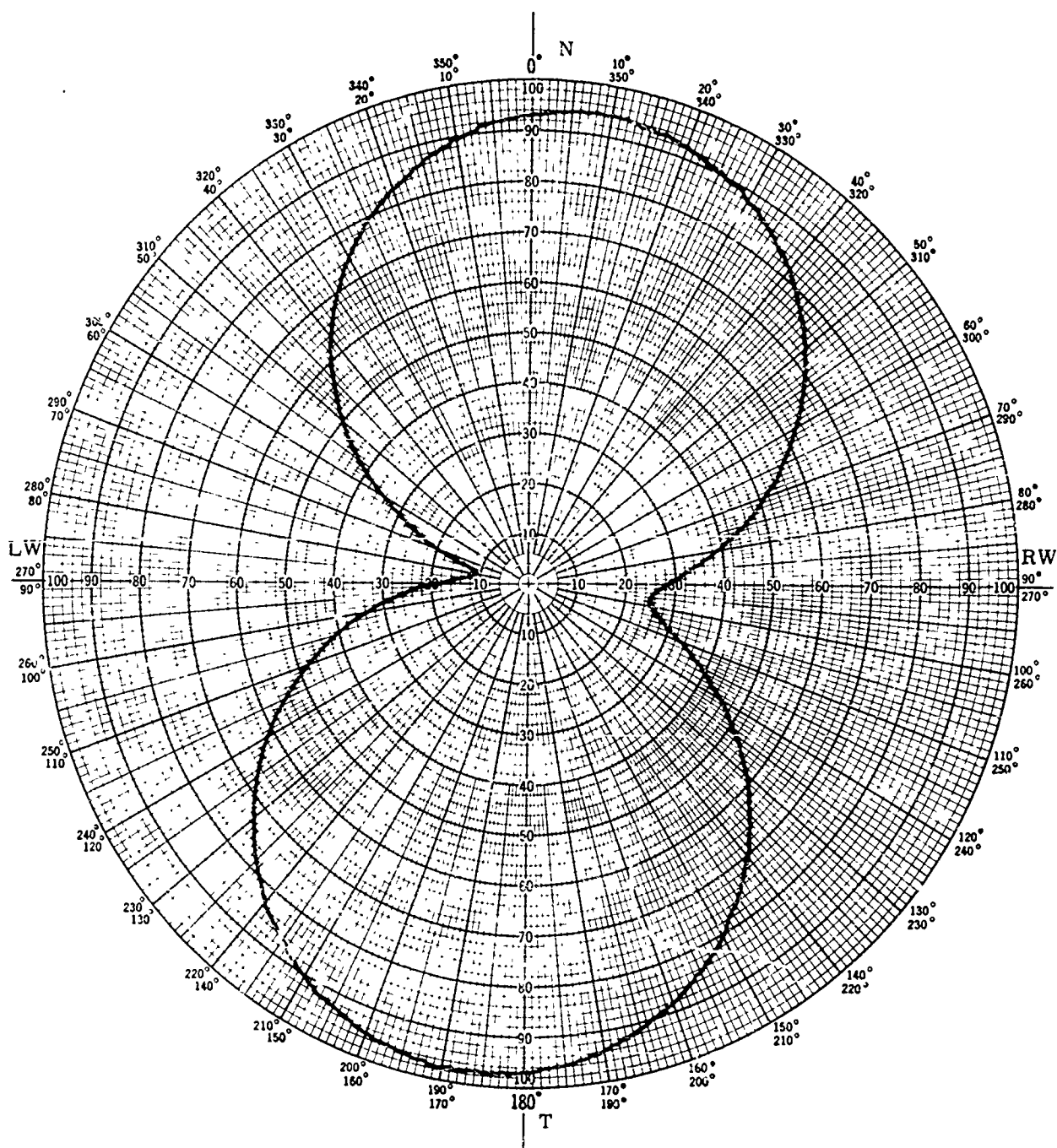


Fig. 33. Patterns of Low Profile Wire Antenna, 1/50 Caribou






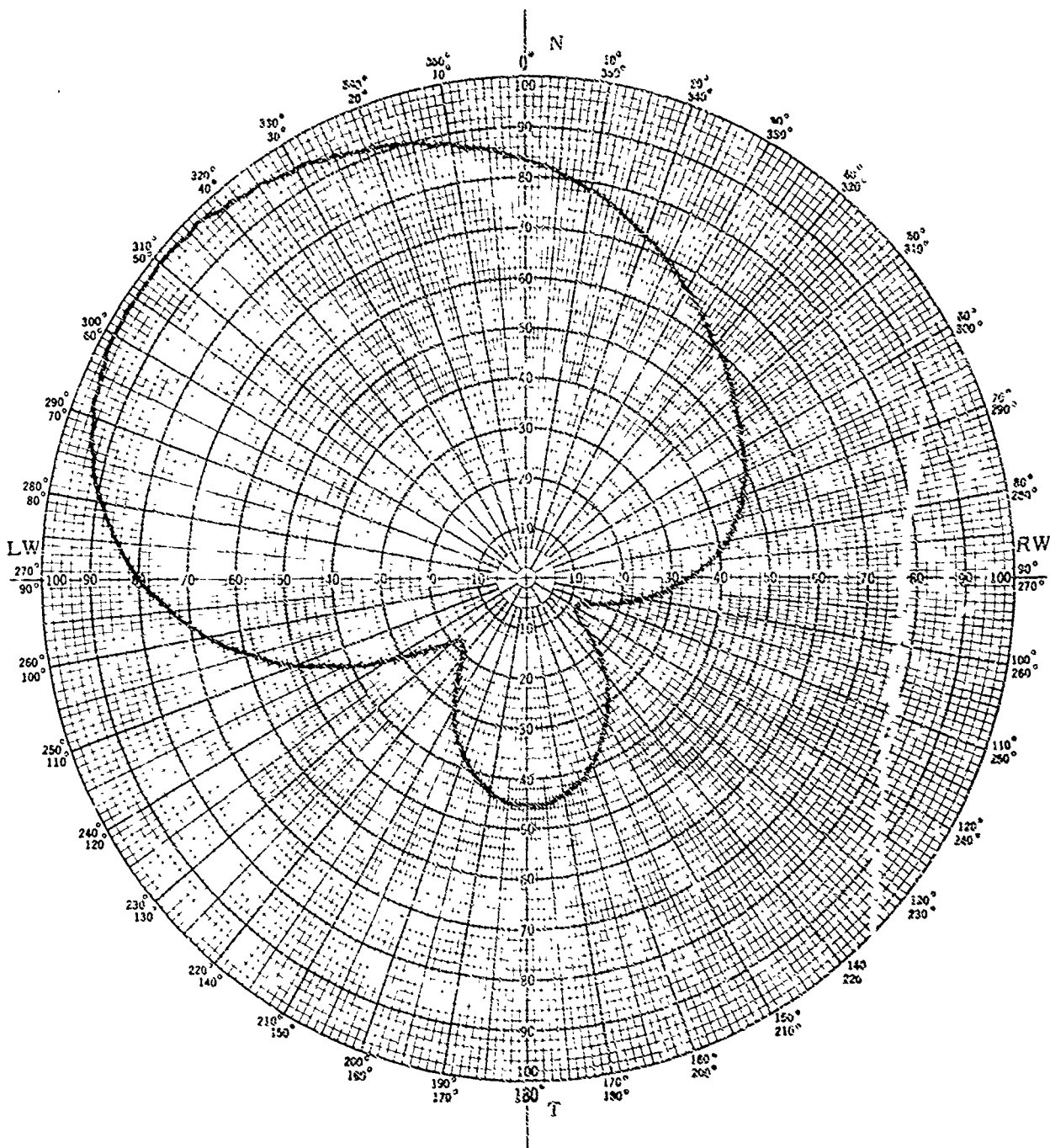
ANTENNA TYPE	Low Profile Wire	LOCATION	No. 3	USE	
TEST MODEL:	Caribou	FREQUENCY:	4 MHz		
MODEL SCALE:	1/50	SCALE FREQUENCY:	200 MHz		
CONDITIONS:	Spacing = 0.050 in.	POLARIZATION:	Vertical		
CURVES PLOTTED IN:		E θ:			
VOLTAGE		E φ:			
POWER		PATTERN AREA:			

Fig. 34. Patterns of Low Profile Wire Antenna, 1/50 Caribou



ANTENNA TYPE	Low Profile Wire	LOCATION	No. 3	USE	
TEST MODEL:	Caribou	FREQUENCY:	8 MHz		
MODEL SCALE:	1/50	SCALE FREQUENCY:	300 MHz		
CONDITIONS:	Spacing = 0.055 in.	POLARIZATION:	Vertical		
CURVES PLOTTED IN:		E θ:			
VOLTAGE	X	E φ:			
POWER		PATTERN AREA:			



Fig. 35. Patterns of Low Profile Wire Antenna, 1/50 Caribou

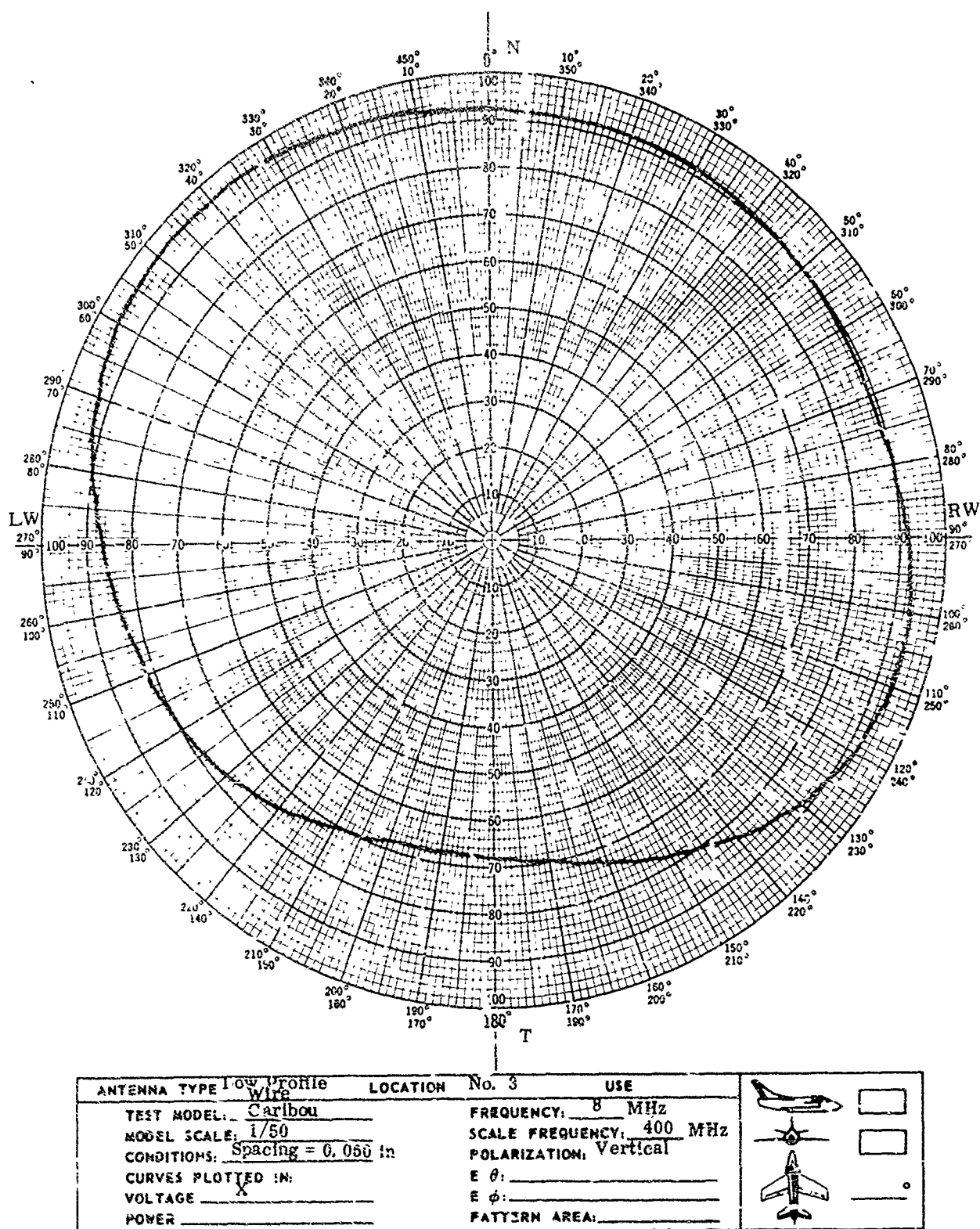
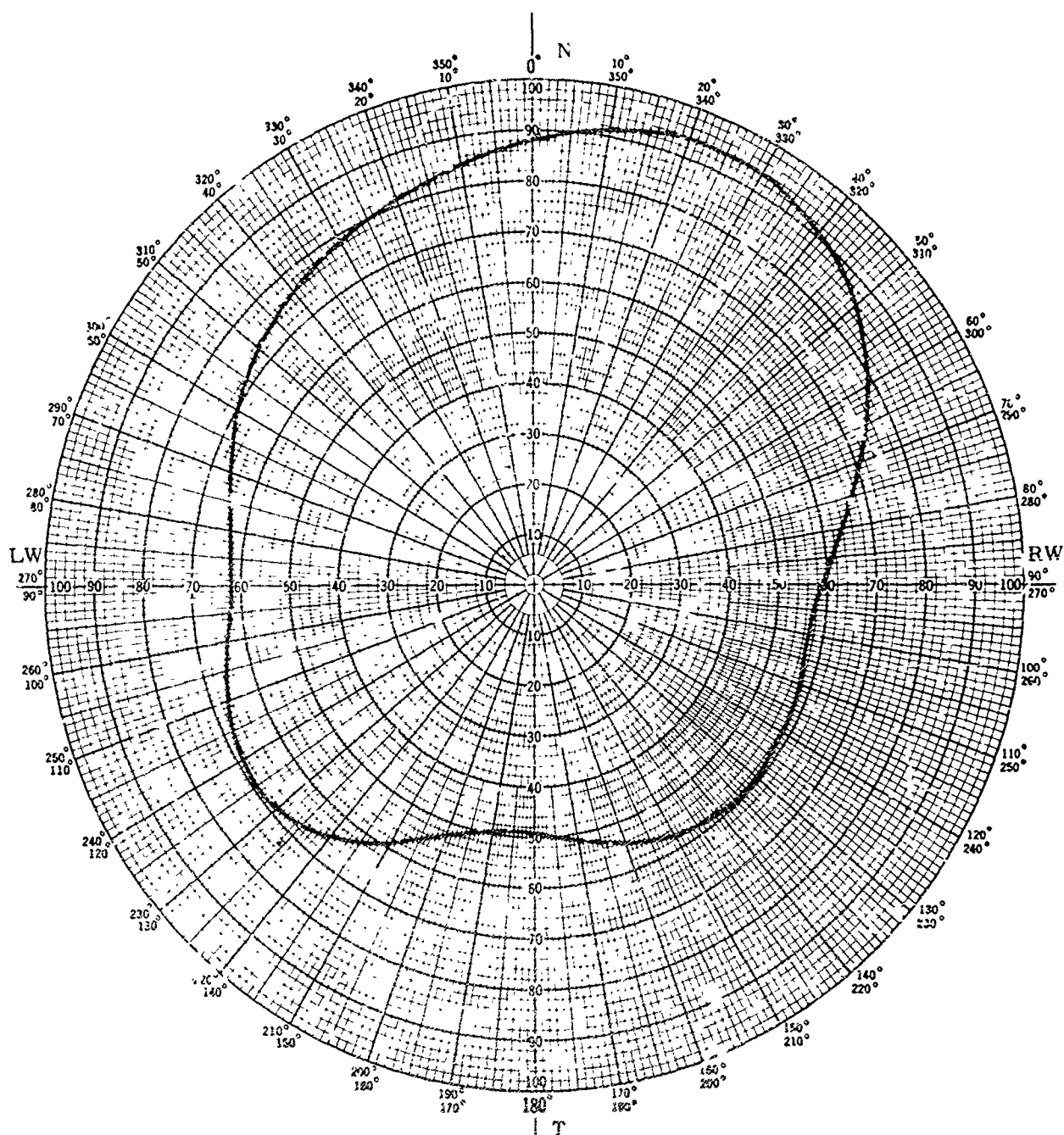


Fig. 36. Patterns of Low Profile Wire Antenna, 1/50 Caribou



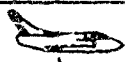


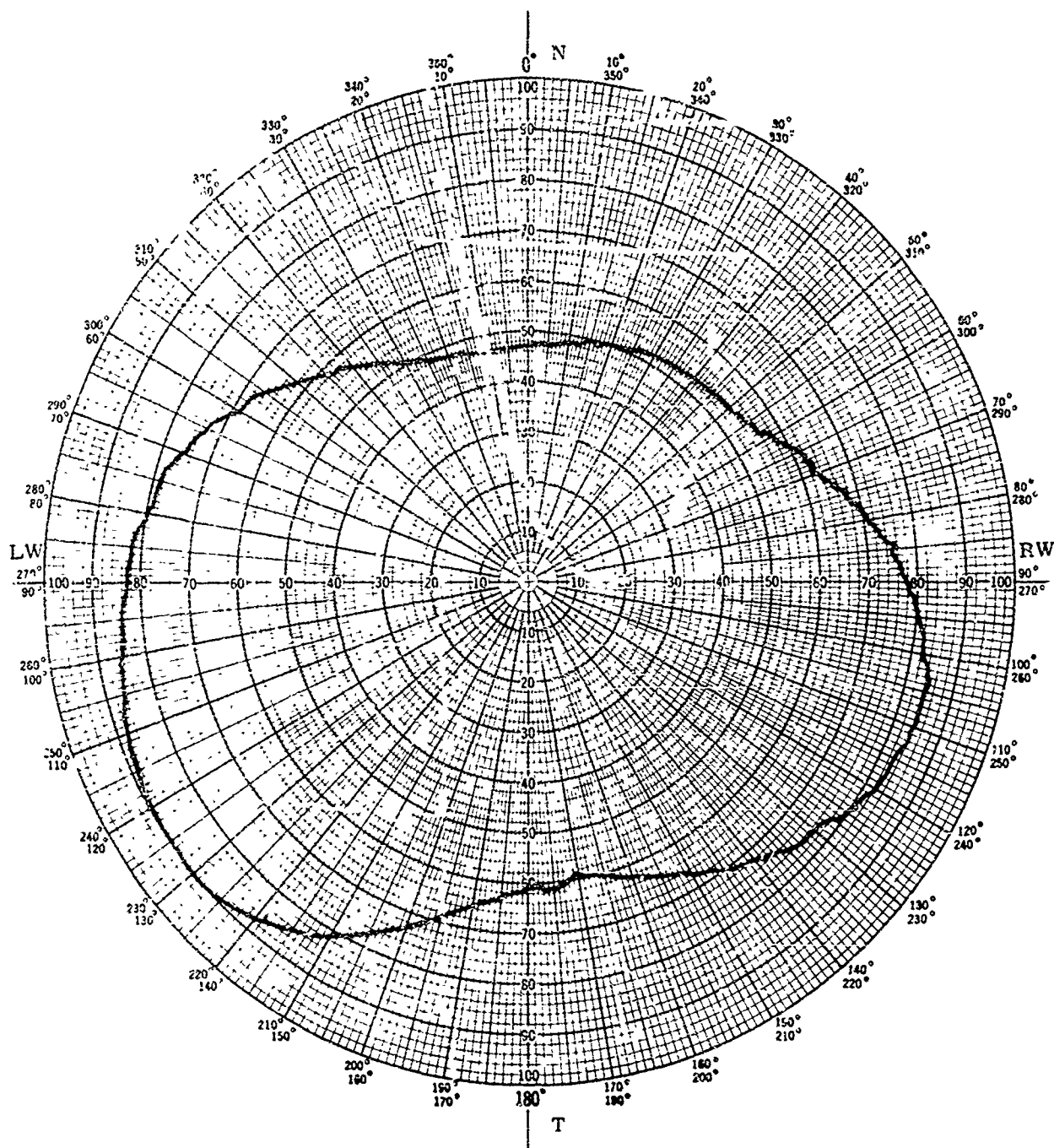
ANTENNA TYPE <u>Low Profile Wire</u>	LOCATION <u>No. 3</u>	USE
TEST MODEL: <u>Caribou</u>	FREQUENCY: <u>10</u> MHz	 <input type="checkbox"/>
MODEL SCALE: <u>1/50</u>	SCALE FREQUENCY: <u>500</u> MHz	 <input type="checkbox"/>
CONDITIONS: <u>Spacing = 0.050 in.</u>	POLARIZATION: <u>Vertical</u>	 <input type="checkbox"/>
CURVES PLOTTED IN: <u>X</u>	E θ : _____	
VOLTAGE _____	E ϕ : _____	
POWER _____	PATTERN AREA: _____	

Fig. 37. Patterns of Low Profile Wire Antenna, 1/50 Caribou






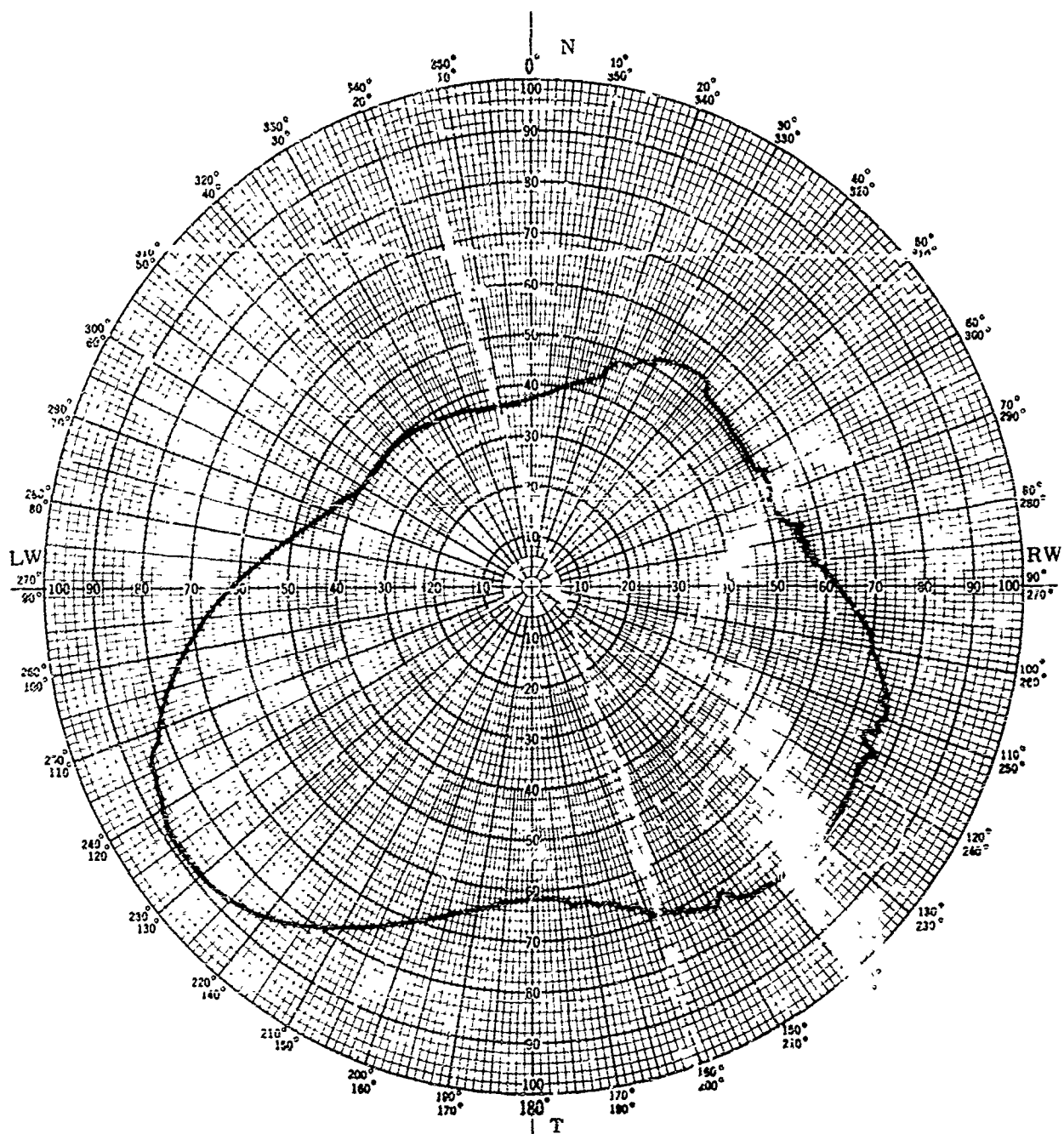
ANTENNA TYPE	Low Profile Wire	LOCATION	No. 3	USE	
TEST MODEL:	Caribou	FREQUENCY:	12 MHz		
MODEL SCALE:	1/50	SCALE FREQUENCY:	600 MHz		
CONDITIONS:	Spacing = 0.050 in.	POLARIZATION:	Vertical		
CURVES PLOTTED IN:		E θ:			
VOLTAGE	X	E φ:			
POWER		PATTERN AREA:			

Fig. 38. Patterns of Low Profile Wire Antenna, 1/50 Caribou



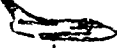


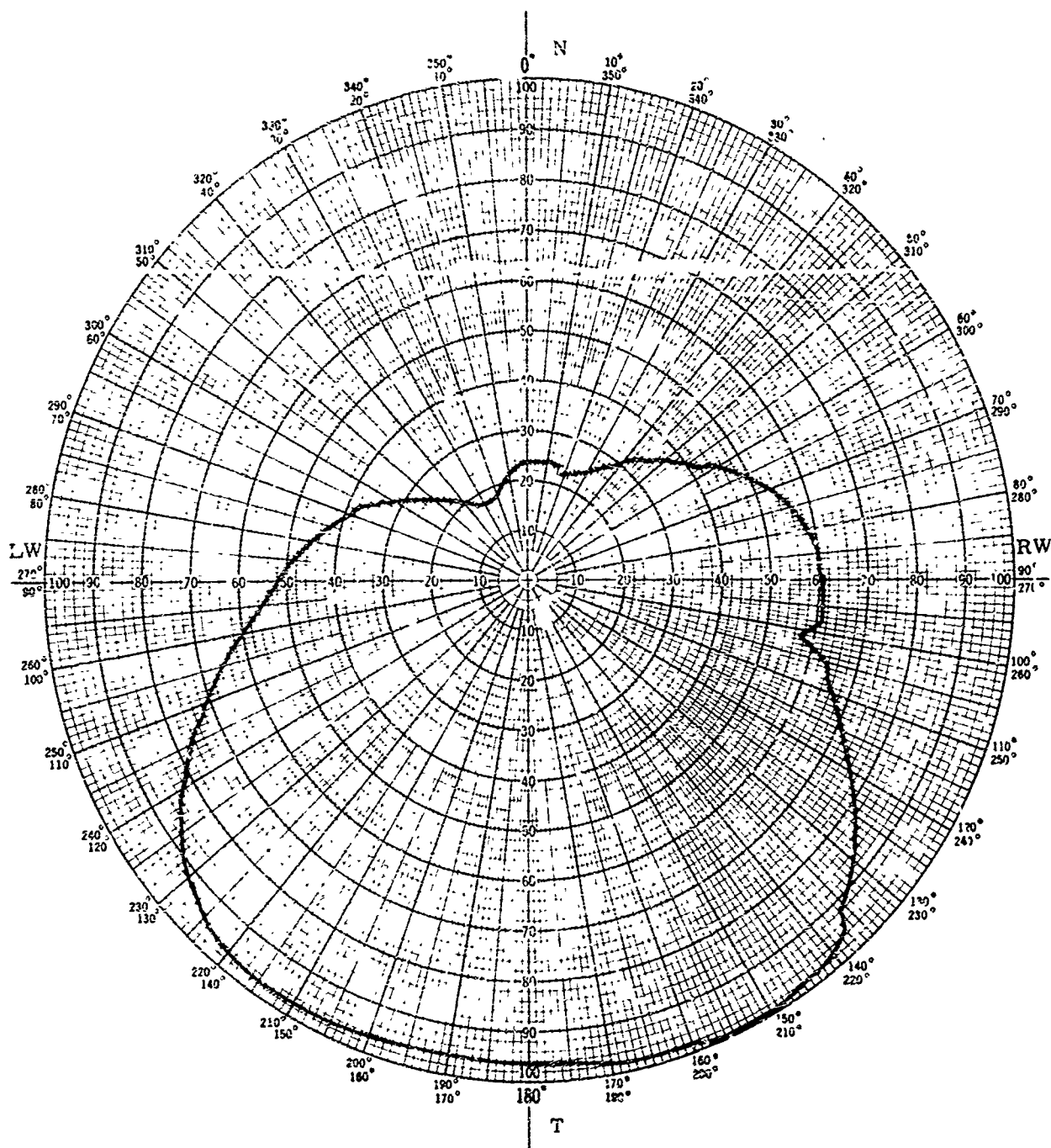
ANTENNA TYPE	Low Profile Wire	LOCATION	No. 3	USE	
TEST MODEL:	Caribou	FREQUENCY:	14 MHz		 <input type="checkbox"/>
MODEL SCALE:	1/50	SCALE FREQUENCY:	700 MHz		 <input type="checkbox"/>
CONDITIONS:	Spacing = 0.050 in.	POLARIZATION:	Vertical		 <input type="checkbox"/>
CURVES PLOTTED IN:		E θ:			
VOLTAGE	X	E φ:			
POWER		PATTERN AREA:			

Fig. 39. Patterns of Low Profile Wire Antenna, 1/50 Caribou



ANTENNA TYPE	Low Profile Wire	LOCATION	No. 3	USE	
TEST MODEL	Caribou	FREQUENCY	16 MHz		
MODEL SCALE	1/50	SCALE FREQUENCY	800 MHz		
CONDITIONS	Spacing = 0.350 in.	POLARIZATION	Vertical		
CURVES PLOTTED IN:		E θ :			
VOLTAGE	X	E ϕ :			
POWER		PATTERN AREA			

Fig. 40. Patterns of Low Profile Wire Antenna, 1/50 Caribou

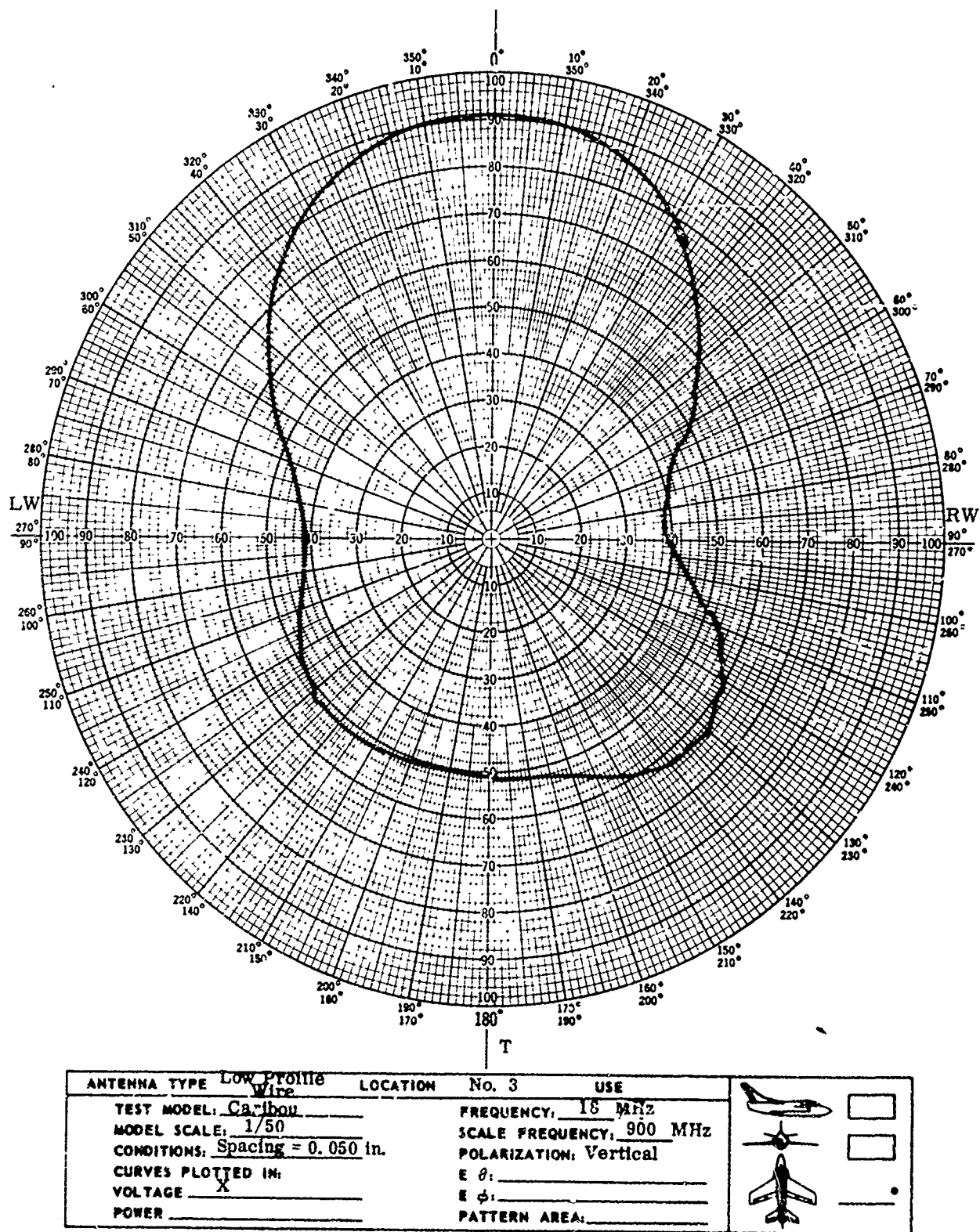


Fig. 41. Patterns of Low Profile Wire Antenna, 1/50 Caribou

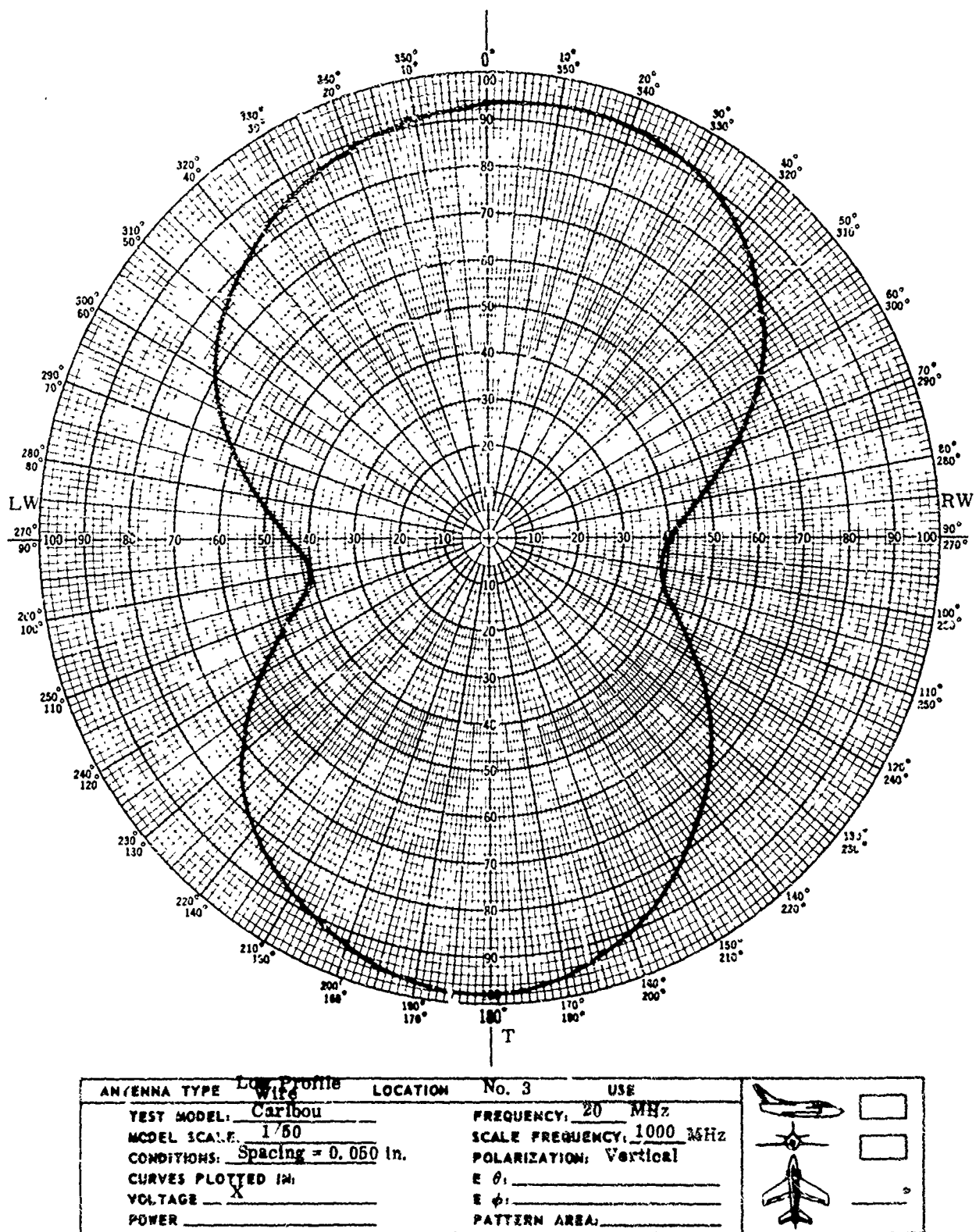


Fig. 42. Patterns of Low Profile Wire Antenna, 1/50 Caribou

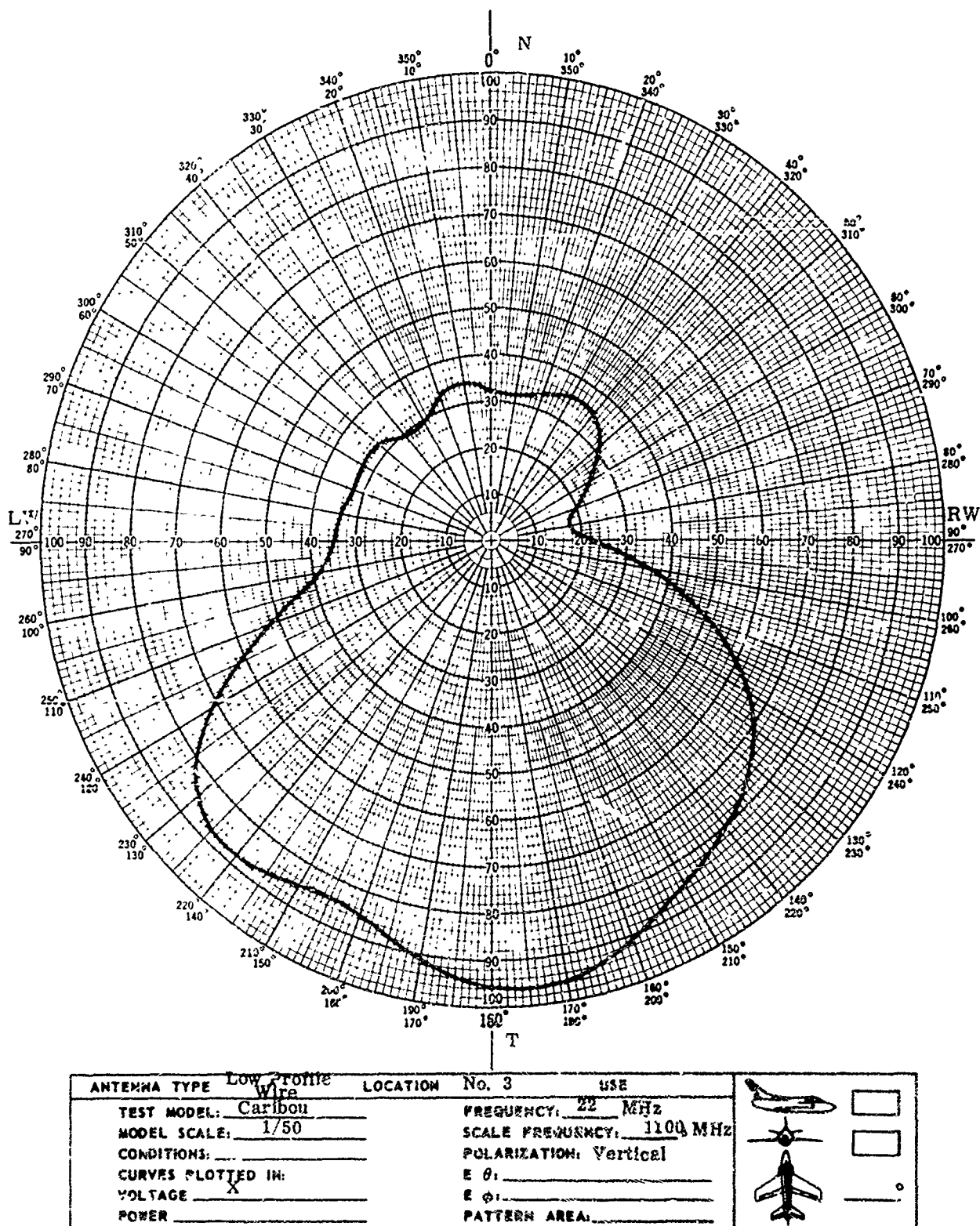


Fig. 43. Patterns of Low Profile Wire Antenna, 1/50 Caribou

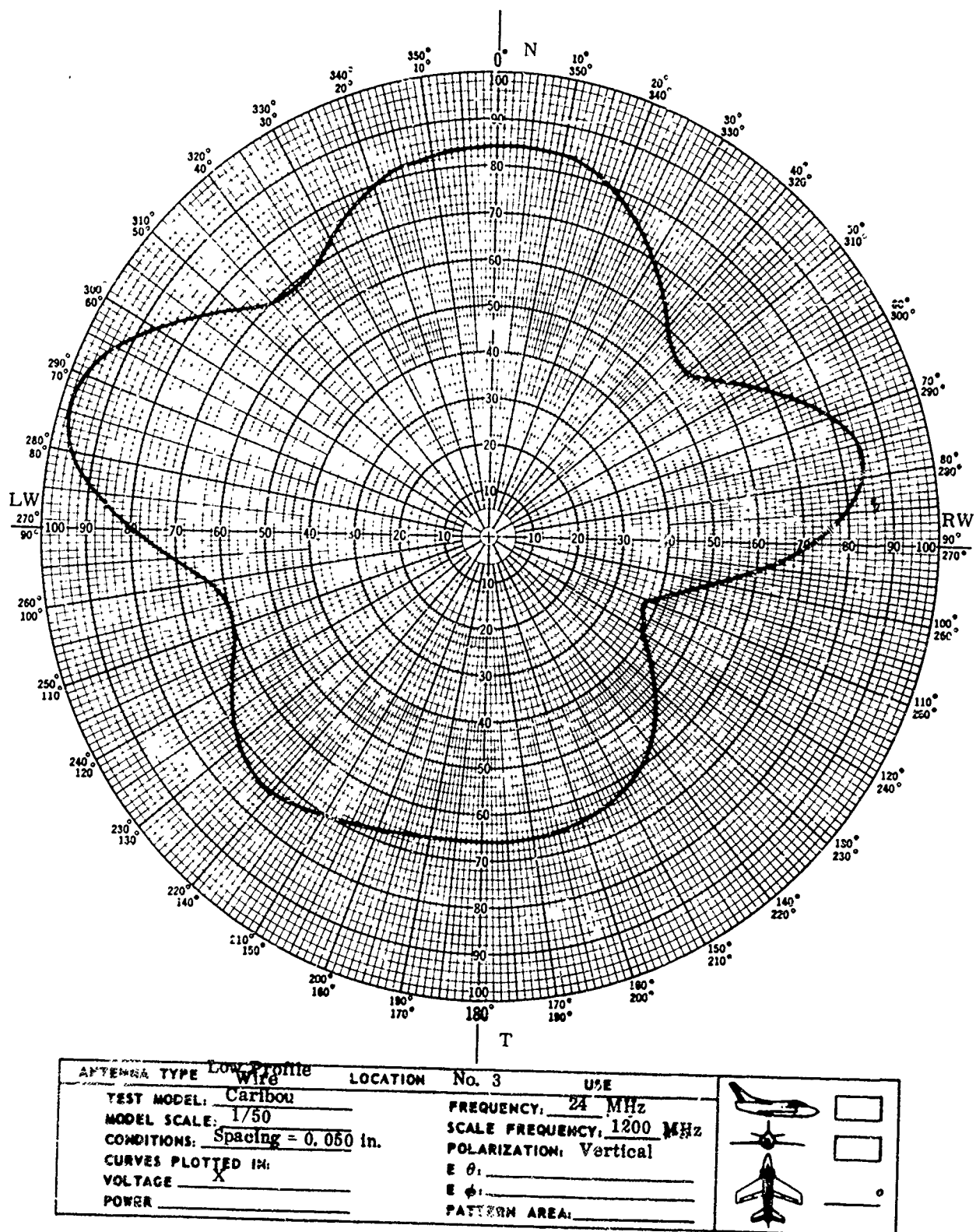
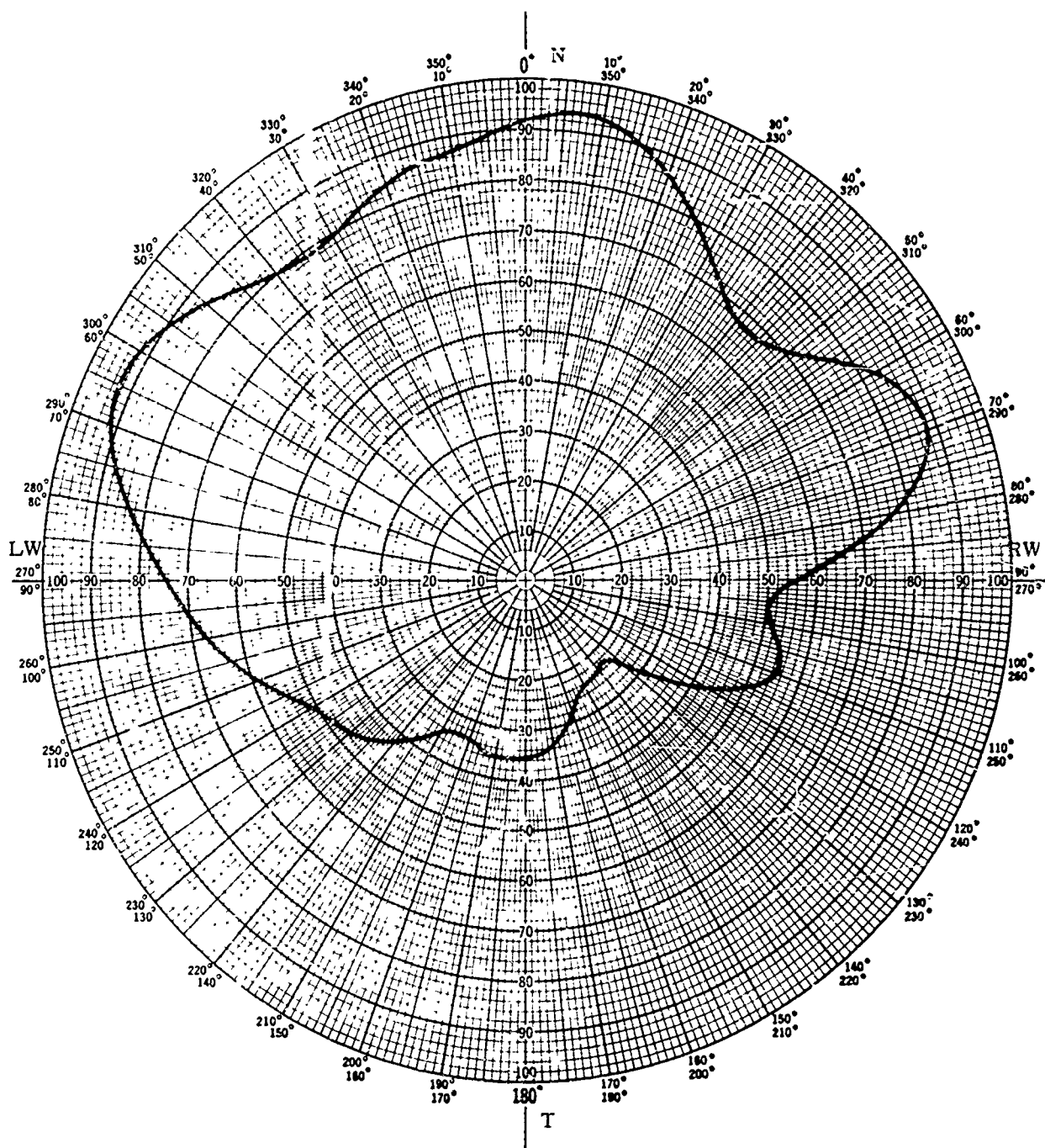


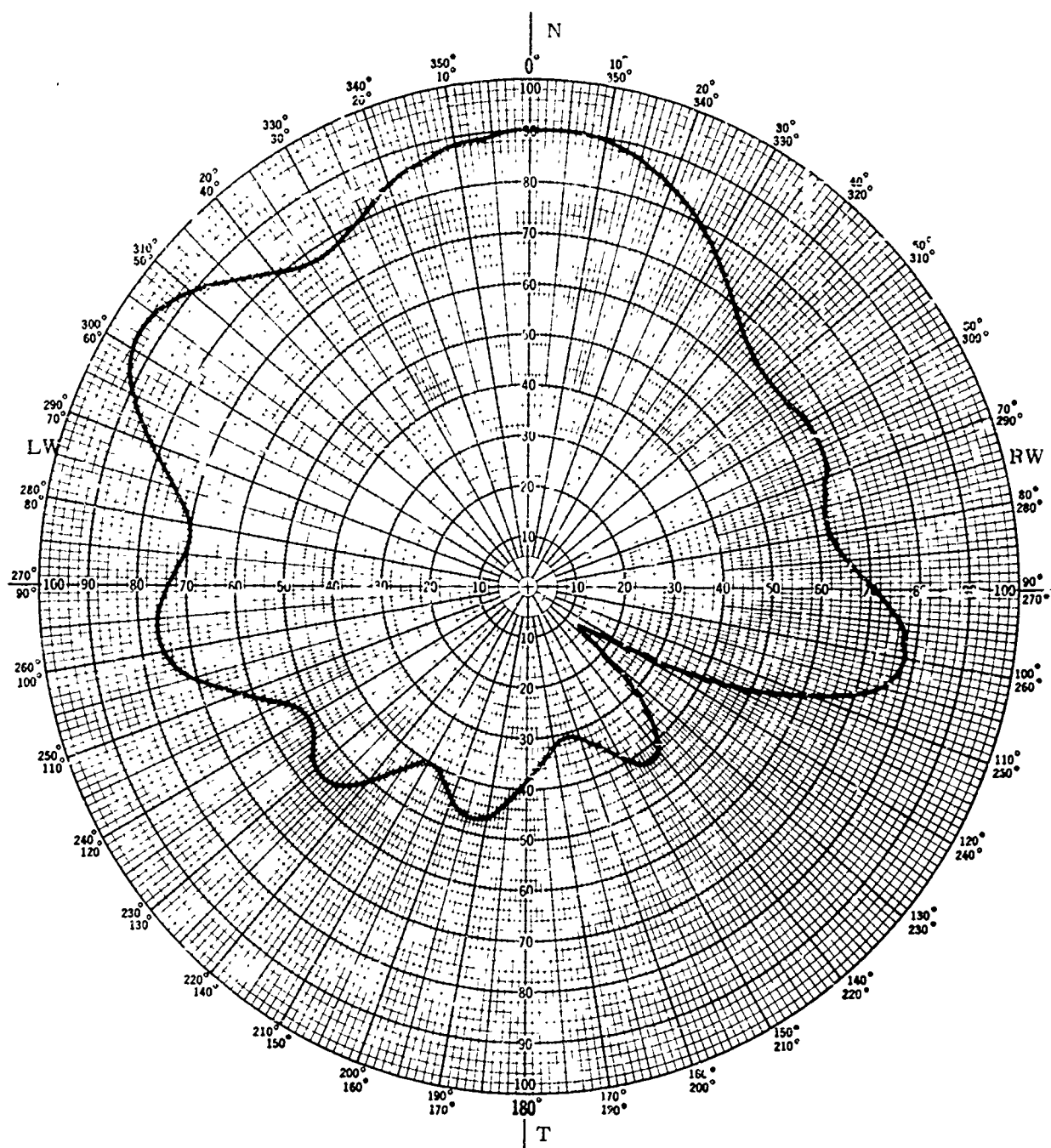
Fig. 44. Patterns of Low Profile Wire Antenna, 1/50 Caribou



ANTENNA TYPE	Low Profile	LOCATION	No. 3	USE
TEST MODEL:	Caribou			FREQUENCY: 28 MHz
MODEL SCALE:	1/50			SCALE FREQUENCY: 1300 MHz
CONDITIONS:	Spacing = 0.050 in.			POLARIZATION: Vertical
CURVES PLOTTED IN:				E θ : _____
VOLTAGE	X			E ϕ : _____
POWER				PATTERN AREA: _____

☐
☐
☐

Fig. 45. Patterns of Low Profile Wire Antenna, 1/50 Caribou






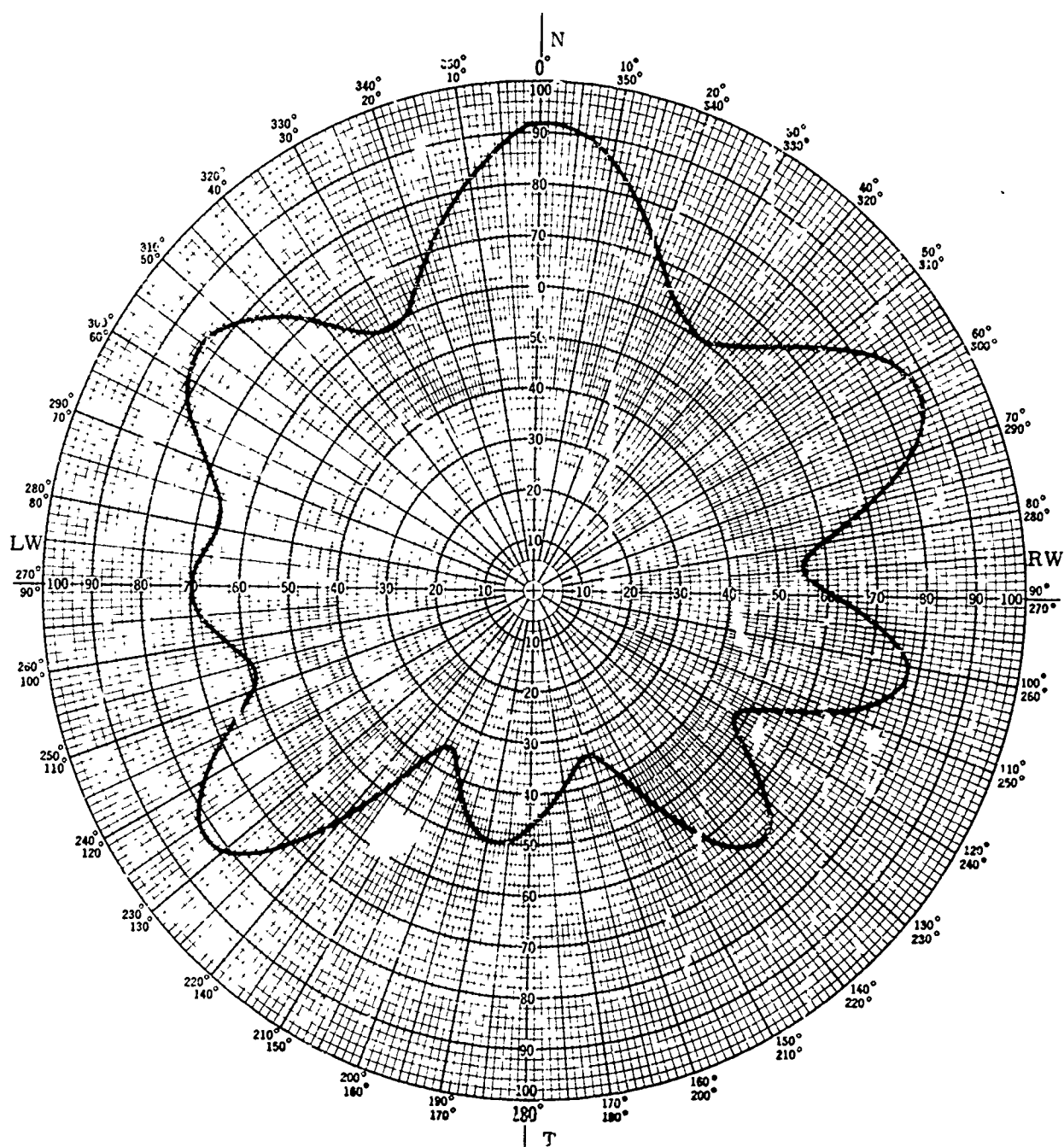
ANTENNA TYPE <u>Low-Profile Wire</u>	LOCATION <u>No. 3</u>	USE
TEST MODEL: <u>Caribou</u>	FREQUENCY: <u>28</u> MHz	 <input type="checkbox"/>  <input type="checkbox"/>  <input checked="" type="checkbox"/>
MODEL SCALE: <u>1/50</u>	SCALE FREQUENCY: <u>1400</u> MHz	
CONDITIONS: <u>Spacing = 0.050 in.</u>	POLARIZATION: <u>Vertical</u>	
CURVES PLOTTED IN:	E θ : _____	
VOLTAGE <u>X</u>	E ϕ : _____	
POWER _____	PATTERN AREA: _____	

Fig. 46. Patterns of Low Profile Wire Antenna, 1/50 Caribou






ANTENNA TYPE	Low Profile Wire	LOCATION	No. 3	USE	
TEST MODEL:	Caribou	FREQUENCY:	30 MHz		
MODEL SCALE:	1/50	SCALE FREQUENCY:	1500 MHz		
CONDITIONS:	Spacing = 0.057 in.	POLARIZATION:	Vertical		
CURVES PLOTTED IN:		E θ:			
VOLTAGE	X	E φ:			
POWER		PATTERN AREA:			

Fig. 47. Patterns of Low Profile Wire Antenna, 1/50 Caribou

REFERENCES/REPORTS

1. Hendershot, J., "Compact H-F Aircraft Antennas (2-30 MHz), " First Semi Annual Report, Technical Report ECOM-00477-1.
2. Hendershot, J. and Thomas, R. K., "Compact H-F Aircraft Antennas (2-30 MHz), " Second Semi Annual Report, Technical Report ECOM-00477-2.
3. Hendershot, J., "Compact H-F Aircraft Antennas (2-30 MHz), " Third Semi Annual Report, Technical Report ECOM-00477-3.

APPENDIX A
DESIGN PLAN
FOR
COMPACT H-F AIRCRAFT ANTENNAS

I. INTRODUCTION

This plan covers the design of a 1/5-scale antenna unit with manually controlled tuning network. Two such combinations will be delivered as "exploratory development models." The 1/5-scale factor is a necessary consequence of the design procedures as will be shown.

The work is organized under two principal topics: (2) patterns and (b) impedance. These are essentially separable, and the investigations will be carried out using scale factors appropriate for each situation, taking all electrical and physical factors into account. These investigations are based upon the Caribou and Iroquois aircraft.

II. PATTERNS

A 1/50-scale model will be used for the Caribou (Figs. A-1 and A-2) and a 1/25-scale for the Iroquois. It is desirable to keep the frequency range as high as possible in order to minimize ground reflections. Thus, for the Caribou, the lowest frequency required is 100 MHz which is compatible with the largest source antenna, a 12-ft parabola. The 1/50-scale factor is impractical for the Iroquois, however, since the model size becomes too small to permit detector mounting and to provide adequate illumination around the tower head. The lowest operating frequency becomes 50 MHz, at a sacrifice in range performance insofar as reflections are concerned.

A variety of antenna configurations and locations will be used and principal plane patterns taken for each situation, in both polarizations. The design objective is vertically polarized radiation, omnidirectional in azimuth, over the band. The best approximation to this is the practical solution to the problem.

At the lower end of the band, the aircraft itself is actually the radiator; the "antennas" being merely means of coupling to its natural radiation modes. As the frequency is increased, contributions, from the antennas themselves become more noticeable in some areas. Locations on the vertical stabilizer will couple to currents flowing on the stabilizer and fuselage, and the desired vertical polarization is that due to the stabilizer component. Best coupling will correspond to regions of highest current density, which are those where curvatures are sharpest and located as far as possible from aircraft extremities. Three principal locations have been chosen for the Caribou investigation, as shown in Figs. A-1 and A-2.

Based upon the foregoing discussion, location 2 should produce better coupling than location 3. This will be of importance in the impedance investigation, since higher coupling implies more desirable properties

in this regard. In addition, at the high end of the band, location 2 will yield better omnidirectionality due to symmetry.

For the Iroquois, locations 2 and 3 are probably impractical due to the configuration and small size, and a location corresponding to 1, on the fuselage, may be the best of the three. In this location, a loop current mode is induced around the fuselage.

The antennas themselves are essentially loops, or notches. The configurations to be tried involve variations in the dimensions of the overall structure, limited to a maximum of 24 in., and in the dimensions of the point of attachment to the airframe. Fixed tuning compensation, which may be built into the 1/5-scale impedance models, cannot be included in the pattern models due to their very small physical size. This does not affect the patterns except that, in the cases of extreme mismatch, it becomes difficult to realize enough signal to take patterns.

The coordinate system which will be used throughout the pattern study is the standard aircraft system included as Fig. A-3. The study will be based on the three principal planes indicated in the figure with emphasis on obtaining the optimum coverage in the azimuth plane. The preliminary patterns (Figs. A-4 through A-21) were taken on the 1/50-scale model of the Caribou with the exciting device located at the three locations referred to earlier. It is evident from the enclosed patterns that the performance of the device is affected considerably by the point of attachment. The coverage, coupling efficiency and polarization response are all affected by location. The goal of the pattern study will be the optimum combination of the above parameters.

The retransmission mode requirement is also covered in the pattern study. This involves the use of two antennas in the full-scale operation, one for receiving and the other for transmitting. Patterns will be taken for each antenna of the dual installation in order to verify that each can operate in the presence of the other. The decoupling requirement will be covered under the impedance study.

III. IMPEDANCE

Both the Caribou and Iroquois impedance models will be built to 1/5 scale. This produces a Caribou having a wingspan of approximately 20 ft, which is as large as can reasonably be handled. A smaller scale would be undesirable, since the Iroquois would then be too small to contain the measuring equipment. It is necessary that both models be built to the same scale, in order that the same antennas may be used for each.

The models are of wood, covered with hardware mesh. The model shown in Fig. A-22 shows the type of construction which is being used.

They are to be mounted interchangeably on a movable wooden tower about 15 ft high (not as shown in the picture). The measuring equipment will be installed by moving the model next to one of the laboratory buildings and working from the roof. After the equipment is in place and adjusted, the access door will be closed and the model will be moved away from the building. Measurements will be made by an engineer on the ground who will control the equipment dial by nylon cord, observing the meter indication through a transit.

The equipment will be mounted in the center of the fuselage, where there is the most room, and the necessary a-c connection will be made through a filter in order to isolate the R-F current from the line. All impedance measurements will be referred to the point of cable attachment to the instrument, since the "antenna terminals" cannot be identified until later. They are defined as that point on the cable nearest the antenna where the automatic tuning unit may be located in an actual installation.

In this frequency range, impedance measurements are made with either the PRD 219 Standing Wave Indicator, an R-F Bridge, or a Q-meter. The PRD 219 has been rejected for this particular application for two reasons, both of which are concerned with the high standing wave ratios to be expected from these antennas before matching. Under such circumstances, the signal required for a good null reading exceeds that available from the laboratory oscillators, and it is also necessary to change the decade knob on the indicating instrument (typically a HP 415-B). The latter feature is objectionable due to the measurement technique described previously, requiring remote control. For this same reason the R-F Bridge technique is considered unsatisfactory; two controls are required for R and X components. However, the bridge may be employed as a backup for the Q-meter on the upper end of the frequency band.

The Q-meter is initially adjusted from the roof top position, and Q_1 , C_1 readings are taken. Then the antenna cable is connected and the access door is closed. The only control required is the capacitor. Q_2 and C_2 may be read by a transit. The parallel components of impedance, which are determined from the values of Q and C read on the Q-meters, are given by:

$$R_p = \frac{Q_1 Q_2}{\omega C_1 (Q_1 - Q_2)} , \quad X_p = \frac{1}{\omega (C_2 - C_1)}$$

These values are converted to their series equivalents by the relationships:

$$R_s = \frac{R_p X_p^2}{R_p^2 + X_p^2}, \quad X_s = \frac{R_p^2 X_p}{R_p^2 + X_p^2}$$

The antenna impedance is due to the loop inductance in combination with the coupled impedance of the airframe. Partial compensation for the loop inductance component may be achieved by inserting a shunt capacity on the line. This will be necessary in some cases in order to read Q_2 , C_2 . It may be possible to incorporate this capacity in the antenna structure itself in order to present a more satisfactory impedance to the automatic tuning system required for the full-scale antennas. The measurements will be made at the following frequencies:

10 MHz (2 x 5), 15, 20, 30, 40, 50, 75, 100, 125 and 150.

Once the impedance is determined, a manually adjusted lumped constant tuning network will be designed and built to reduce the standing wave ratio to below 2:1. The characteristics of the network depend, of course, upon the point at which the measurement is made on the cable. Information will be made available by this time to define the "antenna terminals," and the measured values will be referred back to this point by means of the transmission line equations. The Smith Chart cannot be used in most of the cases, due to the degraded resolution in regions of low resistance and high reactance. The equation relating Z_{measured} to Z_{load} is

$$\frac{Z_m}{Z_0} = \frac{\frac{Z_l}{Z_0} \cosh(\alpha + j\beta)l + \sinh(\alpha + j\beta)l}{\cosh(\alpha + j\beta)l + \frac{Z_l}{Z_0} \sinh(\alpha + j\beta)l}$$

where

α = attenuation factor; nepers per unit length

β = phase factor; radians per unit length

l = line length

Z_0 = line characteristic impedance.

Z_l = load impedance at the antenna terminals

In order to facilitate data reduction, a two part computer program has been prepared for the IBM 1620. The first part converts the measured

Q and C values to series components of Z_m and the second solves the above transmission line equation for Z_p .

Two antennas, matched by their tuning units, will be mounted for the purpose of making coupling measurements. The initial matching will be a reiterated converging process, involving several readjustments and measurements, due to the nature of the measurement technique. The coupled signal will be measured by a crystal and HP 415-B combination, compared against a known reference input from GR oscillator. From these measurements, the isolation requirements may then be specified for the filter to be used in an actual isolation.

Measurements are called for which compare the performance of these antennas to that of a 15-ft (full scale) vertical whip above a ground plane. A 3-ft reference whip, simulating the full-scale 15-ft whip, will be mounted on a 12-ft x 12-ft screen at ground level. The impedance model of the aircraft, with test antenna, will be placed on the ground. With reference and test antennas tuned for maximum input to a standard detector crystal, comparison will be made against a source located equidistant from both antennas. The losses of the tuning units will later be compared by connecting each to the same signal generator without changing the output level, and without altering the tuning adjustments set in the model. The measurement will be made as shown in Fig. A-23. The losses due to mismatch between the tuner and the detector will be eliminated by employing two identical tuners as indicated.

IV. R-F POWER

The manually controlled tuner designed for the exploratory development models is not intended to meet the 1-kw power requirement. The advanced development models, at full scale, will be tested in conjunction with a 1-kw transmitter and high power automatic tuner as will be described in the forthcoming test plan. The principal burden of the high power requirement is upon the tuner rather than the antennas, due to their loop nature. Any problems that may arise in this connection are thus deferred until the advanced development models are built.

V. BANDWIDTH

Full-scale system bandwidth depends upon the properties of antenna and automatic tuning system, and will therefore be determined by means of the advanced development model as described in the forthcoming test plan.

At the low end of the band, the bandwidth of the antennas, resonated by a lossless tuner, will be very narrow. Consider the 15-ft reference whip to be used as a standard of comparison. As shown in our proposal, the Q of a short dipole with lossless tuner is given by the expression.

$$Q = \frac{Z_0}{160} \left(\frac{\lambda_0}{h} \right)^3$$

where

$$Z_0 = 120 \ln \left(\frac{2h}{r} - 1 \right), \text{ according to Schelkunoff}$$

$$\lambda_0 = \text{wavelength}$$

$$h = \text{dipole half-length}$$

$$r = \text{dipole radius.}$$

The Q of a monopole of length h, above an ideal infinite ground plane, is equal to that of the dipole since the ratios of stored energy to energy dissipated per cycle are the same in both cases. Thus, at the 10 MHz scale frequency, the Q of an ideal 3-ft reference whip is given by

$$\frac{120}{160} \ln \left(\frac{6 \times 12}{1/16} - 1 \right) \cdot \left(\frac{98.5}{3} \right)^3 = 6000$$

assuming that the whip radius is 1/16 in. The scaled 3-dB bandwidth is therefore $\frac{10,000}{6,000}$ KHz = 1.67 KHz. The bandwidth of the full-scale 15-ft reference whip is 1/3 KHz. This is the worst case; as the frequency is increased the antenna Q decreases and the absolute bandwidth, even for a constant Q, increases. In addition to this, the effect of the unavoidable losses in an actual tuning system is to broaden the frequency response at the expense of efficiency.

Antenna configurations arrived at in accordance with foregoing discussion will be referred to mechanical and aeronautical engineers in order that their design requirements may be observed and incorporated. The final design will be satisfactory from an aerodynamic point of view, and will not exceed the 24 in. - 10 lb full-scale limitation.

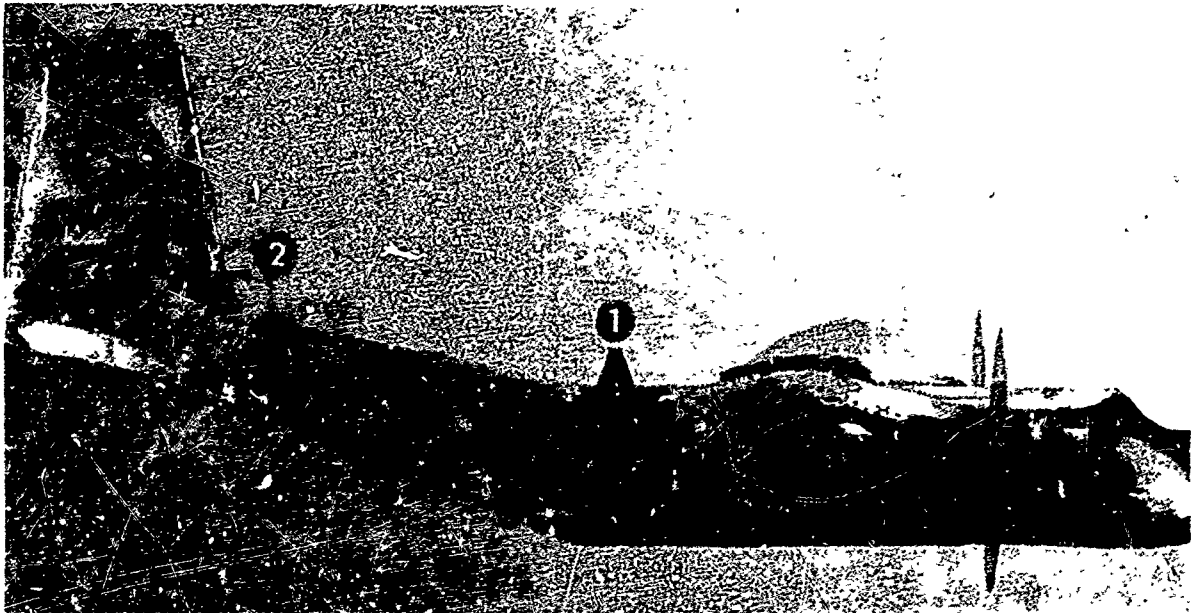


Fig. A-1. 1/50-Scale Model of Caribou

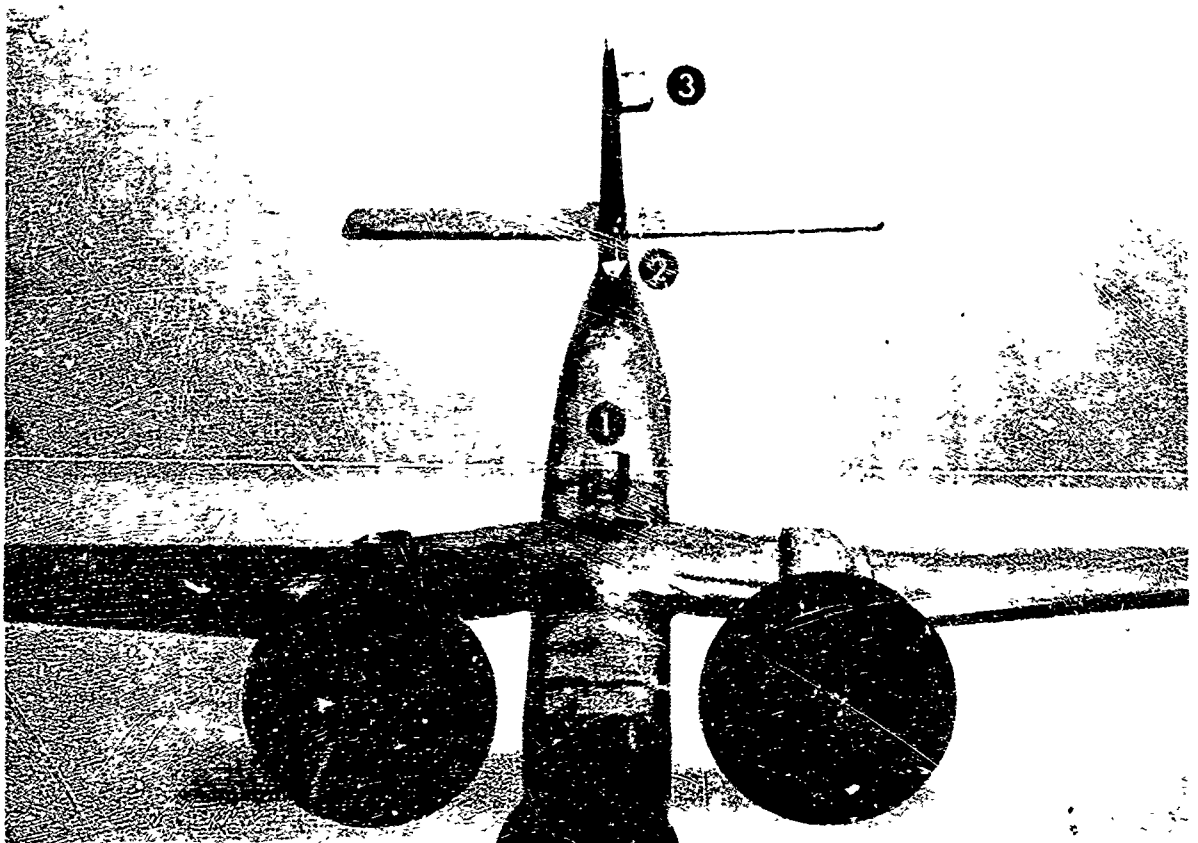


Fig. A-2. Pattern Model--1/5 Scale

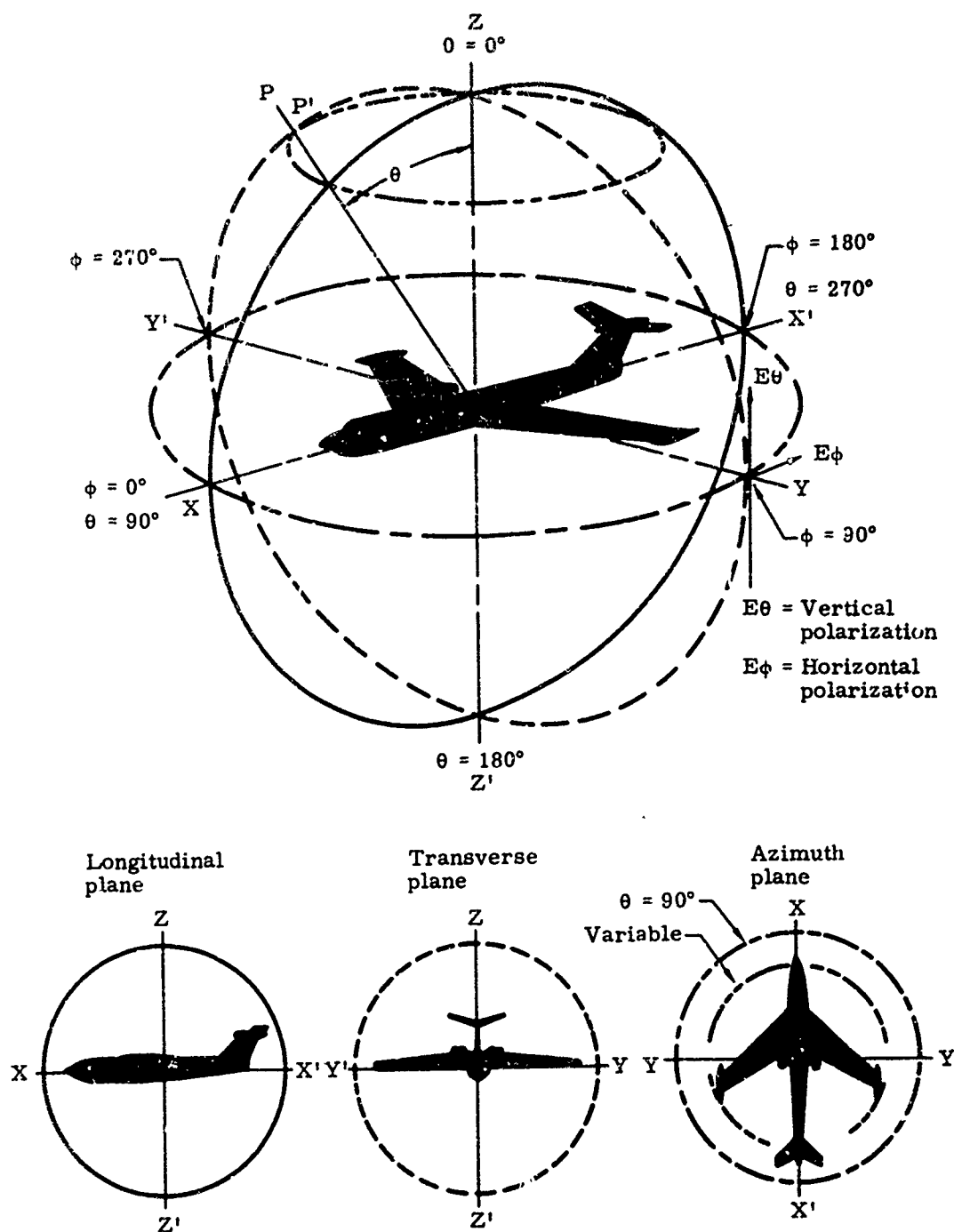
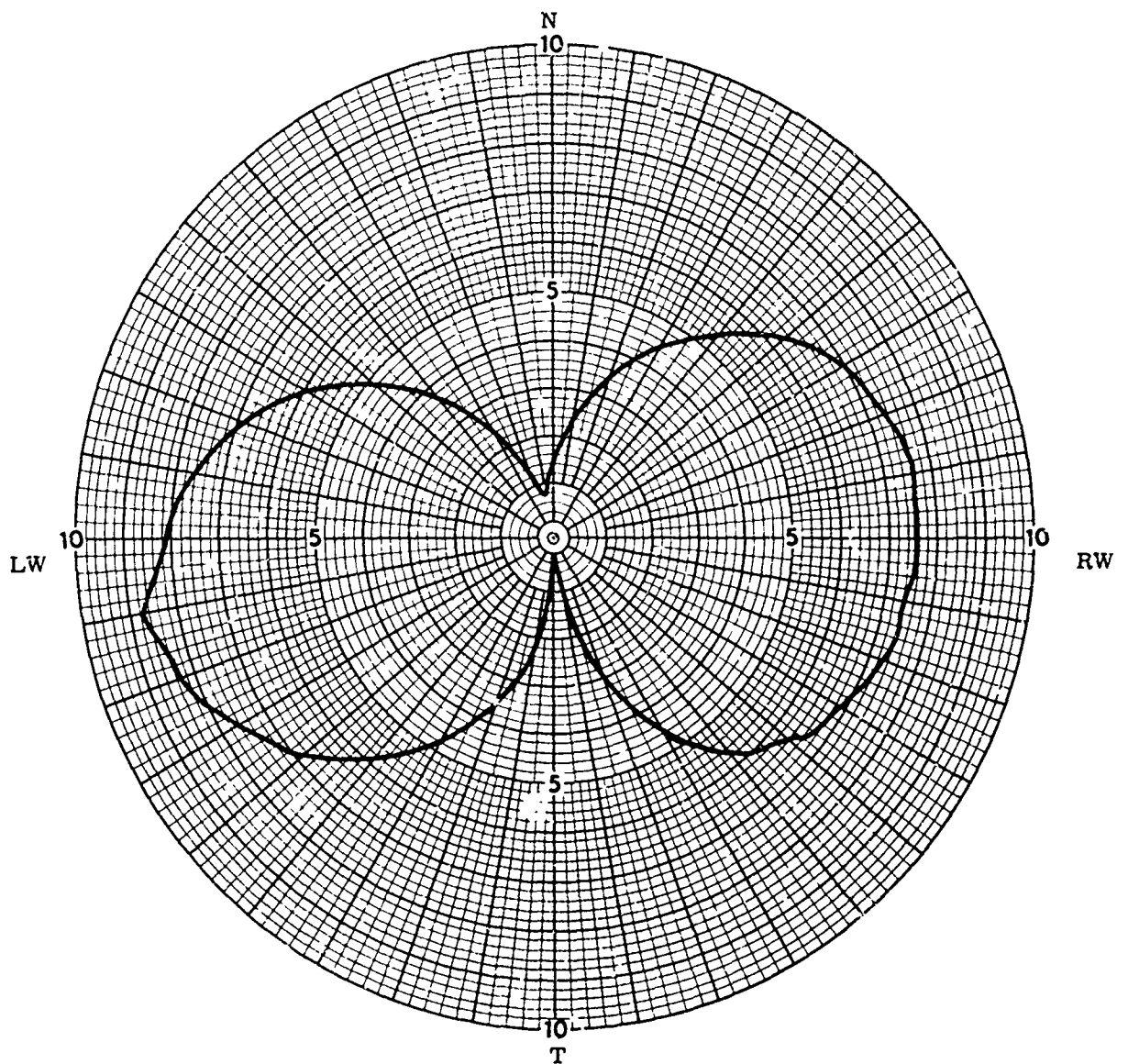


Fig. A-3. Aircraft Model Coordinate System (right-hand spherical coordinates)






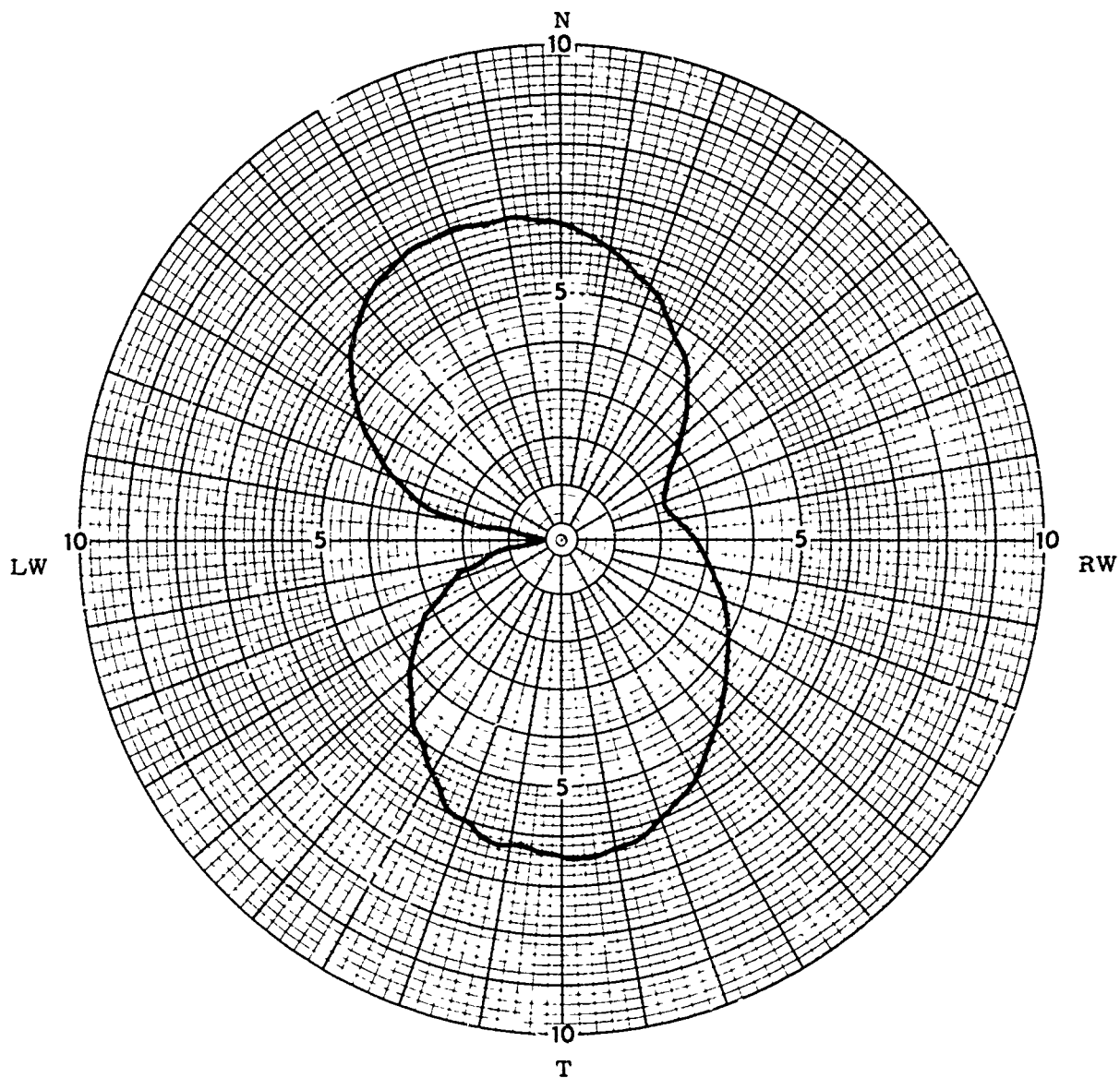
ANTENNA TYPE	LOCATION No. 1.	USE		<input type="checkbox"/>
TEST MODEL: <u>Caribou</u>	FREQUENCY: <u>2</u> MCS	SCALE FREQUENCY: <u>100</u> MCS		<input type="checkbox"/>
MODEL SCALE: <u>1/50</u>	POLARIZATION:			<input type="checkbox"/>
CONDITIONS: <u>Azimuth $\theta = 90^\circ$</u>	E θ : <input checked="" type="checkbox"/>	E ϕ : <input type="checkbox"/>		
CURVES PLOTTED IN:	PATTERN AREA: <input type="text"/>			
VOLTAGE <input checked="" type="checkbox"/>				
POWER <input type="checkbox"/>				
ENGINEER	OPERATOR	FILE NO.	DATE	

Fig. A-4.



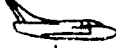


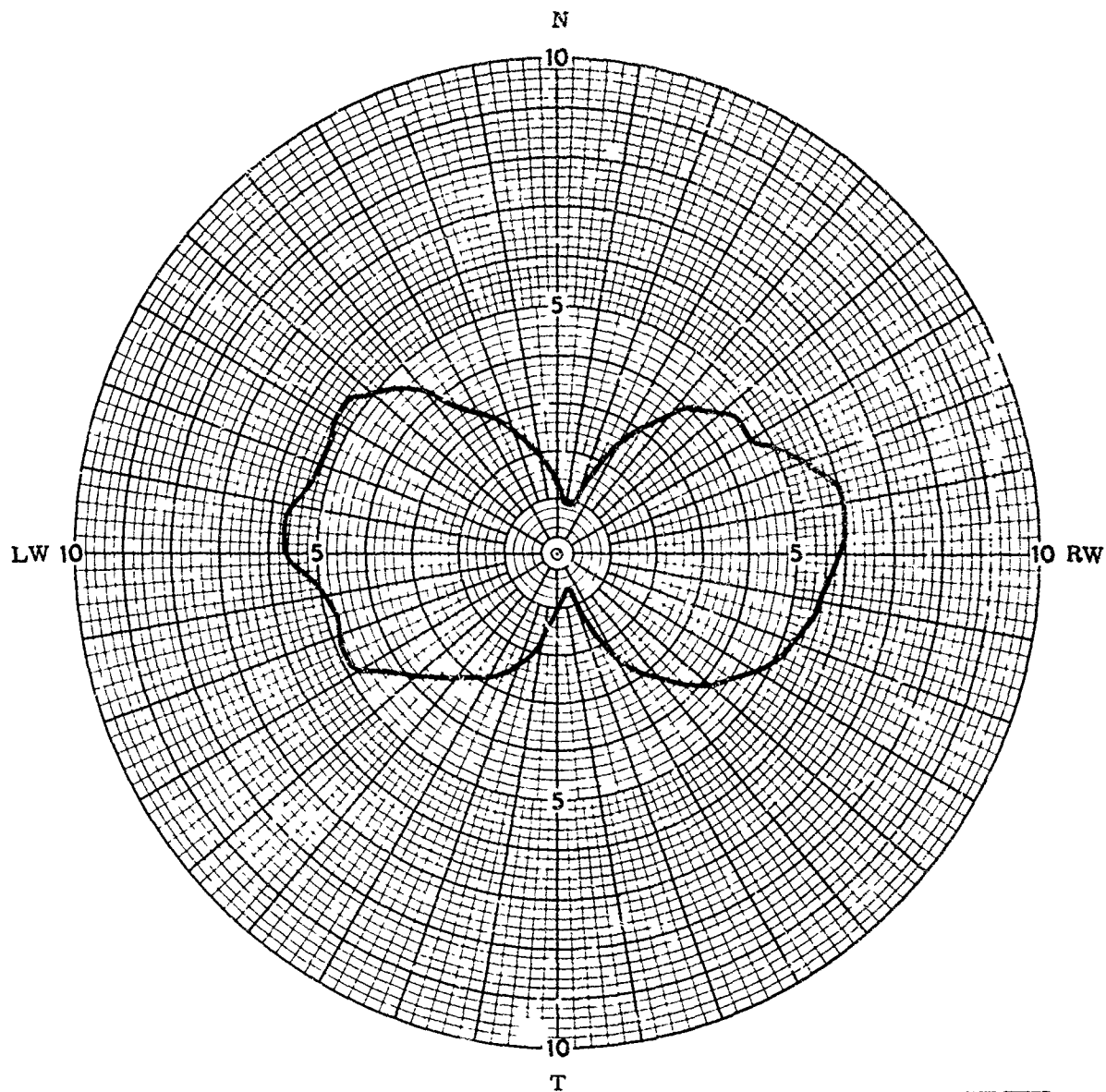
ANTENNA TYPE	LOCATION	No. 1	USE	
TEST MODEL: <u>Caribou</u>			FREQUENCY: <u>2</u> MCS	 <input type="checkbox"/>
MODEL SCALE: <u>1/50</u>			SCALE FREQUENCY: <u>100</u> MCS	 <input type="checkbox"/>
CONDITIONS: <u>Azimuth</u>	$\theta = 90^\circ$		POLARIZATION:	
CURVES PLOTTED IN:			E θ : _____	
VOLTAGE \downarrow _____			E ϕ : \downarrow _____	 _____°
POWER _____			PATTERN AREA: _____	
ENGINEER _____	OPERATOR _____	FILE NO. _____	DATE _____	

Fig. A-5.



ANTENNA TYPE	LOCATION	No. 1	USE
TEST MODEL: <u>Caribou</u>			FREQUENCY: <u>15</u> MCS
MODEL SCALE: <u>1/50</u>			SCALE FREQUENCY: <u>750</u> MCS
CONDITIONS: <u>Azimuth $\theta = 90^\circ$</u>			POLARIZATION:
CURVES PLOTTED IN:			E θ : <u>Y</u>
VOLTAGE <u>1</u>			E ϕ : _____
POWER _____			PATTERN AREA: _____
ENGINEER _____	OPERATOR _____	FILE NO. _____	DATE _____

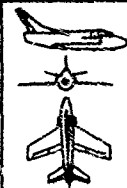
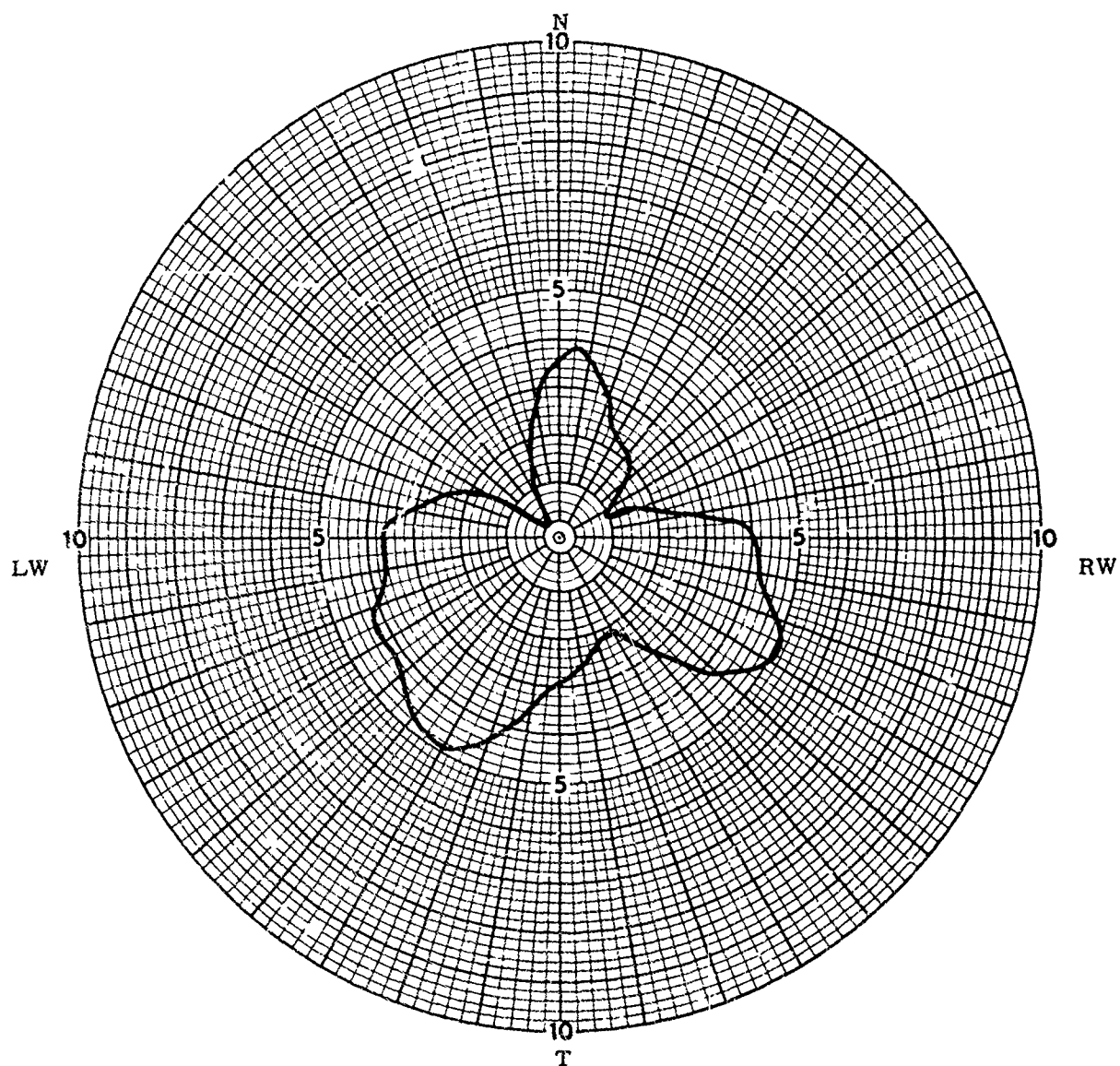


Fig. A-6. Azimuth Patterns--Location 1, 750 MHz, E



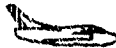


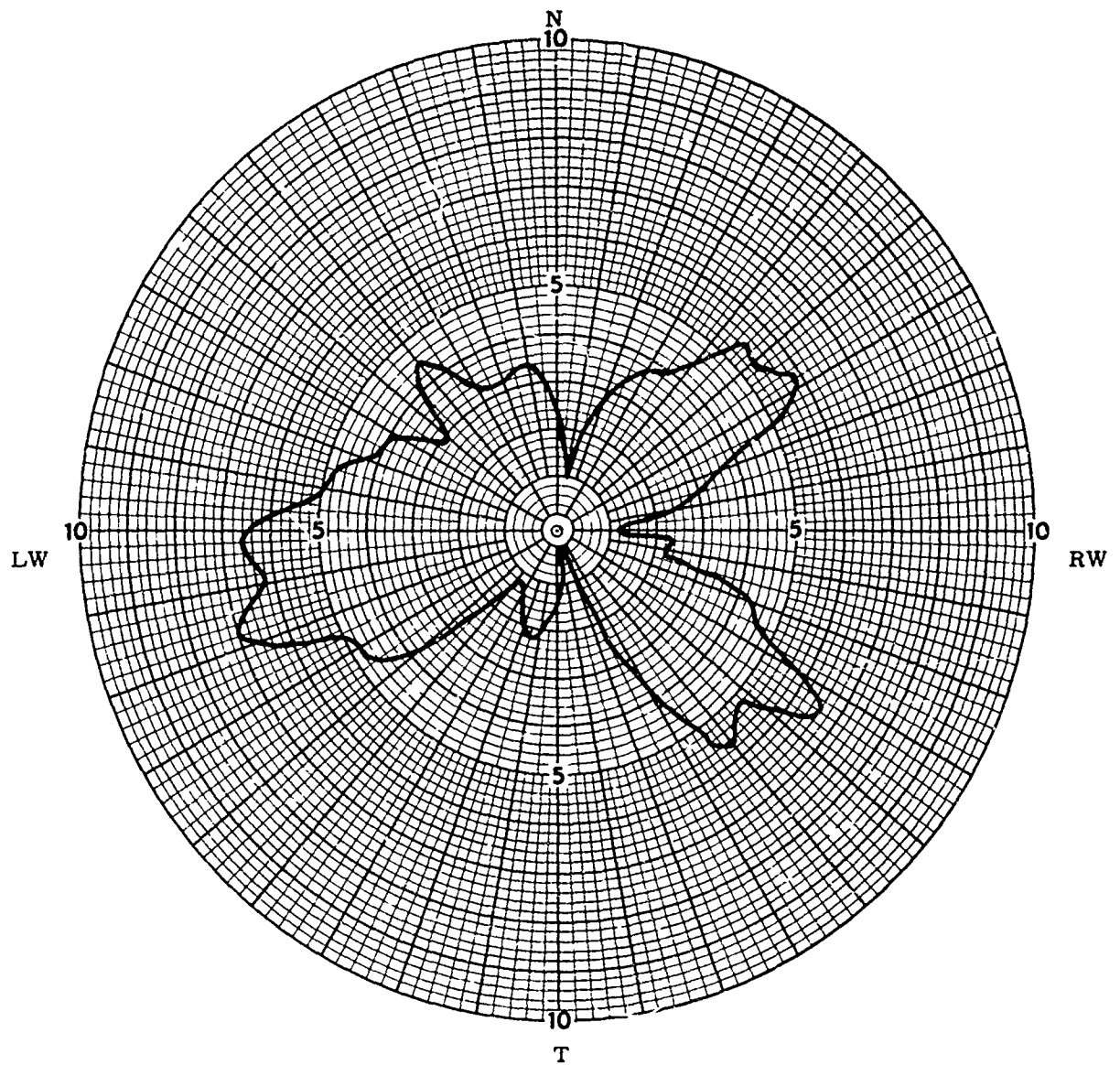
ANTENNA TYPE	LOCATION	No. 1	USE		<input type="checkbox"/>
TEST MODEL: <u>Caribou</u>			FREQUENCY: <u>15</u> MCS		<input type="checkbox"/>
MODEL SCALE: <u>1/50</u>			SCALE FREQUENCY: <u>750</u> MCS		<input type="checkbox"/>
CONDITIONS: <u>Azimuth $\theta = 90^\circ$</u>			POLARIZATION:		<input type="checkbox"/>
CURVES PLOTTED IN:			E θ :		<input type="checkbox"/>
VOLTAGE <u>V</u>			E ϕ :		<input type="checkbox"/>
POWER			PATTERN AREA:		<input type="checkbox"/>
ENGINEER	OPERATOR	FILE NO	DATE		

Fig. A-7. Azimuth Patterns--Location 1, 750 MHz, E



ANTENNA TYPE	LOCATION	No. 1	USE
TEST MODEL: <u>Caribou</u>			FREQUENCY: <u>30</u> MCS
MODEL SCALE: <u>1/50</u>			SCALE FREQUENCY: <u>1500</u> MCS
CONDITIONS: <u>Azimuth $\theta = 90^\circ$</u>			POLARIZATION:
CURVES PLOTTED IN:			E θ : <u>V</u>
VOLTAGE <u>3</u>			E ϕ : _____
POWER _____			PATTERN AREA: _____
ENGINEER	OPERATOR	FILE NO.	DATE

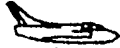
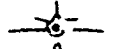

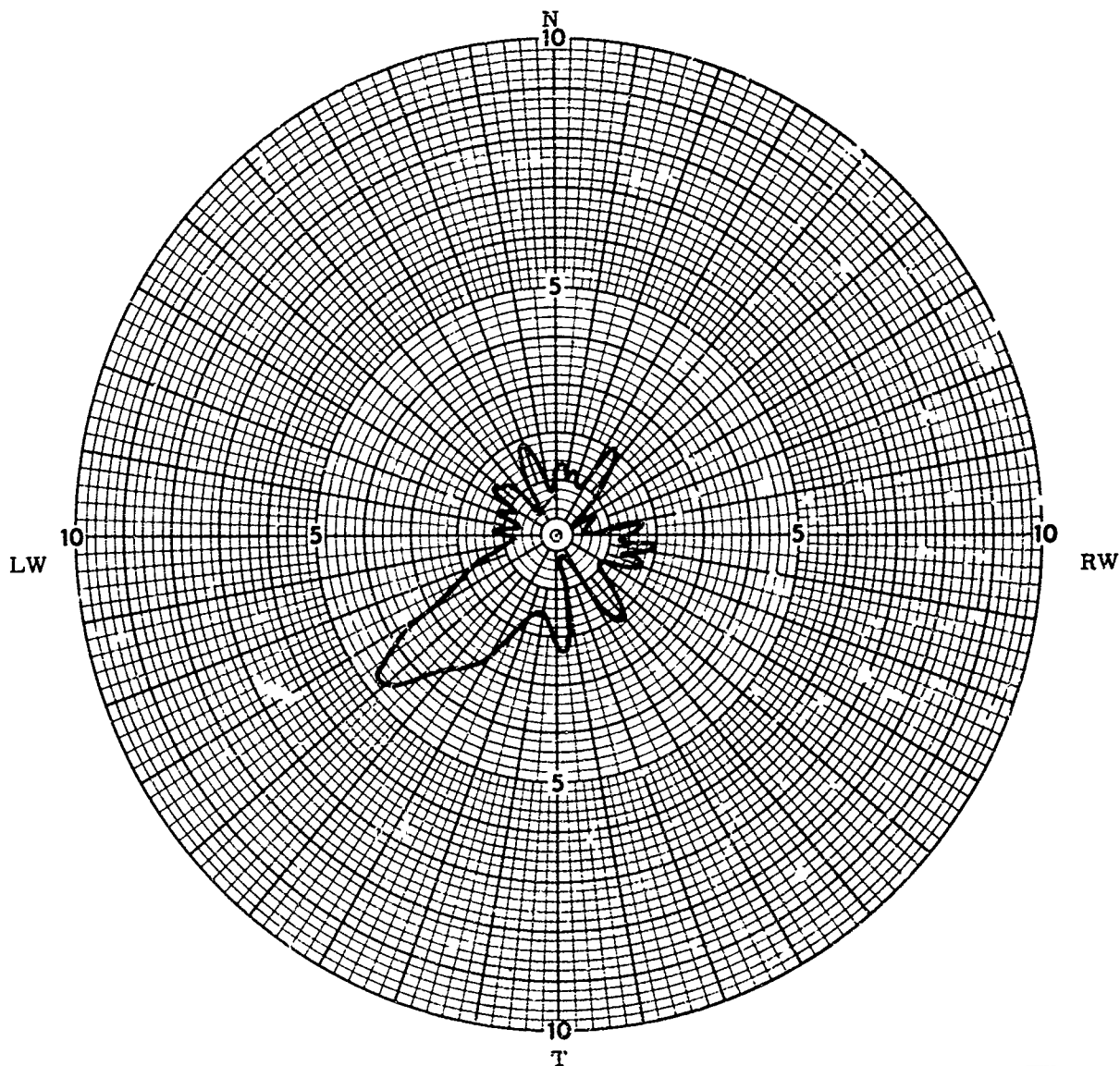

☐

☐

☐

Fig. A-8. Azimuth Patterns--Location 1, 1500 MHz, E






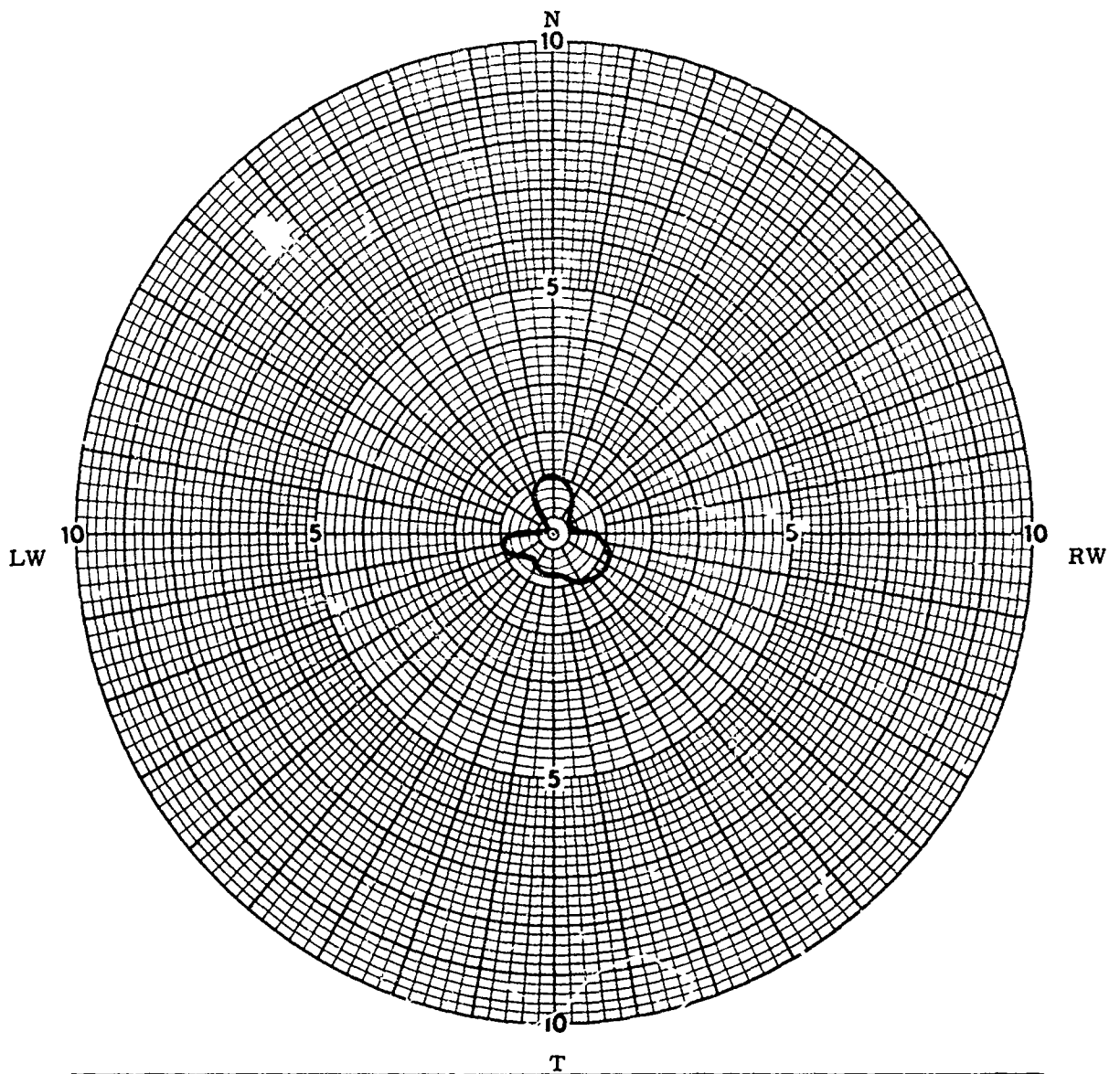
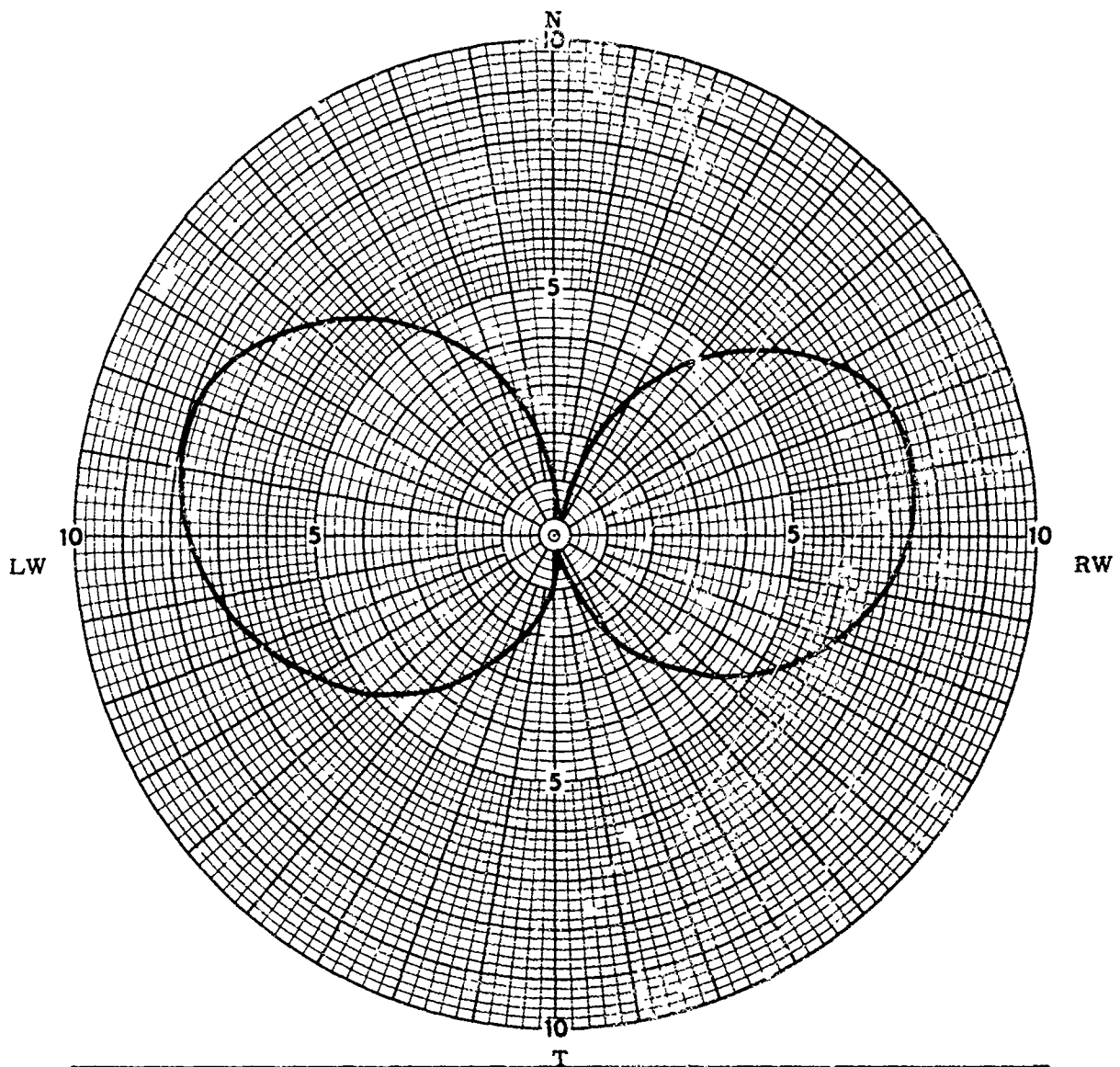
ANTENNA TYPE	LOCATION No. 1	USE
TEST MODEL: <u>Caribou</u>	FREQUENCY: <u>30</u> MCS	 <input type="checkbox"/>
MODEL SCALE: <u>1/50</u>	SCALE FREQUENCY: <u>1500</u> MCS	 <input type="checkbox"/>
CONDITIONS: <u>Azimuth $\theta = 90^\circ$</u>	POLARIZATION:	 <input type="checkbox"/>
CURVES PLOTTED IN:	E θ : _____	_____°
VOLTAGE <u>V</u>	E ϕ : <u>V</u>	
POWER _____	PATTERN AREA: _____	
ENGINEER	OPERATOR	FILE NO. DATE

Fig. A-9. Azimuth Patterns--Location 1, 1500 MHz, E



ANTENNA TYPE	LOCATION	No. 2	USE
TEST MODEL: <u>Caribou</u>			FREQUENCY: <u>2</u> MCS
MODEL SCALE: <u>1/50</u>			SCALE FREQUENCY: <u>100</u> MCS
CONDITIONS: <u>Azimuth $\theta = 90^\circ$</u>			POLARIZATION:
CURVES PLOTTED/IN:			E θ : <u>↓</u>
VOLTAGE <u>↓</u>			E ϕ : <u> </u>
POWER <u> </u>			PATTERN AREA: <u> </u>
ENGINEER	OPERATOR	FILE NO.	DATE

Fig. A-10. Azimuth Patterns--Location 2, 100 MHz. E






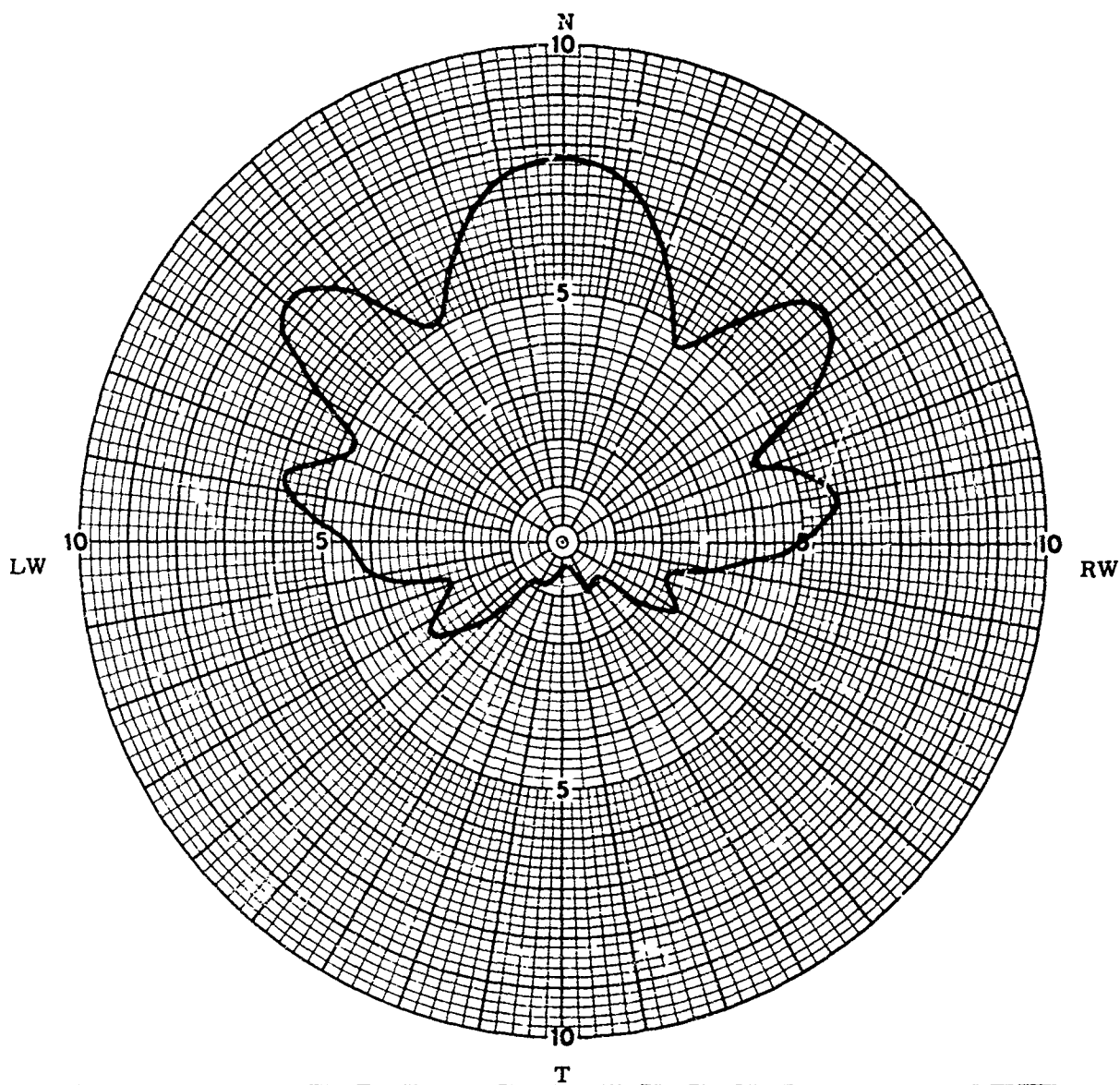
ANTENNA TYPE	LOCATION	No. 2	USE		<input type="checkbox"/>
TEST MODEL: <u>Caribou</u>			FREQUENCY: <u>2</u> MCS		<input type="checkbox"/>
MODEL SCALE: <u>1/50</u>			SCALE FREQUENCY: <u>100</u> MCS		<input type="checkbox"/>
CONDITIONS: <u>Azimuth $\theta = 90^\circ$</u>			POLARIZATION:		<input type="checkbox"/>
CURVES PLOTTED IN:			E θ : _____		<input type="checkbox"/>
VOLTAGE <u>V</u>			E ϕ : <u>V</u>		<input type="checkbox"/>
POWER _____			PATTERN AREA: _____		<input type="checkbox"/>
ENGINEER	OPERATOR		NO.	DATE	

Fig. A-11. Azimuth Patterns--Location 2, 100 MHz, E






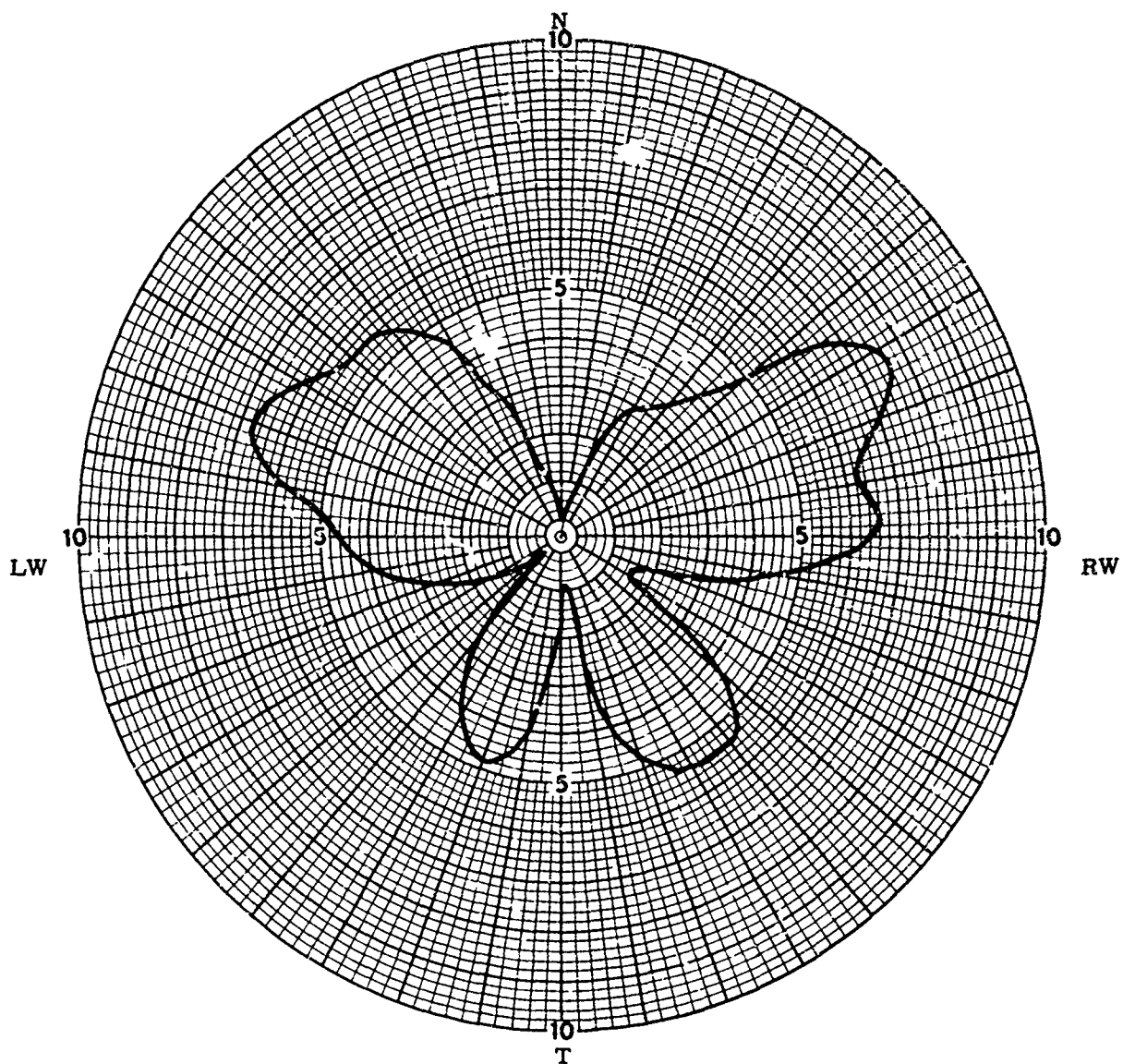
ANTENNA TYPE	LOCATION	No. 2	USE		<input type="checkbox"/>
TEST MODEL: <u>Caribou</u>			FREQUENCY: <u>15</u> MCS		<input type="checkbox"/>
MODEL SCALE: <u>1/50</u>			SCALE FREQUENCY: <u>750</u> MCS		<input type="checkbox"/>
CONDITIONS: <u>Azimuth $\theta = 90^\circ$</u>			POLARIZATION:		<input type="checkbox"/>
CURVES PLOTTED IN:			E θ : <u>V</u>		<input type="checkbox"/>
VOLTAGE: <u>V</u>			E ϕ :		<input type="checkbox"/>
POWER:			PATTERN AREA:		<input type="checkbox"/>
ENGINEER	OPERATOR	FILE NO.	DATE		

Fig. A-12. Azimuth Patterns--Location 2, 750 MHz, E



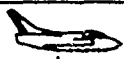


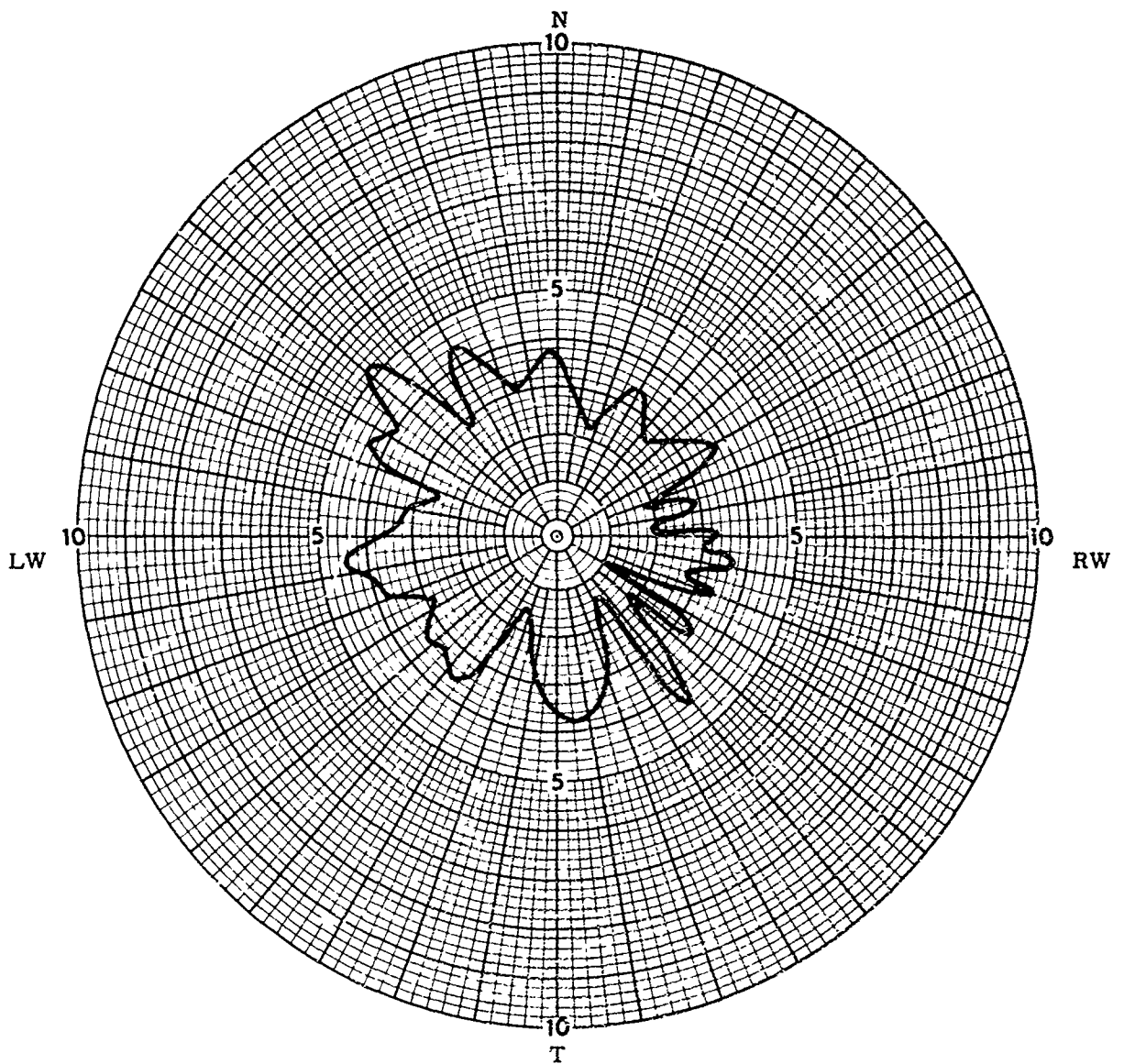
ANTENNA TYPE	LOCATION	No. 2	USE	 <input type="checkbox"/>  <input type="checkbox"/>  <input type="checkbox"/>
TEST MODEL: <u>Caribou</u>	FREQUENCY: <u>15</u> MCS			
MODEL SCALE: <u>1/50</u>	SCALE FREQUENCY: <u>750</u> MCS			
CONDITIONS: <u>Azimuth $\theta = 90^\circ$</u>	POLARIZATION:			
CURVES PLOTTED IN:	E θ : <u> </u>			
VOLTAGE <u>V</u>	E ϕ : <u>V</u>			
POWER <u> </u>	PATTERN AREA: <u> </u>			
ENGINEER	OPERATOR	FILE NO.	DATE	

Fig. A-13. Azimuth Patterns--Location 2, 750 MHz, E



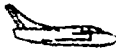
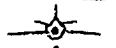

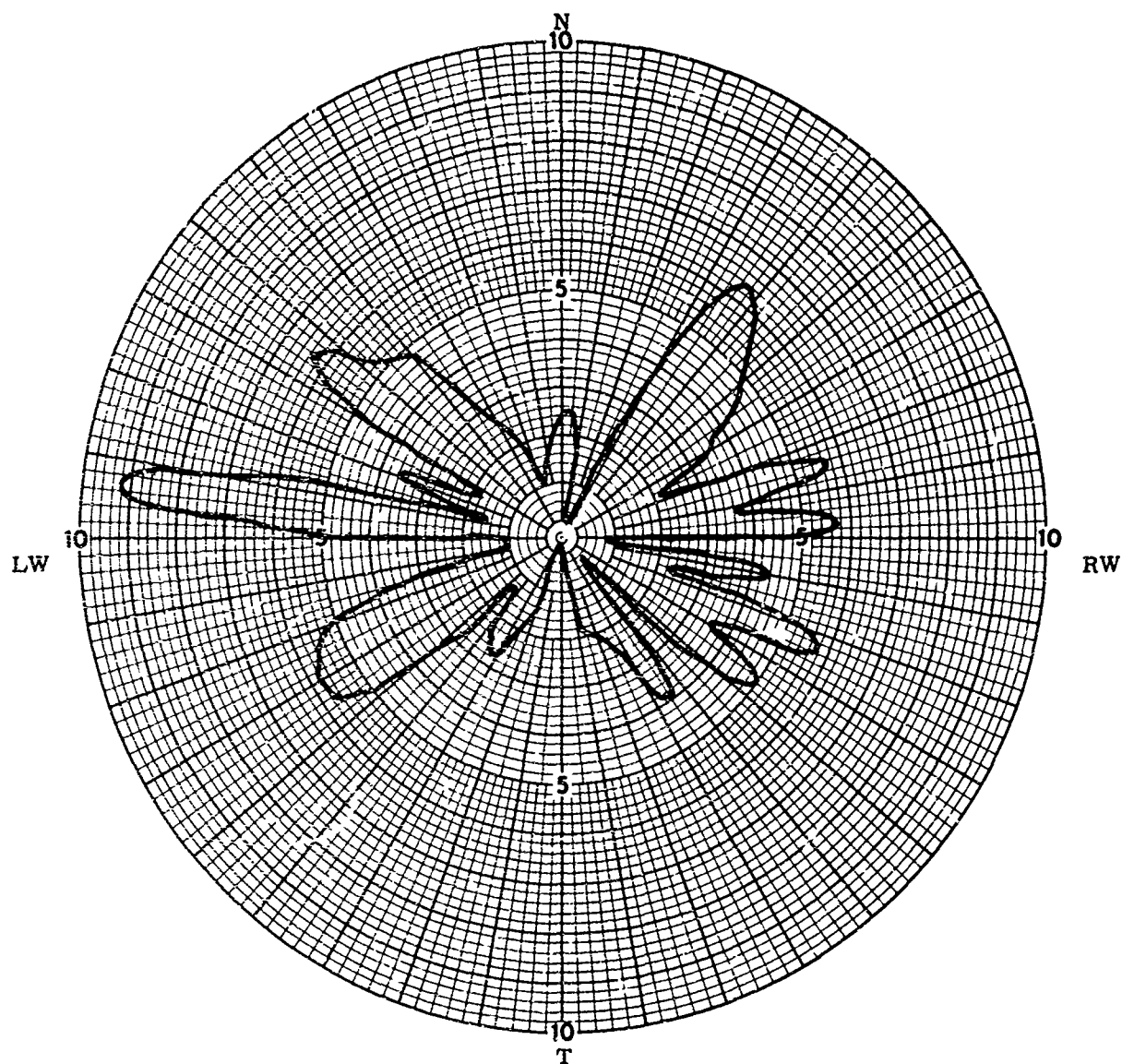
ANTENNA TYPE	LOCATION	No. 2	USE		<input type="checkbox"/>
TEST MODEL: <u>Caribou</u>			FREQUENCY: <u>30</u> MCS		<input type="checkbox"/>
MODEL SCALE: <u>1/50</u>			SCALE FREQUENCY: <u>1500</u> MCS		<input type="checkbox"/>
CONDITIONS: <u>Azimuth $\theta = 90^\circ$</u>			POLARIZATION:		<input type="checkbox"/>
CURVES PLOTTED IN:			E θ : <u>✓</u>		<input type="checkbox"/>
VOLTAGE <u>✓</u>			E ϕ : <u>✓</u>		<input type="checkbox"/>
POWER			PATTERN AREA:		<input type="checkbox"/>
ENGINEER	OPERATOR	FILE NO.	DATE		

Fig. A-14. Azimuth Patterns--Location 2, 1500 MHz, E



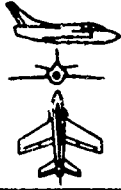
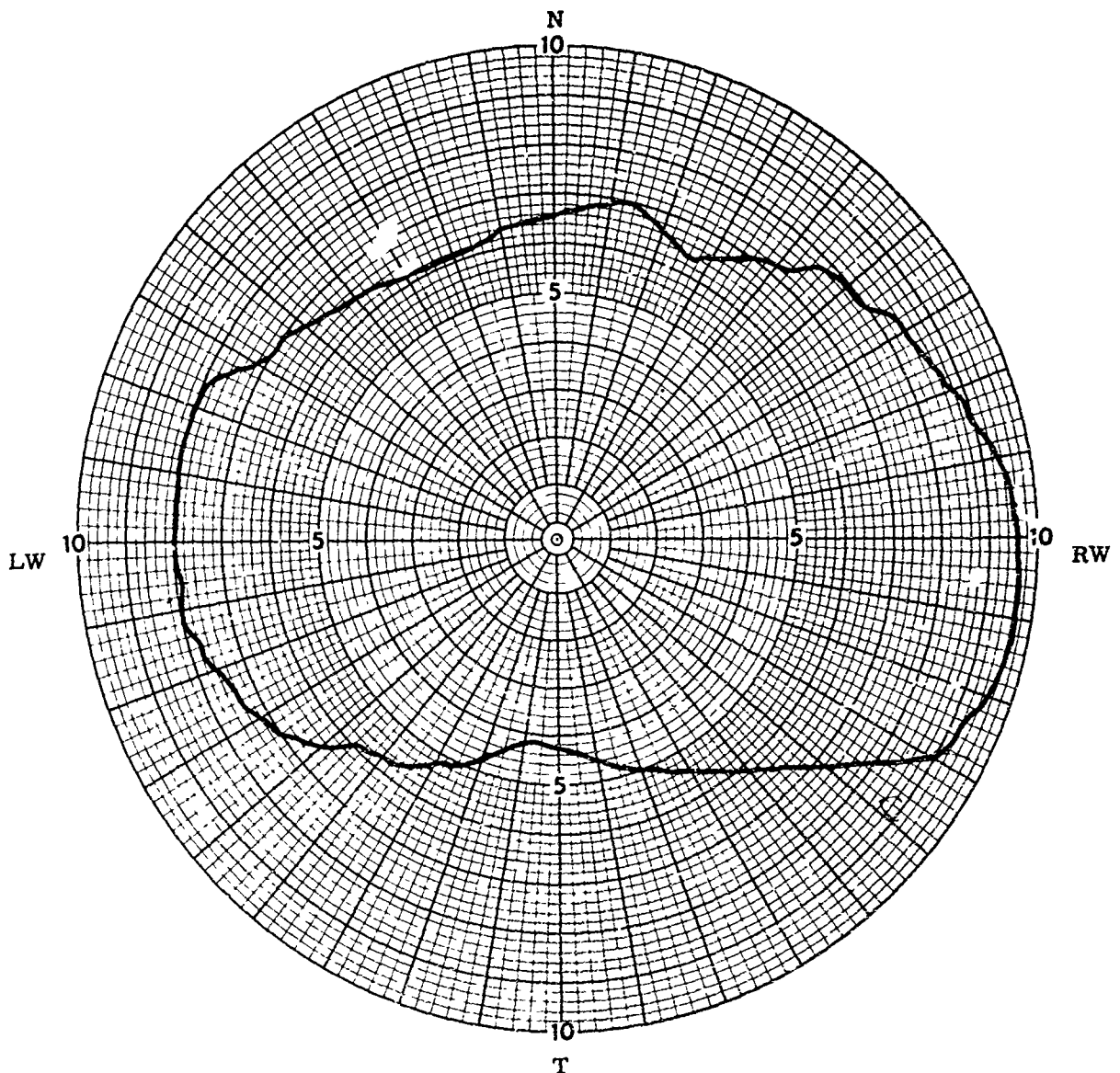
ANTENNA TYPE	LOCATION No. 2	USE	 <input type="checkbox"/> <input type="checkbox"/> <input type="checkbox"/>
TEST MODEL: <u>Caribou</u>	FREQUENCY: <u>30</u> MCS		
MODEL SCALE: <u>1/50</u>	SCALE FREQUENCY: <u>1500</u> MCS		
CONDITIONS: <u>Azimuth $\theta = 90^\circ$</u>	POLARIZATION:		
CURVES PLOTTED IN:	E θ : <u>✓</u>		
VOLTAGE <u>✓</u>	E ϕ : <u>✓</u>		
POWER	PATTERN AREA:		
ENGINEER	OPERATOR	FILE NO.	DATE

Fig. A-15. Azimuth Patterns--Location 2, 1500 MHz, E



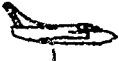


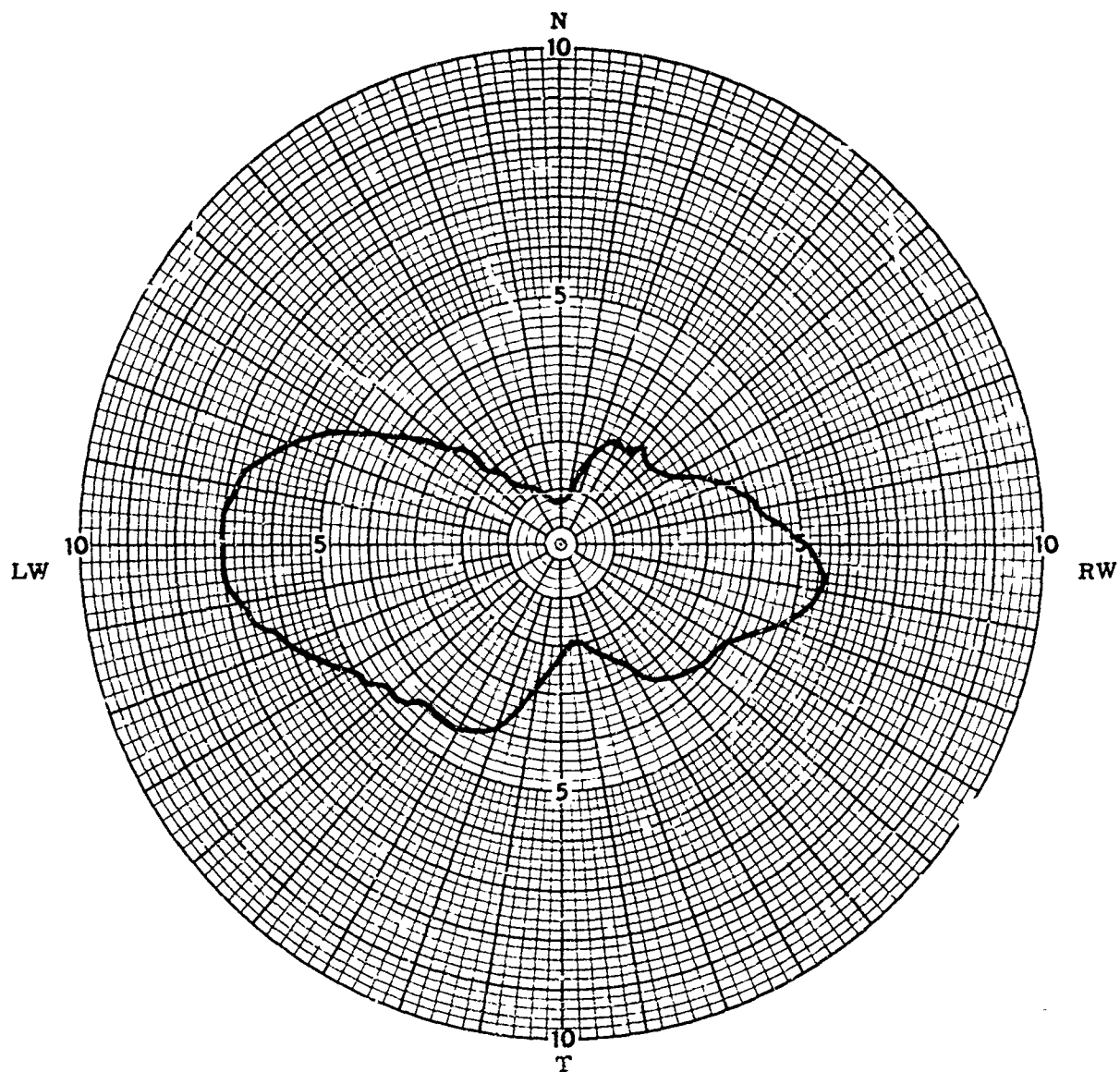
ANTENNA TYPE	LOCATION	No. 3	USE	 <input type="checkbox"/>  <input type="checkbox"/>  <input type="checkbox"/>
TEST MODEL: <u>Caribou</u>	FREQUENCY: <u>2</u> MCS			
MODEL SCALE: <u>1/50</u>	SCALE FREQUENCY: <u>100</u> MCS			
CONDITIONS: <u>Azimuth $\theta = 90^\circ$</u>	POLARIZATION:			
CURVES PLOTTED IN:	E θ : <u> </u>			
VOLTAGE <u> </u>	E ϕ : <u> </u>			
POWER <u> </u>	PATTERN AREA: <u> </u>			
ENGINEER	OPERATOR	FILE NO.	DATE	

Fig. A-16. Azimuth Patterns--Location 3, 100 MHz, E






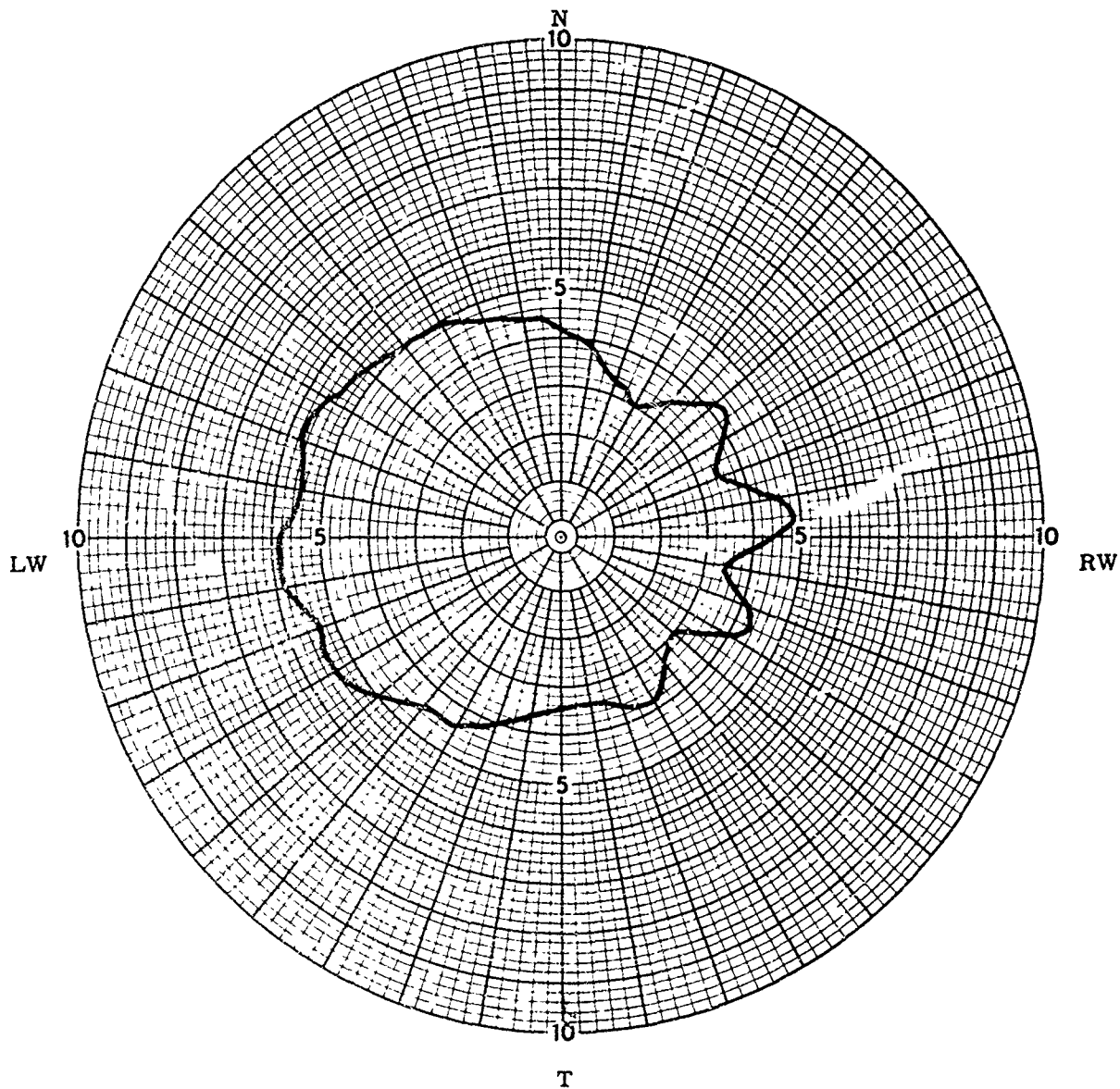
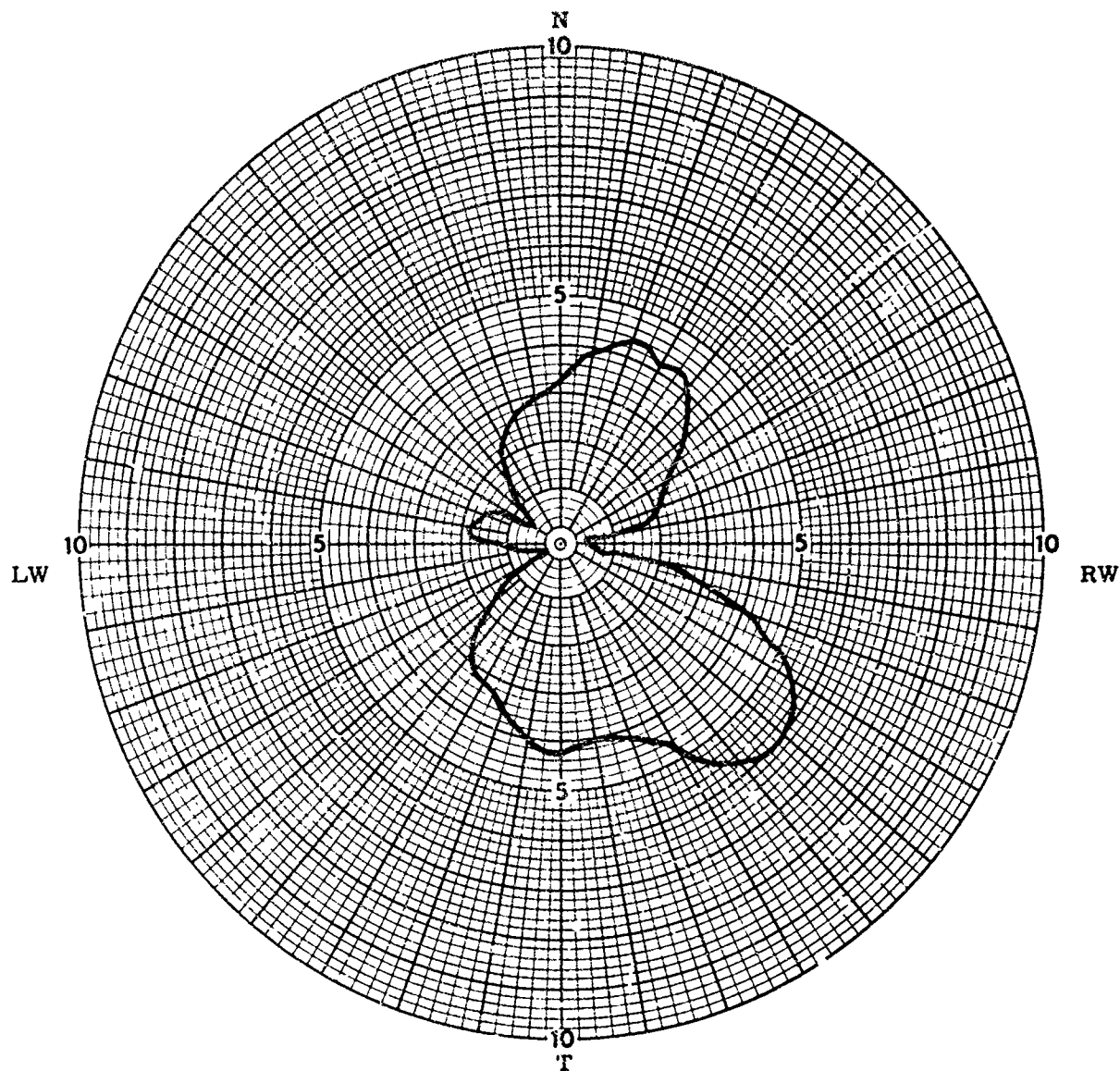
ANTENNA TYPE	LOCATION No. 3	USE		<input type="checkbox"/>
TEST MODEL: <u>Caribou</u>	FREQUENCY: <u>2</u> MCS			<input type="checkbox"/>
MODEL SCALE: <u>1/50</u>	SCALE FREQUENCY: <u>100</u> MCS			<input type="checkbox"/>
CONDITIONS: <u>Azimuth $\theta = 90^\circ$</u>	POLARIZATION:			<input type="checkbox"/>
CURVES PLOTTED IN:	E θ : <u> </u>			<input type="checkbox"/>
VOLTAGE <u>V</u>	E ϕ : <u>V</u>			<input type="checkbox"/>
POWER <u> </u>	PATTERN AREA: <u> </u>			<input type="checkbox"/>
ENGINEER	OPERATOR	FILE NO.	DATE	

Fig. A-17. Azimuth Patterns--Location 3, 100 MHz, E



ANTENNA TYPE	LOCATION	No. 3	USE
TEST MODEL: <u>C. ribou</u>	FREQUENCY: <u>15</u> MCS		
MODEL SCALE: <u>1/50</u>	SCALE FREQUENCY: <u>750</u> MCS		
CONDITIONS: <u>Azimuth $\theta = 90^\circ$</u>	POLARIZATION:		
CURVES PLOTTED IN:	E θ : <u>✓</u>		
VOLTAGE <u>V</u>	E ϕ :		
POWER	PATTERN AREA:		
ENGINEER	OPERATOR	FILE NO.	DATE

Fig. A-18. Azimuth Patterns--Location 3, 750 MHz, E



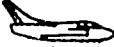


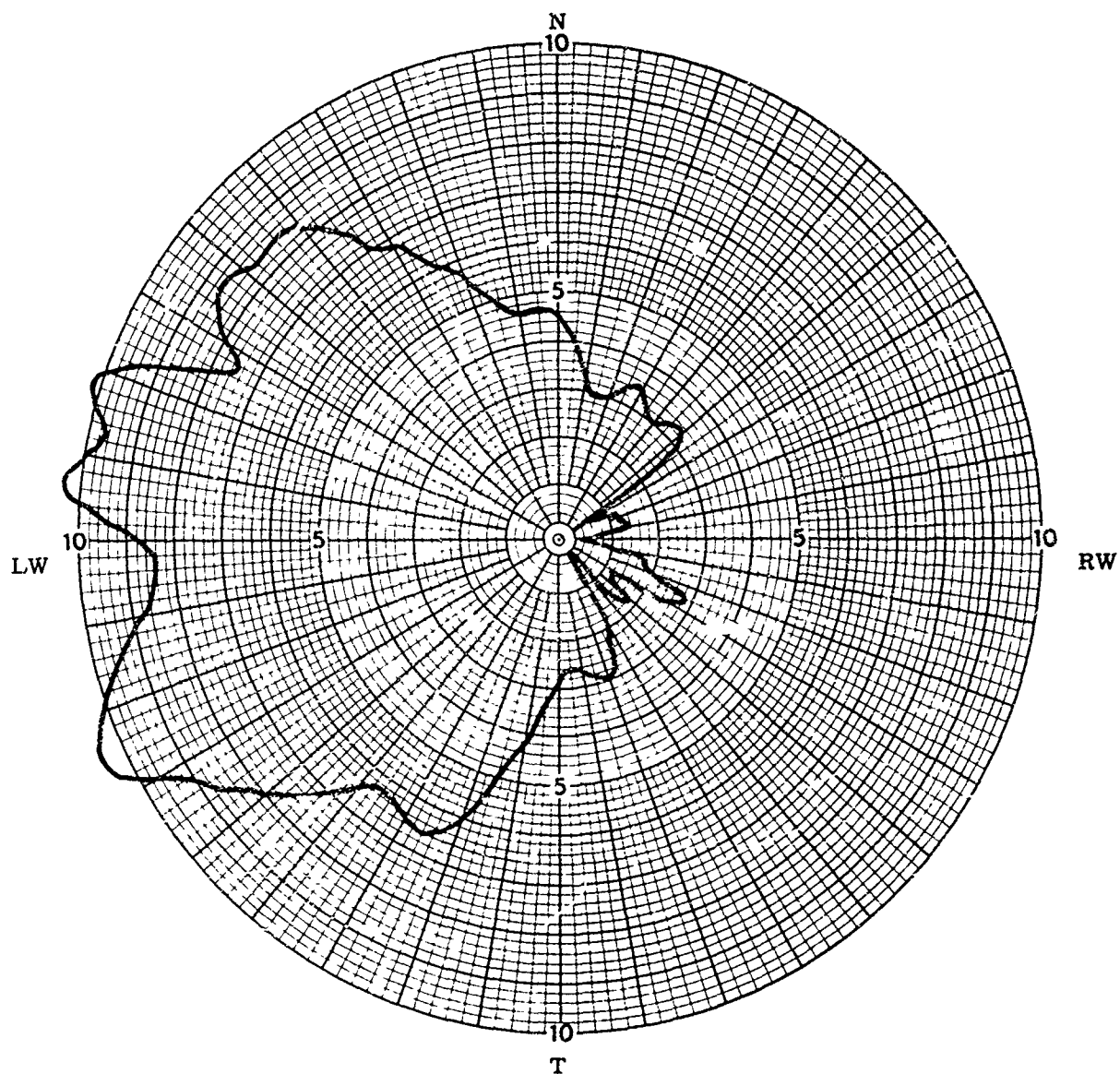
ANTENNA TYPE	LOCATION	No. 3	USE		<input type="checkbox"/>
TEST MODEL: <u>Caribou</u>			FREQUENCY: <u>15</u> MCS		<input type="checkbox"/>
MODEL SCALE: <u>1/50</u>			SCALE FREQUENCY: <u>750</u> MCS		<input type="checkbox"/>
CONDITIONS: <u>Azimuth $\theta = 90^\circ$</u>			POLARIZATION:		<input type="checkbox"/>
CURVES PLOTTED IN:			E θ : _____		<input type="checkbox"/>
VOLTAGE <u>V</u>			E ϕ : <u>V</u>		<input type="checkbox"/>
POWER _____			PATTERN AREA: _____		<input type="checkbox"/>
ENGINEER	OPERATOR	FILE NO.	DATE		

Fig. A-19. Azimuth Patterns--Location 3, 750 MHz, E



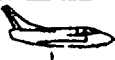


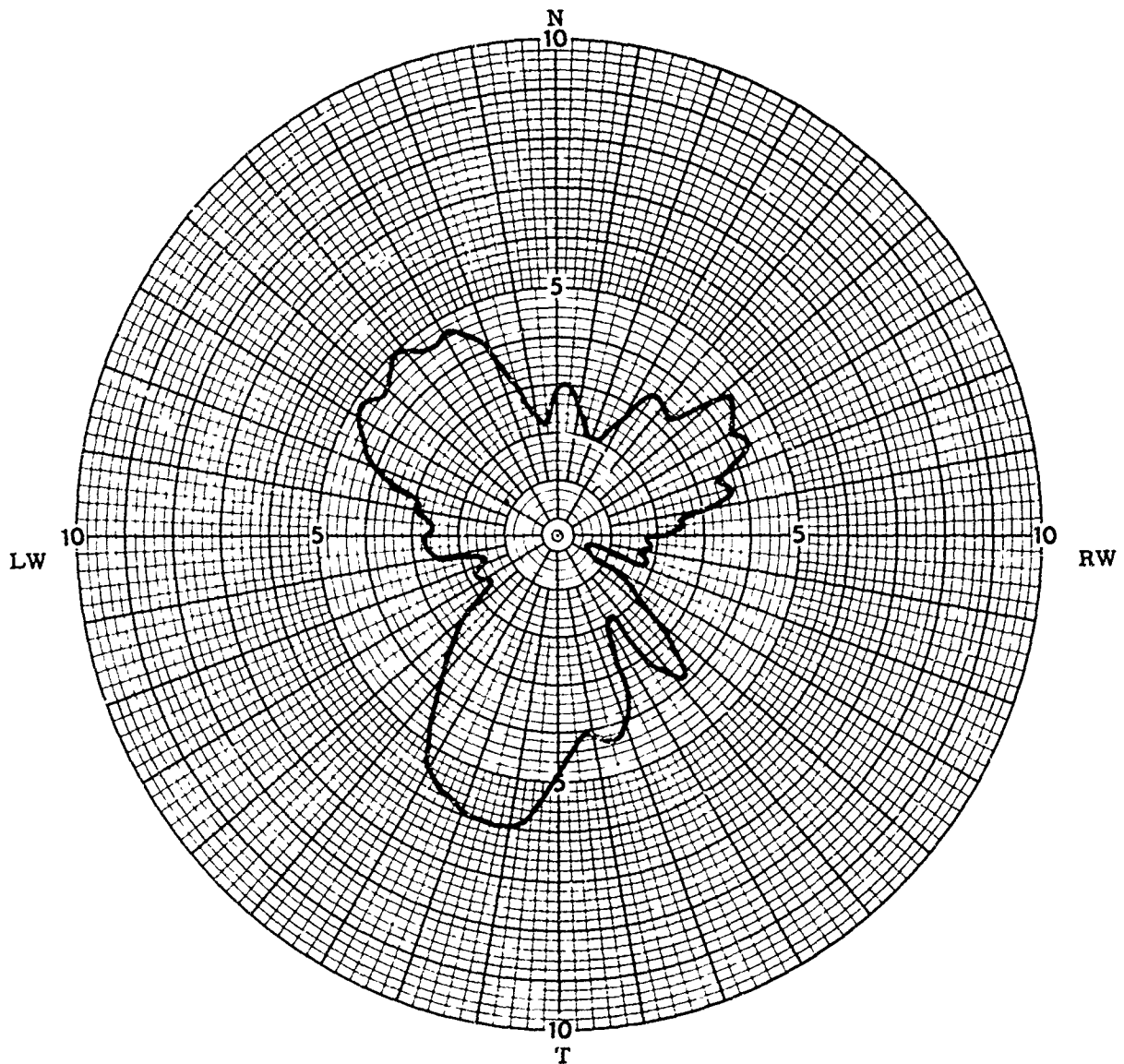
ANTENNA TYPE	LOCATION No. 3	USE	 <input type="checkbox"/>  <input type="checkbox"/>  <input type="checkbox"/>
TEST MODEL: <u>Caribou</u>	FREQUENCY: <u>30</u> MCS		
MODEL SCALE: <u>1/50</u>	SCALE FREQUENCY: <u>1500</u> MCS		
CONDITIONS: <u>Azimuth $\theta = 90^\circ$</u>	POLARIZATION:		
CURVES PLOTTED IN:	E θ : <u>3</u>		
VOLTAGE: <u>3</u>	E ϕ :		
POWER	PATTERN AREA:		
ENGINEER	OPERATOR	FILE NO.	DATE

Fig. A-20. Azimuth Patterns--Location 3, 1500 MHz, E






ANTENNA TYPE	LOCATION	No. 3	USE		<input type="checkbox"/>
TEST MODEL: <u>Caribou</u>			FREQUENCY: <u>30</u> MCS		<input type="checkbox"/>
MODEL SCALE: <u>1/50</u>			SCALE FREQUENCY: <u>1500</u> MCS		<input type="checkbox"/>
CONDITIONS: <u>Azimuth $\theta = 90^\circ$</u>			POLARIZATION:		
CURVES PLOTTED IN:			E θ : <input checked="" type="checkbox"/>		
VOLTAGE <input checked="" type="checkbox"/>			E ϕ : <input checked="" type="checkbox"/>		
POWER			PATTERN AREA:		
ENGINEER	OPERATOR	FILE NO.	DATE		

Fig. A-21. Azimuth Patterns--Location 3, 1500 MHz, E



Fig. A-22. Typical Construction of Impedance Mockup (Sikorsky C-4-3C shown)

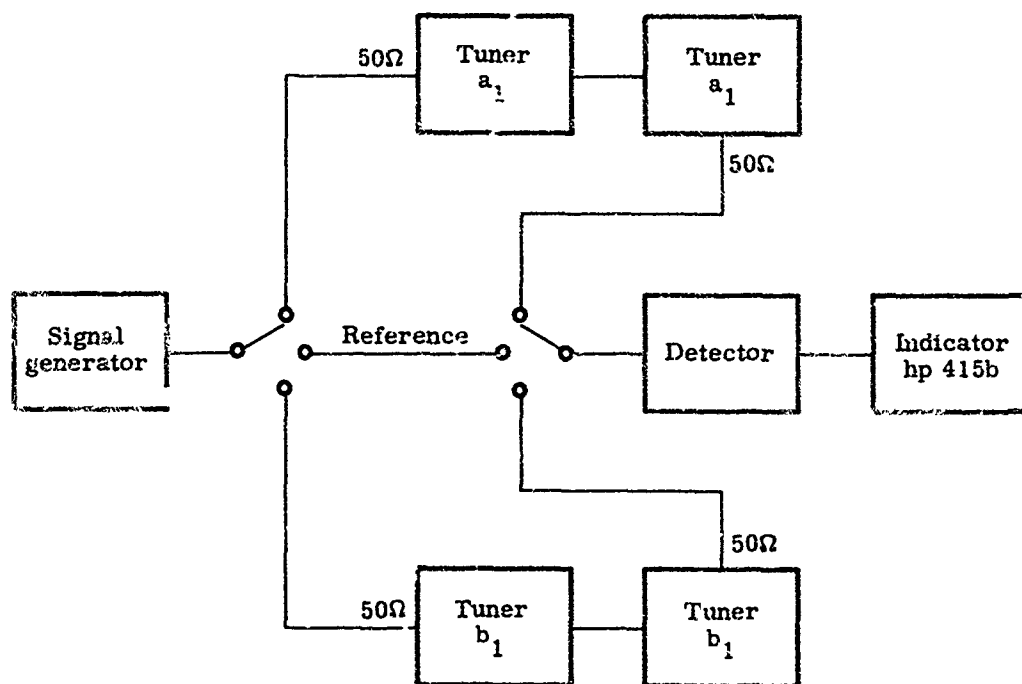


Fig. A-23. Test Setup for Determining Tuner Losses

APPENDIX B
TEST PLAN
FOR
COMPACT H-F AIRCRAFT ANTENNAS

I. INTRODUCTION

This test plan describes the procedures, methods, techniques and limits to be utilized in testing the 1/5-scale Exploratory Development Model H-F antennas. A brief discussion of the design objectives applicable to these 1/5-scale models is presented. The tests to be performed are outlined in the following order: Impedance, Gain, Radiation Patterns.

II. GENERAL DESIGN OBJECTIVES

The Exploratory Development Models are comprised of two 1/5-scale antennas with manual tuners. Since these models are 1/5 scale, the frequency range of interest for these tests will be from 10 to 150 MHz as outlined in the Design Plan.

The design objectives relevant to these 1/5-scale models are listed as follows:

Tuning range	10 to 150 MHz
Efficiency and gain	Better than a 3-ft monopole over a good ground plane
Polarization	Vertical
Azimuth coverage	Omnidirectional
VSWR	2:1 max
Input impedance	50 ohms unbalanced
Size	4.8 in. in the maximum dimension

The power and bandwidth requirements are not listed here since these parameters are applicable to the full-scale models.

III. IMPEDANCE

The impedance testing is divided into two parts: measurement of the antenna impedance without manual tuner and measurement of VSWR with the manual tuner installed.

The basic test setup for measuring the antenna impedance is illustrated in Fig. B-1. A Boonton Radio R-X meter, Model 250-A, is mounted within the 1/5-scale aircraft with its measurement terminals (coaxial fitting) protruding through the aircraft skin. The outer conductor of the coaxial connector is grounded to the skin of the aircraft, while the antenna is connected to the center conductor of the same coaxial adapter. Preliminary adjustments are made from the roof top of the laboratory building with the mockup and support stand adjacent to the building. The movable test stand with mockup is then wheeled about 15 ft away from the building. Remote tuning of the R-X meter is then performed by employing a long bamboo pole approximately 16 ft in length.

At the low frequency end of the band, auxiliary shunt capacitors are employed at the antenna terminals when the test instrument lacks adequate capacity for tuning. Values of parallel resistance and parallel capacitance are recorded at each frequency. An IBM 1620 computer is then used to reduce the data to the series equivalent resistance and reactance components, as well as the magnitude of the complex impedance at the antenna terminals. If cable lengths are employed between the test instrument and the antenna terminals, the computer program is also set up to handle this condition. Details of the computer program relating Z_{measured} to Z_{load} are outlined in the Design Plan. Values of R, X, and Z for each frequency of measurement will be recorded on the provided data sheets.

The measurement test setup for VSWR with the manual tuner installed is illustrated in Fig. B-2. The manual tuner, comprised of LC networks, is shown in Fig. B-3. Initially, a 50-ohm coaxial load is placed at the output end of the cable connected to the R-X meter. The R-X meter bridge instrument is balanced to read $R_p = 50$ ohms and $C_p = 0$ pf. With the bridge (R-X meter) balanced for a 50-ohm resistive load, the manual tuner is then connected to the R-X meter cable and the antenna matched out. The range of R_p can vary from 25 to 100 ohms which corresponds to a VSWR of 2:1 or less.

In order to accommodate the physical location of the test equipment and to ensure the best accuracy of measurement, the antenna will be located atop the fuselage at the trailing edge of the wings of the Caribou. For the Iroquois aircraft, the antenna location for these tests will be atop the fuselage above the cabin area.

IV. GAIN

The gain measurement test setup is shown in Fig. B-4. This test will consist of comparing the gain of the 1/5-scale H-F antenna relative to a 3-ft monopole.

The vertical polarized source antenna will be located equidistant from the monopole and H-F antenna. The 1/5-scale aircraft mockup will be mounted on a swivel platform and rotated for a maximum detected power level on a HP-415, 1000-cycle amplifier. The variable attenuators, detector, and amplifier and manual tuner are enclosed within the mockup. The reference monopole is mounted on a 12- x 12-ft wire mesh ground plane with wire mesh enclosure (3 x 3 x 3 ft) located underneath. The 3-ft monopole with ground plane and the 1/5-scale Caribou with the rotating platform are shown in Fig. B-5.

The basic gain measuring test sequence is now described. The choice of antenna to be measured first is arbitrary. With the vertical polarized source antenna radiating at some prescribed distance (50 to 100 ft) toward the test antenna, the manual tuner is manipulated for maximum received power. When the H-F antenna is matched out, the aircraft is then rotated for maximum received power. A reference level and attenuator settings are then noted remotely by a transit. The source generator is then disconnected from its antenna, and a piece of RG-58A/U coaxial cable is connected between the generator and attenuator input. The amount of attenuation required to obtain the original reference level is then noted as $-G_{12}(\text{dB})$ or $-G_{13}(\text{dB})$ which are the insertion losses of the H-F and whip links, respectively. The gain of the H-F antenna relative to the monopole with tuner losses present is therefore $-G_{12}(\text{dB}) - [-G_{13}(\text{dB})]$.

Manual tuner losses will be accounted for in each to obtain the true relative gain. The manual tuners for both the H-F and 3-ft monopole antennas will be precalibrated before the gain measurement tests. Each will be calibrated for component settings and insertion loss from 10 to 150 MHz. The tuner insertion loss measurement test setup is shown in Figs. B-6a and B-6b. Initially, the manual tuner is tuned for a matched condition as outlined in the impedance tests. A reference power level is set on the receiver shown in Fig. B-6a. Two manual tuners are then connected as shown in Fig. B-6b. The second conjugate tuner is employed and required to simulate the antenna impedance for maximum power output in order to account for the true tuner losses. The H-F antenna tuner remains fixed, while the conjugate tuner is manipulated for a maximum power output indication noted on the receiver. The difference in this level and the indicated reference level of Fig. B-6a is noted. The actual insertion loss of a single H-F manual tuner is this difference in power levels divided by two. The tuners will be calibrated at each frequency of interest from 10 through 150 MHz. The calibration of the monopole manual tuner is accomplished by the same procedure. Tuner insertion loss, relative gain levels in dB, and true relative gain will be recorded as a function of frequency. The true relative gain expression from the data is expressed as follows:

$$(-G_{12} + IL_2) - (-G_{13} + IL_3) \text{ where:}$$

- G_{12} is insertion loss of H-F link
- G_{13} is insertion loss of monopole link
- IL_2 is the insertion loss of H-F antenna tuner
- IL_3 is the insertion loss of monopole tuner.

The retransmission mode decoupling measurement between two antennas is shown in Fig. B-7. This test will consist of measuring the insertion loss (decoupling) between two 1/5-scale antennas with a minimum separation of one foot. Each antenna will be matched out with a manual tuner as previously outlined. Tuner losses are again accounted for to obtain the true decoupling losses. Decoupling measurements will be taken from 10 through 150 MHz. The measured results will be recorded on the provided data sheets.

V. PATTERNS

A 1/50-scale model of the Caribou and a 1/25-scale model of the Iroquois aircraft are used for the radiation pattern testing. For the sake of brevity and economy, spot frequency checks will be made at frequencies appropriate to each model aircraft. Patterns will be taken in the azimuth plane with vertical polarization. These patterns will then be included as part of the test data results. The coordinate system will be as outlined in the Design Plan. Frequency, aircraft, location and polarization will be noted on each pattern plot.

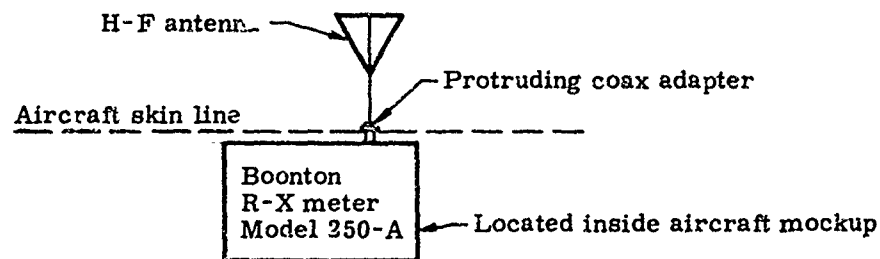


Fig. B-1. Impedance Test Setup

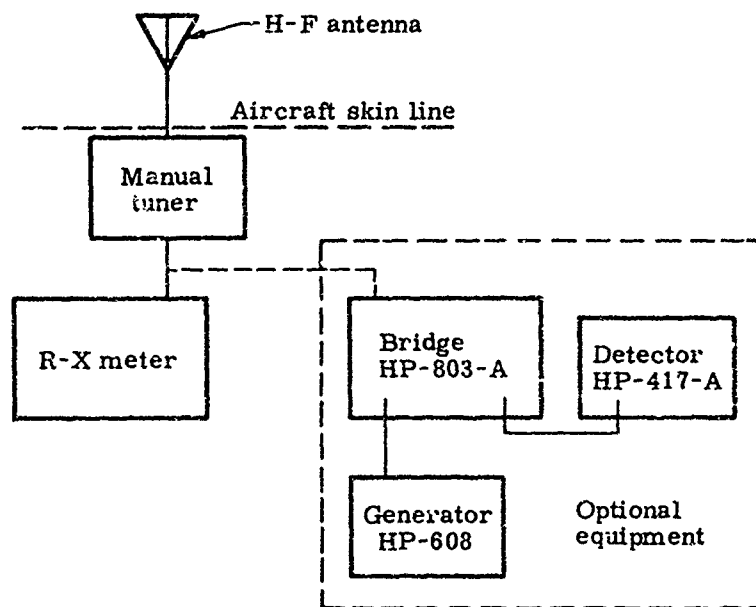


Fig. B-2. Test Setup to Verify $VSWR \leq 2:1$

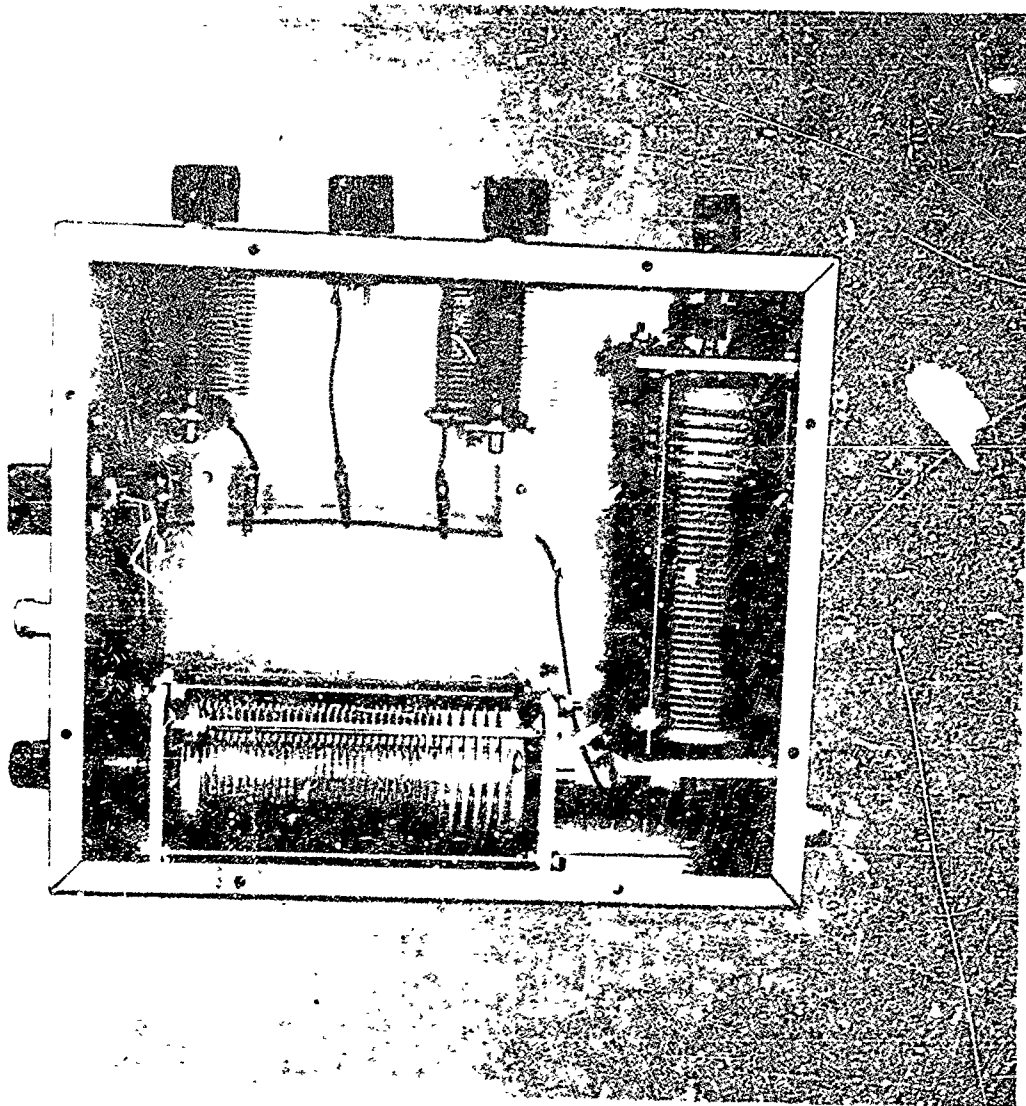


Fig. B-3. H-F and Monopole Manual Tuner

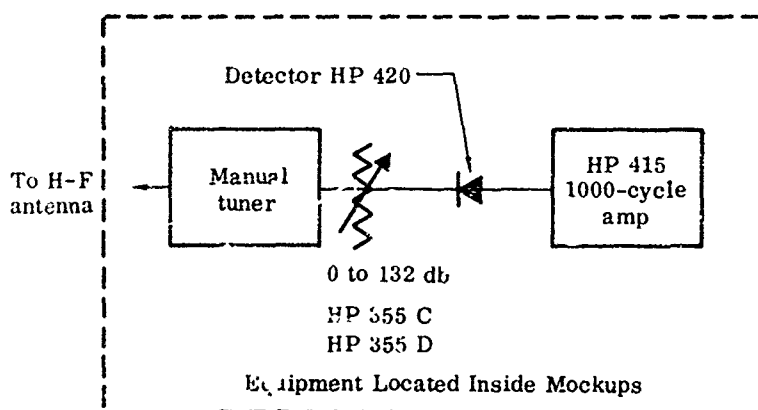
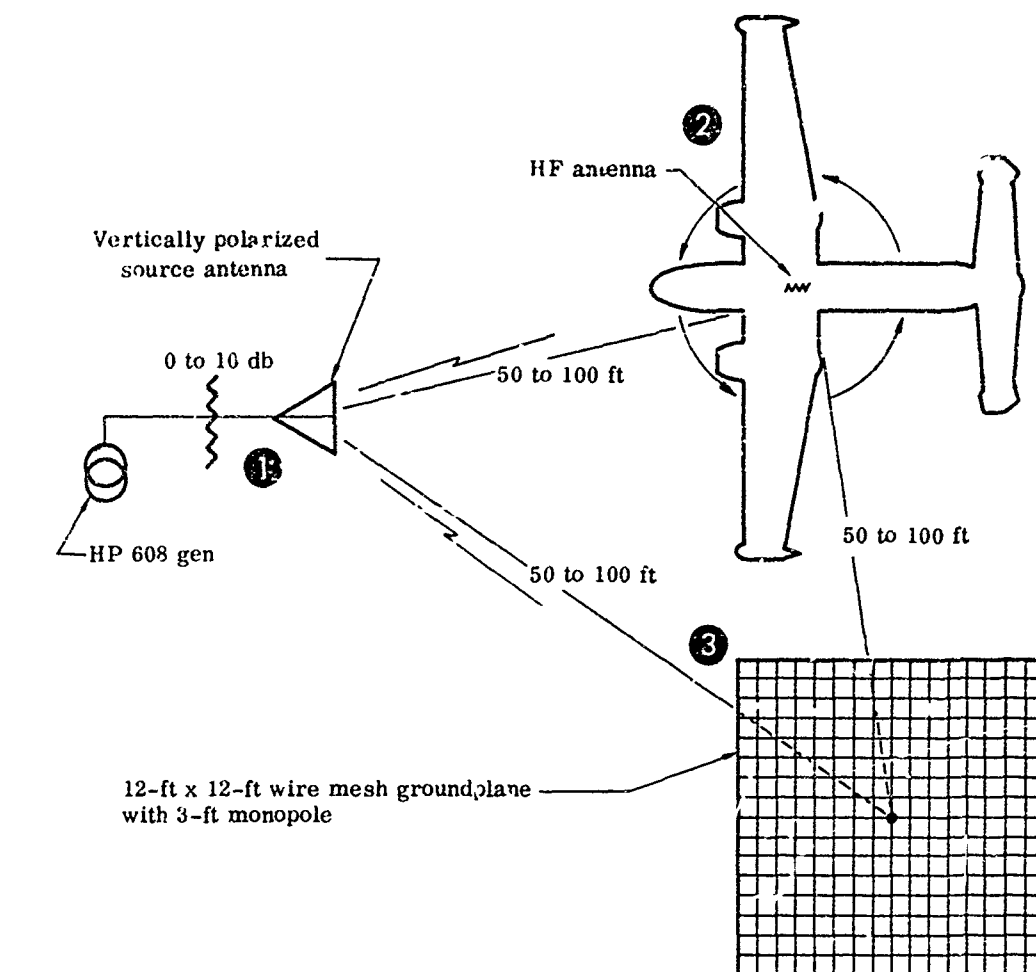


Fig. 17. Gain Measurement Test Setup



Fig. B-5. 3-ft Monopole with Ground Plane and 1/5-Scale Caribou on Rotary Platform

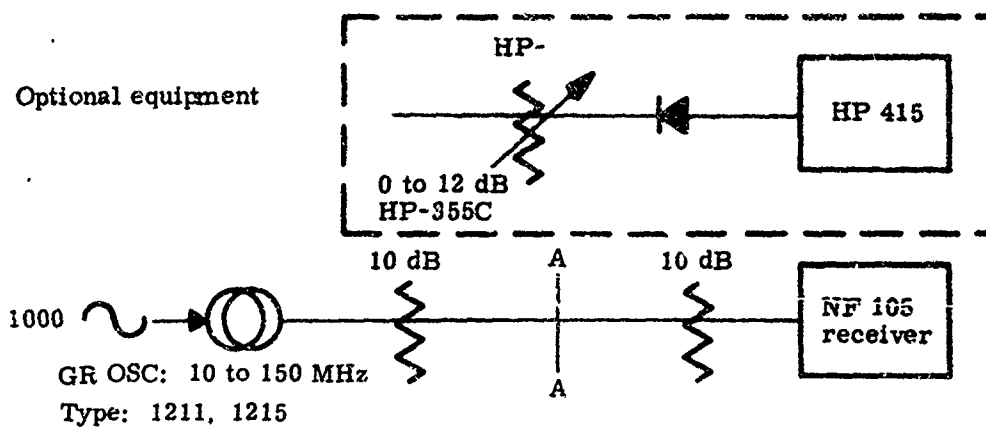


Fig. B-6a. Reference Level Setup for Manual Tuner Calibration

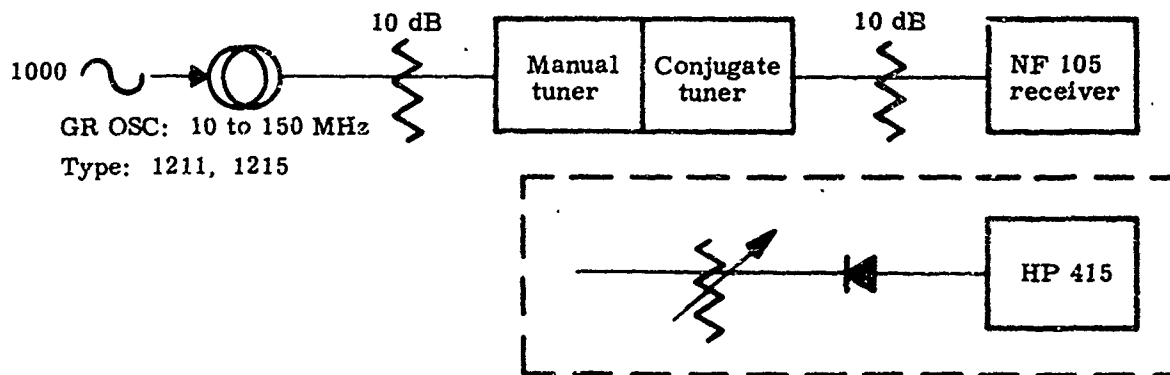


Fig. B-6b. Manual Tuner Insertion Loss Test Setup

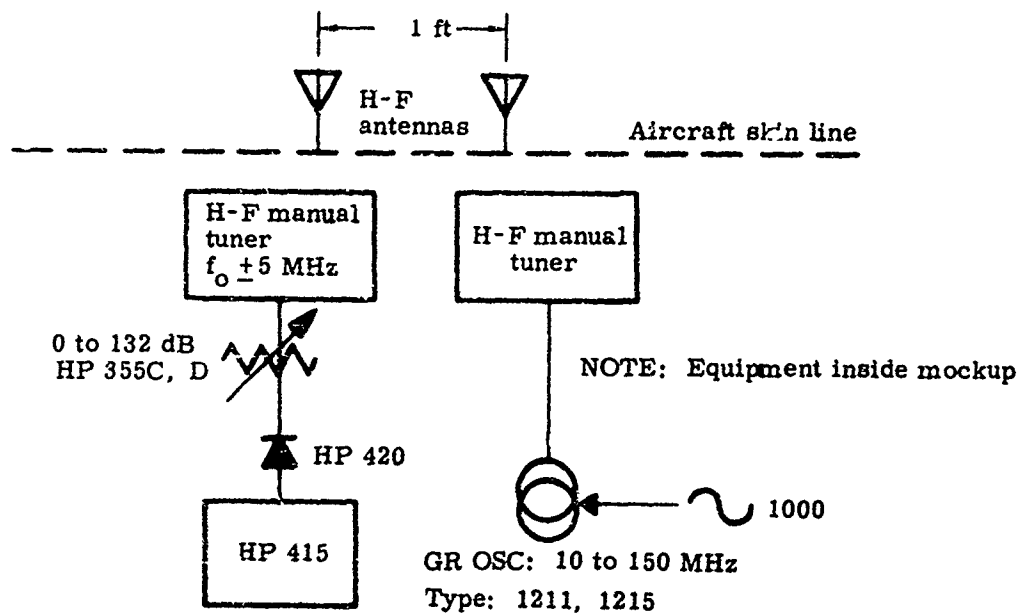


Fig. B-7. Decoupling Test Setup

APPENDIX C
ENVIRONMENTAL TEST RESULTS

1.0 Purpose

The testing was conducted in order to determine the ability of the Compact H-F Aircraft Antenna, Dwg. No. DH 225661, to withstand the shock and vibration requirements of: "Test Plan for Compact H-F Aircraft Antenna, Item 4, Contract DA 28-043-AMC-00477(E)."

2.0 Test Specimen

The test specimen consisted of one Compact H-F Aircraft Antenna as shown in Fig. C-1. All antenna locations and orientations used in this report are referenced to Fig. C-1.

3.0 Procedure

Except where otherwise noted, all testing herein was conducted in accordance with "Environmental Qualification Test Procedure for the Compact H-F Aircraft Antenna DH 225661."

3.1 Vibration

- 3.1.1 The antenna was mounted for exposure to vibration in the lateral axis (see Fig. C-1).
- 3.1.2 A frequency sweep from 5 to 500 to 5 cps at qualification levels as shown in Fig. C-2 was started. At 52 cps (5-g input), one of the solid fiberglass stanchions (Leg No. 2) broke away from the baseplate, and testing was discontinued. This was the first lateral resonant frequency of the antenna.
- 3.1.3 Legs Nos. 2 and 4 were reinforced with metal screws, and the antenna was again mounted for vibration in the lateral axis.
- 3.1.4 An upsweep from 5 to 500 cps was made, and a downsweep from 500 to 5 cps was started. When the resonant frequency of 52 cps was reached, one of the antenna stanchions (Leg No. 2) cracked where it joined the baseplate and testing was again discontinued.
- 3.1.5 The antenna configuration was then modified so that Legs Nos. 2 and 4 were not attached to the baseplate, and an evaluation at reduced input levels was conducted. For results of this evaluation see Table C-1.
- 3.1.6 The antenna was then modified to stiffen all four stanchions and returned to the laboratory for evaluation. The evaluation was conducted at reduced levels both with and without clamped crossbars between the upper members of the antenna (see Fig. C-1. For results of the evaluation see Table C-1.

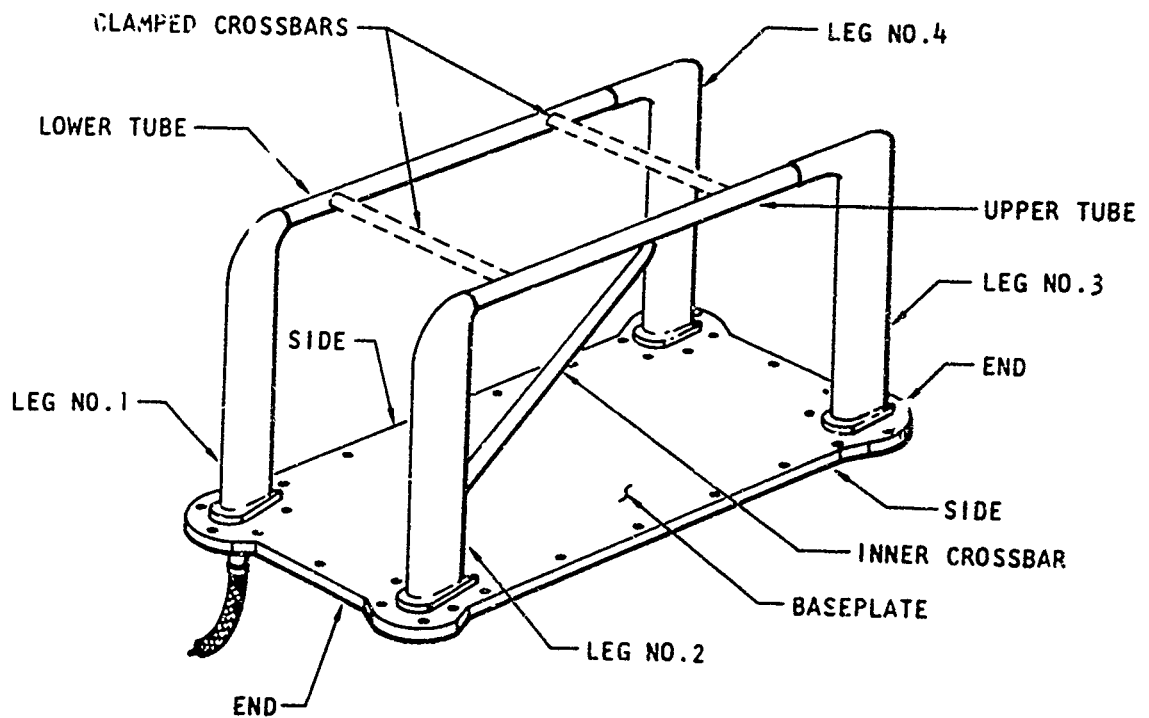
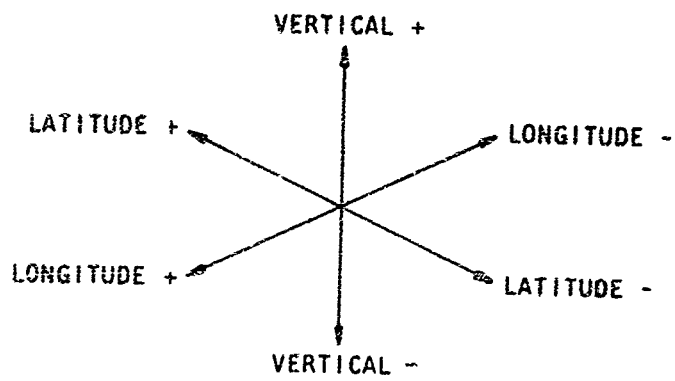


Fig. C-1. Compact H-F Aircraft Antenna

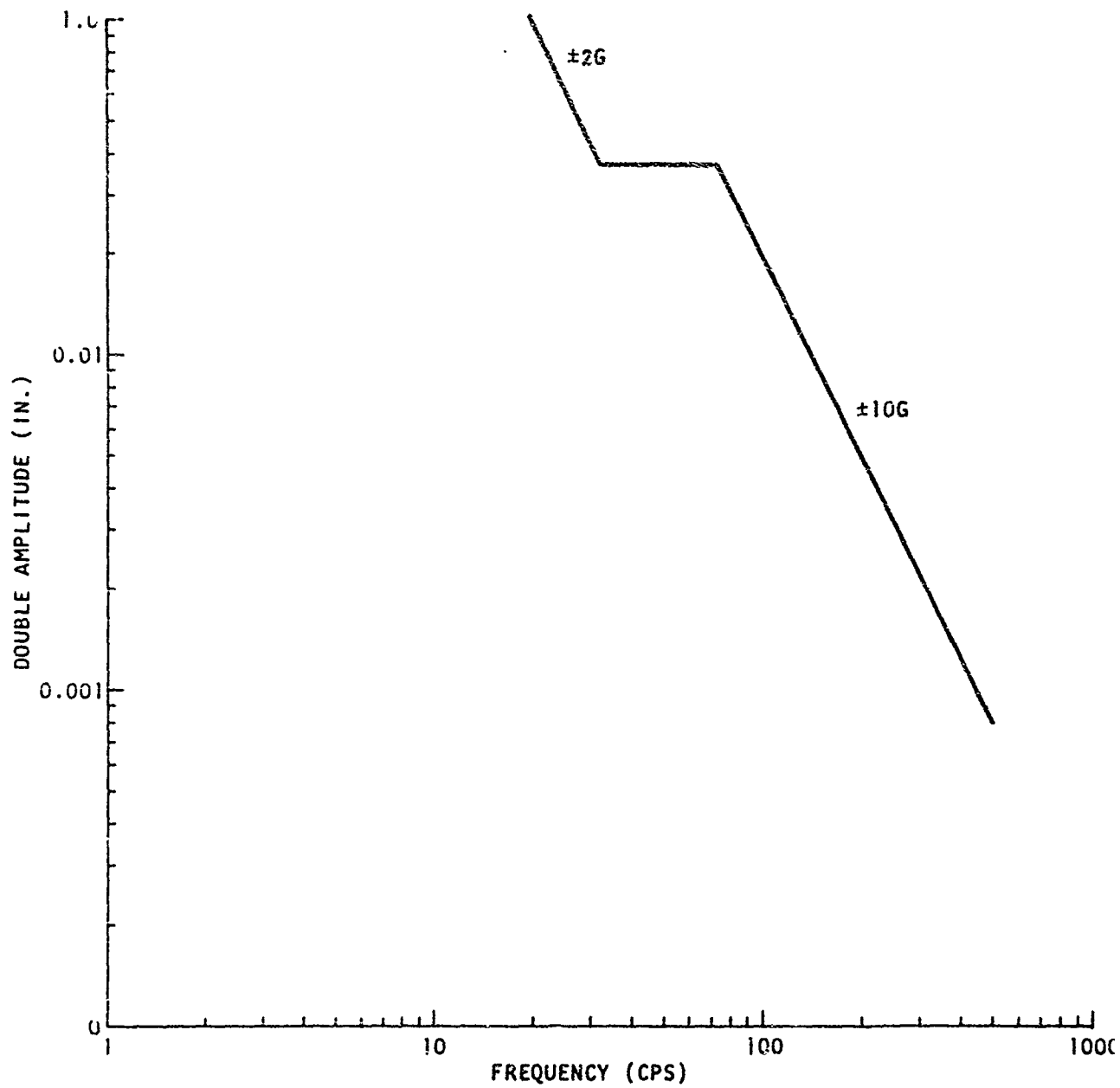


Fig. C-2. Vibration Requirements Qualification Level

- 3.1.7 The specimen was mounted for vibration in the vertical direction and subjected to three sweeps from 5 to 500 to 5 cps at full specification level (see Table C-1 for test data). This and all subsequent testing was conducted without clamped crossbars.
- 3.1.8 The first resonant dwell at 150 cps was started; however, after 1 min and 55 sec, the vibrator shut down due to overheating of the amplifier and the dwell was discontinued.
- 3.1.9 A fourth vertical sweep (see Table C-2) was conducted to complete vertical axis sweep requirements, and the dwell postponed until the vibrator was repaired. During repairs to the vibrator, the antenna shock test was conducted (see paragraph 3.2).
- 3.1.10 With the vibrator repaired, the first resonant dwell of the vertical axis was completed. Three additional dwells were also completed in this axis (see Table C-2 for data).
- 3.1.11 A low level evaluation was then conducted in the longitudinal axis. Upon completion of evaluation, four sweeps from 5 to 500 to 5 cps were conducted at full level. Due to severe response of the antenna at resonant vibration frequencies, and desire to gain more information, dwells in this axis were postponed, and the antenna was oriented for vibration in the lateral axis (see Tables C-1 and C-2 for data).
- 3.1.12 A low level evaluation was conducted in the lateral axis, and six full level sweeps from 5 to 500 to 5 cps were conducted. Upon completion of sweeps, a 30-min dwell at 359 cps was conducted (see Tables C-1 and C-2 for data).
- 3.1.13 To allow as much testing as possible before chance of failure, dwells at 50 to 60 cps and 63 to 70 cps were postponed until after testing in the longitudinal axis.
- 3.1.14 The specimen was oriented for vibration in the longitudinal axis, and four sweeps from 5 to 500 to 5 cps were conducted (a total of eight sweeps for this axis, as four sweeps had already been conducted in Step 3.1.11). Upon completion of the sweeps, one full 30-min dwell at 110 cps was conducted, and a second dwell at 98 cps was started. After 22 min of vibration at 98 cps, the antenna failed and testing was discontinued (see Table C-2 for data).

3.2 Shock

- 3.2.1 The Barry 1200-1 VD Medium Impact Shock Machine was set up to produce an 11 msec, 15-g peak shock pulse.
- 3.2.2 The antenna (with connector downward) was mounted to be subjected to shock in the lateral axis and subjected to three shock pulses set up for in step 3.2.1.
- 3.2.3 The antenna was rotated 180° and subjected to the three shock pulses set up for in step 3.2.1.
- 3.2.4 The antenna was then inspected for any signs of failure.
- 3.2.5 Steps 3.2.2 through 3.2.4 were then repeated for the remaining two orthogonal axes.

4.0 Test Data

A summary of evaluation and test data is given in Tables C-1 and C-2.

5.0 Test Results and Conclusions

5.1 Shock

The shock test produced no adverse effects on the antenna.

5.2 Vibration

Three configurations of the antenna were tested. The configurations, and the results of the evaluations of each, are given in Table C-1.

The original and second configurations were inadequate to withstand qualification level vibration at their primary resonant frequencies. Failure of one of the fiberglass stanchions was experienced at 52 cps in the first case. While testing of the second configuration was not carried to failure, the extremely high magnifications noted at the reduced input level demonstrated that the structure could not endure testing at full level.

The last configuration to be tested also incurred a vibration failure, during testing in the longitudinal axis. This failure was of a fatigue type, however, and occurred after subsection of the specimen to the following tests:

Vertical axis, --completion of the specified three hours of testing (six frequency sweeps and four resonant dwells).

Lateral axis. --two hours of testing (six frequency sweeps and one resonant dwell).

Longitudinal axis. --two hours and 52 min of testing (eight frequency sweeps, one resonant dwell, and 22 min of a second dwell. During this second dwell, the failure occurred.

The failure occurred in the form of a crack in the baseplate under and adjacent to legs Nos. 1 and 3, due to flexing of the plate. It is anticipated that this situation would be improved by stiffening or providing additional restraint of the baseplate at the leg junctions.

TABLE C-1

Evaluation of Compact H-F Aircraft Antenna at Reduced Vibration Levels

I. Original Configuration

A. Resonant frequency 52 cps (lateral axis)

B. Resonant frequency (stanchion repaired with metal screws) 52 cps (lateral axis).

II. Two Stanchions Cut off at Baseplate

<u>Axis</u>	<u>Resonant Frequency (cps)</u>	<u>Input</u>	<u>Output</u>	<u>Magnification Factor (Q)</u>
Lateral	18-3/4	0.011 in. DA	0.877 in. DA	79.7
	105 (slight)	--	--	--
	490 (slight)	--	--	--

III. Heavier Fiberglass on all Four Stanchions

Low Level Sweeps with Crossbars

<u>Axis</u>	<u>Resonant Frequency (cps)</u>	<u>Input (g)</u>	<u>Output</u>	<u>Magnification Factor (Q)</u>
Lateral	75	0.5	13 to 15 g	26 to 30
	355	0.5	3 g	6
Vertical	453	0.5	18.5 g (center tube)	37
			12 g (upper tube)	24
	500	0.5	33 g (center tube)	66
			5.7 to 8.5 g (upper tubes)	11.4 to 17
	508	6.5	20 to 24 g (upper tubes)	40 to 48
			52 g (center tube)	104

TABLE C-1 (continued)

Low Level Sweeps Without Crossbars

<u>Axis</u>	<u>Resonant Frequency (cps)</u>	<u>Input</u>	<u>Output</u>	<u>Magnification Factor (Q)</u>
Lateral	73 to 77	0.0007 in. DA	0.04 in. DA	56
	91	0.0065 in. DA	0.02 in. DA	40
	105 to 110	--	--	--
Vertical	145 to 160	--	--	--
	180	--	--	--
	360	--	--	--
	480	0.5 g	5.4 g (upper tube)	10.8
	528	0.5 g	32 g (upper tube)	64
			27 g (center tube)	54
Longitudinal	135	0.5 g	14 or 15 g	28 to 30
	184	0.53 g	15 g (upper tube)	27.2
	233	0.54 g	17.5 g (upper tube)	32.4

Magnification factor $Q = \text{output}/\text{input}$

DA = double amplitude

TABLE C-2

Summary of Vibration Test Data at Qualification Levels

A. Vertical Axis

Frequency Sweeps from 5 to 500 to 5 cps

<u>Sweep No.</u>	<u>Resonant Frequency (cps)</u>	<u>Input (g)</u>	<u>Output (g)</u>	<u>Magnification Factor (Q)</u>
1	145 to 160	--	--	--
	180	--	--	--
	360	--	--	--
	480	--	--	--
2	150 to 160	10	80 (upper tube)	8
	255	10	47	4.7
	370	10	60	6
	420	10	60	6
3	145 to 150	10	45 (center tube)	4.5
	235	10	62	6.2
	380	10	100	10
	470	10	700	70
	150	10	80 (upper tube)	8
	260	10	40	4
	390	10	60	6
4	150	10	70	7
	260	10	37	3.7

Dwells

<u>Frequency (cps)</u>	<u>Remarks</u>
149 to 144	Resonant frequency decreased during dwell and amplification increased. Torsional motion present.
229	Inner crossbar mostly vertical motion. Stanchions mostly lateral motion.
396	Same motion as 329 cps.
460	Motion of whole antenna mostly vertical.

TABLE C-2 (continued)

B. Lateral Axis

Frequency Sweeps from 5 to 500 to 5 cps

<u>Sweep No.</u>	<u>Resonant Frequency (cps)</u>	<u>Remarks</u>
1	68 73 100 360 to 370	At 73 cps, a magnification factor of about 30. Several 1/4-in. screws became loose during vibration and had to be retightened.
2	64 to 68 70 to 72 98 to 105 360	Crack appeared where Leg No. 1 joins the baseplate (Fig. C-1).
3	55 to 63 67 to 72 100 360 to 370	
4	50 to 60 63 to 70 105 to 110 360	Inspection at the completion of this sweep showed possible cracks in baseplate next to Legs Nos. 1 and 3.
5	45 to 57 60 to 68 94 to 103 360	Cracks in baseplate next to Legs Nos. 1 and 3 appeared to be worse.
6	47 to 56 57 to 67 95 to 100 360	Head of 1/4-in. screw on end of baseplate next to Leg No. 4 snapped off at 56 cps on upsweep.

Dwell

<u>Frequency (cps)</u>	<u>Remarks</u>
359	Near the end of the dwell, the points where the inner cross-bar joins the stanchions were thermally warm. Some vertical motion at previously recorded crack between foot of Leg No. 1 and baseplate.

TABLE C-2 (continued)

C. Longitudinal Axis

Frequency Sweeps from 5 to 500 to 5 cps

<u>Sweep No.</u>	<u>Resonant Frequency (cps)</u>	<u>Remarks</u>
1	80 to 85 110 to 125 140 to 165 210 to 220	Very strong torsional motion at 140 to 165 cps and at 110 to 125 cps.
2	80 110 to 125 140 to 135 205 to 210	
3	78 to 80 105 to 108 143 to 158 206 to 210	
4	80 to 83 108 to 110 140 to 150 205 to 210	No failures noted in visual inspection.
5	92 to 102 105 to 115	
6	90 to 100 105 to 116	
7	88 to 100 105 to 115	
8	90 to 100 105 to 115	

Dwells

<u>Frequency (cps)</u>	<u>Remarks</u>
110	110 cps was resonance of Legs Nos. 2 and 3. There was a beat frequency of about 2 cps that disappeared after 15 min of vibration. After about 16 min of vibration, the head of a 1/4-in. screw on the end of the baseplate next to Leg No. 3 snapped off. The 2-cps beat frequency returned after screw was replaced.

TABLE C-2 (continued)

<u>Frequency</u> <u>(cps)</u>	<u>Dwell</u>	<u>Remarks</u>
98		Six 1/4-in. screws broke during vibration, after 1 min--on side next to Leg No. 4, after 7 min--on side next to Leg No. 2, after 12 min--on side next to Leg No. 1 and on end next to Leg No. 3. After 16 min--on end next to Leg No. 3, after 22 min--on end next to Leg No. 3. After 22 min of vibration, the test was discontinued. The resonant frequency had dropped to 89 cps, and cracks were present in the baseplate and under all four legs of the antenna. Cracks were also present about the hole for the 1/4-in screw on the side of the baseplate next to Leg No. 3.

Unclassified

Security Classification

DOCUMENT CONTROL DATA - R&D		
(Security classification of title, body of abstract and figure caption must be entered when the overall report is classified)		
1 ORIGINATING ACTIVITY (Corporate author)		2a REPORT SECURITY CLASSIFICATION
Martin Marietta Corporation, Baltimore Division, Baltimore, Maryland 21203		Unclassified
		2b GROUP
3 REPORT TITLE		
Compact H-F Aircraft Antenna (2-30 MHz)		
4 DESCRIPTIVE NOTES (Type of report and inclusive dates)		
Final Report 21 January 1965 to 1 August 1967		
5 AUTHOR(S) (Last name, first name, initial)		
J. H. Hendershot		
6 REPORT DATE	7a TOTAL NO OF PAGES	7b NO. OF REFS
August 1967		4
8a CONTRACT OR GRANT NO	9a. ORIGINATOR'S REPORT NUMBER(S)	
DA28-043-AMC-00477(E)	ECOM-00477(E)	
b PROJECT NO		
1J6-41203-D-528-04		
c	9b. OTHER REPORT NO(S) (Any other numbers that may be assigned this report)	
d		
10 AVAILABILITY/LIMITATION NOTICES		
11 SUPPLEMENTARY NOTES		12. SPONSORING MILITARY ACTIVITY
		U. S. Army Electronics Command Fort Monmouth, N. J. (AMSEL-VL-C)
13 ABSTRACT		
<p>The program effort reported here is primarily concerned with the design and development of a broadband, compact, omnidirectional airborne antenna in the H-F communications range (2 to 30 MHz) to be used on several U. S. Army aircraft both fixed and rotary wing.</p> <p>Additional investigations are presented on a low profile wire antenna located on the aircraft tail at close proximity to the aircraft skin.</p> <p>The various exploratory element configurations reported here are loop-type structures intended to induce currents on the airframe for a predominantly vertical polarized system. The final model H-F antenna delivered as the result of this program is a two-turn grounded loop.</p> <p>Scaled models of two aircraft, one rotary and one fixed wing, were built for pattern, impedance, and gain measurements. Data are presented illustrating the effect of the antenna configuration, orientation, and location on the particular scale model aircraft. Pattern measurements were performed on a 1/50-scale Caribou aircraft. Pattern measurements were performed on a 1/50-scale Caribou aircraft and a 1/25-scale Iroquois helicopter. Impedance and gain measurements were made on 1/5-scale models of the same two aircraft.</p> <p>Manual L-C tuners were built for the 1/5-scale antennas to facilitate impedance matching for the relative gain comparison measurements.</p> <p>The application of ferrite to the H-F antenna has been considered. Measured field strength of a matched transmitting coil, with and without ferrite material, is presented.</p> <p>A full-scale breadboard model of the two-turn loop was successfully tested with a Univac automatic tuner for high power and impedance tuning.</p> <p>Environmental tests were performed on the full-scale final model antenna. The antenna was subjected to various vibration levels which resulted in structural modifications to the delivered model antennas.</p> <p>Two full-scale final model antennas, a Univac automatic tuner and a Collins tunable filter were delivered during this program.</p> <p>The Design Plan, Test Plan, and Environmental Test Results are included in the appendix.</p>		

DD FORM 1 JAN 64 1473

Unclassified

Security Classification

Security Classification

14 KEY WORDS	LINK A		LINK B		LINK C	
	ROLE	WT	ROLE	WT	ROLE	WT
Antenna High Frequency (2-30 MHz) Compact Aircraft Antenna Impedance Gain Patterns Low-Profile Wire Antennas Design Plan Test Plan Environmental Test Results						

INSTRUCTIONS

1. **ORIGINATING ACTIVITY:** Enter the name and address of the contractor, subcontractor, grantee, Department of Defense activity or other organization (*corporate author*) issuing the report.

2a. **REPORT SECURITY CLASSIFICATION:** Enter the overall security classification of the report. Indicate whether "Restricted Data" is included. Marking is to be in accordance with appropriate security regulations.

2b. **GROUP:** Automatic downgrading is specified in DoD Directive S200.10 and Armed Forces Industrial Manual. Enter the group number. Also, when applicable, show that optional markings have been used for Group 3 and Group 4 as authorized.

3. **REPORT TITLE:** Enter the complete report title in all capital letters. Titles in all cases should be unclassified. If a meaningful title cannot be selected without classification, show title classification in all capitals in parentheses immediately following the title.

4. **DESCRIPTIVE NOTES:** If appropriate, enter the type of report, e.g., interim, progress, summary, annual, or final. Give the inclusive dates when a specific reporting period is covered.

5. **AUTHOR(S):** Enter the name(s) of author(s) as shown on or in the report. Enter last name, first name, middle initial. If military, show rank and branch of service. The name of the principal author is an absolute minimum requirement.

6. **REPORT DATE:** Enter the date of the report as day, month, year; or month, year. If more than one date appears on the report, use date of publication.

7a. **TOTAL NUMBER OF PAGES:** The total page count should follow normal pagination procedures, i.e., enter the number of pages containing information.

7b. **NUMBER OF REFERENCES:** Enter the total number of references cited in the report.

8a. **CONTRACT OR GRANT NUMBER:** If appropriate, enter the applicable number of the contract or grant under which the report was written.

8b, 8c, & 8d. **PROJECT NUMBER:** Enter the appropriate military department identification, such as project number, subproject number, system numbers, task number, etc.

9a. **ORIGINATOR'S REPORT NUMBER(S):** Enter the official report number by which the document will be identified and controlled by the originating activity. This number must be unique to this report.

9b. **OTHER REPORT NUMBER(S):** If the report has been assigned any other report numbers (either by the originator or by the sponsor), also enter this number(s).

10. **AVAILABILITY/LIMITATION NOTICES:** Enter any limitations on further dissemination of the report, other than those

imposed by security classification, using standard statements such as:

- (1) "Qualified requesters may obtain copies of this report from DDC."
- (2) "Foreign announcement and dissemination of this report by DDC is not authorized."
- (3) "U. S. Government agencies may obtain copies of this report directly from DDC. Other qualified DDC users shall request through _____."
- (4) "U. S. military agencies may obtain copies of this report directly from DDC. Other qualified users shall request through _____."
- (5) "All distribution of this report is controlled. Qualified DDC users shall request through _____."

If the report has been furnished to the Office of Technical Services, Department of Commerce, for sale to the public, indicate this fact and enter the price, if known.

11. **SUPPLEMENTARY NOTES:** Use for additional explanatory notes.

12. **SPONSORING MILITARY ACTIVITY:** Enter the name of the departmental project office or laboratory sponsoring (paying for) the research and development. Include address.

13. **ABSTRACT:** Enter an abstract giving a brief and factual summary of the document indicative of the report, even though it may also appear elsewhere in the body of the technical report. If additional space is required, a continuation sheet shall be attached.

It is highly desirable that the abstract of classified reports be unclassified. Each paragraph of the abstract shall end with an indication of the military security classification of the information in the paragraph, represented as (TS) (S) (C), or (U).

There is no limitation on the length of the abstract. However, the suggested length is from 150 to 225 words.

14. **KEY WORDS:** Key words are technically meaningful terms or short phrases that characterize a report and may be used as index entries for cataloging the report. Key words must be selected so that no security classification is required. Identifiers, such as equipment model designation, trade name, military project code name, geographic location, may be used as key words but will be followed by an indication of technical context. The assignment of links, rules, and weights is optional.